7.6 Geologies of Other Structure Sites

7.6.1 Intake Site

(1) Topography

The intake is planned at the right-bank side of the Zamanti River approximately 100 m upstream of the dam axis.

This site faces a small V-shaped gully running into the Zamanti River on the right-bank side, and the slope at which the intake is planned is a steep one of approximately 65 deg.

(2) Geology

The intake site, similarly to the dam site, is composed of hard, massive peridotite. There are no surface deposits and the bedrock is exposed, with small-scale faults in the north-south direction and northwest-southeast direction crossing each other, while joints are also developed. Parts of these discontinuities are opened at the surface layer portion.

(3) Considerations from the Viewpoint of Engineering Geology

This site, which has a steep slope of approximately 65 deg where bedrock is exposed, is stable as a whole. The open cracks visible at the surface can be expected to be tightly closed underground judging by the results of investigations at the dam site. Consequently, although there is a possibility of spalling or collapse of surface rock, it is judged from the geological structure that there is little possibility for large-scale collapsing to occur.

7.6.2 Headrace Tunnel Route

(1) Topography

The headrace tunnel, approximately 16 km in length, is planned to pass through the right-bank side of the Zamanti River 2.5 km distant from the river channel at maximum.

The tunnel route will generally be mountainland of elevation of 800 m to 1,200 m. The principal streams along this route are the Buyukboz River, Kuzlu Kara River, Kapiz River, and Sogut River in order from the dam site. These streams generally run in a north-westerly direction, that is, perpendicular to the direction of the headrace tunnel, to merge with the Zamanti River.

The earth cover of the headrace tunnel planned at EL. 540 m will be 700 m at maximum near the middle of the tunnel route, and 90 m at minimum at the Kuzlu Kara River, Kapiz River, and Sogut River among the tributaries mentioned previously, and around 400 m on average.

(2) Geology

The geology of the headrace tunnel route is shown in Fig. 7-9.

The geology of the headrace tunnel route, viewed macroscopically, is composed of Paleozoic limestone, sandstone, and shale distributed at the powerhouse-site side and Mesozoic limestone and peridotite distributed at the dam-site side (ophiolite to be called peridotite for the reasons described in the section on the geology of the reservoir and dam site), and it can be comprehended that a complex geological structure is presented at the boundary between the two groups.

The Paleozoic formations distributed roughly on the powerhouse-site side of the Kapiz River may be classified according to age of deposition as a formation (D) consisting of Devonian limestone, dolomitic limestone, shale, sandstone, and quartzite (or quartz sandstone), and a formation (Pk) consisting mainly of Carboniferous to Permian limestone, and also muddy limestone (or sandy limestone), dolomitic limestone, and shale. Repetitions of microfolding are seen and the formations are cut by high-angle faults or low-angle thrust faults extending mainly in the north-south and southwest-northeast directions.

On the other hand, the Mesozoic limestone and peridotite distributed at the dam-site side of the Kapiz River, as described in the preceding section on "Geology of Reservoir," is contacted by a thrust fault with peridotite pushed up on top of limestone. This thrust

fault, macroscopically is thought to form a low angle as seen from
the distributions of limestone and peridotite, and at least from
the Kuzlu Kara River to the Kapiz River, the angle is roughly close
to vertical.

(3) Considerations from the Viewpoint of Engineering Geology

  (a) Sections of Thin Earth Cover

       Of the planned headrace tunnel route, the locations where earth
       cover from the ground surface will be thinnest are directly under
       the Kuzlu Kara River, the Kapiz River, and the Sogut River.

       Of these three, drilling investigations from the ground surface to
       near the planned elevation of the headrace tunnel have been made
       at the Kapiz River and Sogut River sites. According to the
       results, surface deposits at both sites are thin, and hard
       limestone and other rocks are distributed from close to the ground
       surface down to the tunnel elevation. Regarding the Kuzlu Kara
       River site, the thickness of slope wash is small according to the
       results of surface reconnaissances, and it was found that hard
       peridotite is distributed.

       Accordingly, it is judged there are no problematic points with
       regard to driving of the tunnel at the abovementioned three sites.

  (b) Bedrock Strength

       The results of tests on cores obtained in drilling performed at
       the headrace tunnel site are given in Table 7-8. The unconfined
       compressive strengths of the core samples tested were from 223
       kgf/cm^2 to 686 kgf/cm^2 for limestone, 537 kgf/cm^2 for sandy
       limestone, and 389 kgf/cm^2 for quartz sandstone. As for the
       unconfined compressive strength of peridotite, an average of 376
       kgf/cm^2 was indicated as stated in the preceding section, "Geology
       of Dam Site."

7 - 51

The headrace tunnel will pass chiefly through the these rocks, and it is judged there will be no problematic points regarding the strength possessed by the rock itself.

(c) Faults

Numerous faults are distributed along the route of the headrace tunnel.

Among these faults, with regard to the thrust fault comprising the boundary between limestone and peridotite, the following results were obtained in surface geological mapping of the vicinity of the Kuzlu Kara River:

o Limestone and peridotite in this vicinity contact each other at an angle close to vertical,

o Broad altered zones and weak zones are not found in limestone, needless to say, or in peridotite in the vicinity of the fault,

and it is judged that there is little possibility of extreme difficulty being encountered in tunnel excavation over a long section in connection with the thrust fault.

On the other hand, with regard to faults developed in the Paleozoic formations on the powerhouse-site side, the following may be considered:

o These faults are mostly recognized as lineaments which continue for comparatively great lengths in aerial photogeological interpretations.

o However, on making confirmations in the field of a few long, continuous lineaments, it was ascertained that the widths of sheared zones of faults were small at about 1 m or under.

o The directions of faults developed in Paleozoic formations are roughly north-south to northeast-southwest so that they will intersect the headrace tunnel which is to be in the northwest-southeast direction at an angle close to perpendicular. Because of this, even if a fault with a sheared zone of small

width were to be encountered, it would be possible to break through it in the shortest distance.

In view of the above, it is judged there is little possibility that these faults will make tunnel excavation difficult over long distances.

(d) Ground Water

The peridotite distributed on the dam-site side, as described in the preceding section, "Geology of Dam Site," has a high ground-water table and is impermeable, and it is expected that springing of water into the tunnel would be only in small amounts through minute fissures in the bedrock.

On the other hand, limestone is predominant in formations other than the peridotite, and since there are hardly any water flows to be seen in gullies at the ground surface, it is estimated that the groundwater table is generally low and solution cracks are developed inside the rock. At the Kapiz River and Sogut River sites where drilling was done, the groundwater table is at roughly the same height as the headrace tunnel elevation or slightly higher. According to observations of drilled cores, the widths of solution cracks are small, and it is considered that the quantity of ground water springing into the tunnel from these cracks will be small.

However, it is necessary that hydrogeological investigations shall be done further.

7.6.3 Surge Tank, Penstock, and Powerhouse Sites

(1) Topography

The surge tank, penstock, and powerhouse sites are located at the right-bank side of the Zamanti River approximately 2 km upstream from the confluence of the Zamanti River and the Goksu River.

The slope at which these structures are planned is in the form of a ridge sandwiched by small gullies at both sides. This slope shows a

point of change in inclination at about EL. 520 m, the slope being gentle at approximately 20 deg above EL. 520 m and steep at an average of 40 deg and a maximum of about 70 deg below EL. 520 m.

The river-bed elevation of the Zamanti River at this site is approximately 320 m and the river-bed gradient is an average of 1/140.

(2) Geology

The geologies of the surge tank, penstock, and powerhouse sites, as shown in Figs. 7-10 and 7-11, consist of basement rock of Paleozoic sandstone, shale, and limestone, Mesozoic sandstone and shale, and Quaternary deposits such as slope wash and alluvium.

A Cambrian formation (Ea) mainly composed of sandstone and shale which is the oldest formation seen in the Goktas project area is distributed at the powerhouse site, and this is overlain by a Devonian formation (D) mainly composed of limestone and dolomitic limestone, while further, there is a Carboniferous-Permian formation (Pk) mainly composed of limestone on top, which is distributed on the penstock route. The slope at which these formations are distributed has a steep gradient averaging 40 deg. A Cretaceous sandstone-shale formation (Kp) is thinly distributed to make up the surge tank site, and the slope of this distribution zone is gently inclined at approximately 20 deg.

Strikes and dips of formations cannot be measured at the massive limestone distribution zone, but at least the Cambrian sandstone and shale distributed at the powerhouse site show north-south or northeast-southwest strikes roughly parallel to the Zamanti River, and dip gently to the west, that is, toward the right-bank side of the Zamanti River. Large-scale faults are not seen in the surroundings of the projected structures.

Slope wash, which is a Quaternary deposit, is generally thin. Alluvium distributed at the bed of the Zamanti River is estimated to have a thickness of about 20 m, although this needs further ascertainment.

(3) Considerations from the Viewpoint of Engineering Geology

    (a) Selection of Powerhouse Site

        At the Master Plan stage, the powerhouse site was selected at the
right-bank side of the Zamanti River approximately 1.5 km upstream
from the confluence of the Zamanti and the Goksu River. The JICA
Survey Team carried out surface reconnaissances and aerial photo-
geological interpretations of the upstream and downstream
stretches of the Zamanti River including that site and made the
findings below.

      o Distinct arc-shaped cliffs and collapse areas are distributed
        at the powerhouse site planned at the stage of the Master Plan,
        and this is not suitable as the powerhouse site since it is
        estimated to be a landslide zone.

      o At the section downstream from this to the confluence with the
        Goksu River, there is a succession of steep cliffs composed of
        limestone from around EL. 1,000 m down to the bed of the
        Zamanti River, and the topographical conditions are not
        favorable for surge tank, penstock and powerhouse sites.

      o A ridge-shaped slope having many parts of exposed bedrock is
        seen approximately 500 m upstream from the powerhouse site
        planned at the Master Plan stage.

      o Further upstream from this point, in addition to the effective
        head for power generation being reduced, there is a con-
        tinuation of steep cliffs made up of limestone and the
        topographical conditions are unfavorable.

        In view of the above findings, the powerhouse site located
approximately 500 m upstream from the site in the Master Plan was
selected as shown in Fig. 7-10.

    (b) Stability of Slope

        According to surface geological explorations, drilling investiga-
tions, and seismic prospecting, the thickness of surface deposits
distributed at the slope where the surge tank, penstock, and

powerhouse are planned is generally small. Cretaceous sandstone and shale are distributed at the gently-sloped part between EL. 520 m and 700 m, and surface deposits are thin.

Collapse areas are not seen at the slope, while there are no faults distributed to cause concern about collapses being induced, while prominent weathering or loosening of the rock comprising the slope is not recognized as a result of drilling investigations, and so it may be judged that the slope at this site is stable.

(c) Bedrock Strength

The results of tests on cores from drilling done at the projected penstock and powerhouse sites are given in Table 7-9. Unconfined compressive strengths of limestone comprising the foundation of the projected penstock route range from 273 kgf/cm^2 to 409 kgf/cm^2, averaging 341 kgf/cm^2, while the sandstone and shale making up the foundation of the projected powerhouse are from 78 kgf/cm^2 to 529 kgf/cm^2, averaging 272 kgf/cm^2.

According to the results of seismic prospecting, P-wave velocity is 3.7 km/s, which is about normal for a Paleozoic bedrock.

It may be judged from these data that there are no problematic points from the standpoint of strengths of foundations for the projected structures.

The results of seismic prospecting carried out at this slope are discussed in detail in 7.8.

Table 7-8 Laboratory Test Results of Drilled Cores at Headrace Tunnel Route

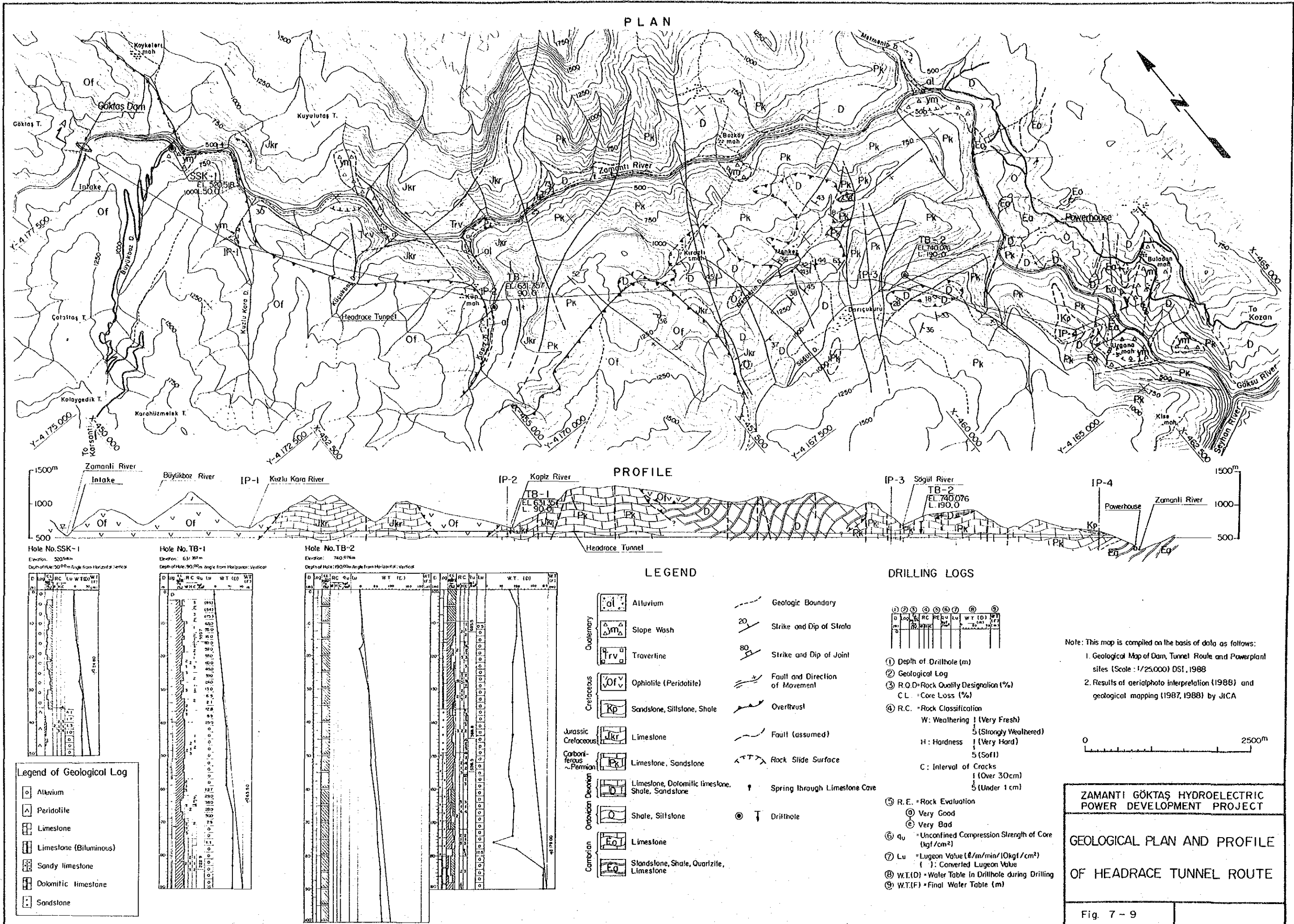| Drillhole No.	Depth (m)	Rock Name	Specific Gravity *(1)	Absorption (%) *(1)	Unconfined Compression Strength (kgf/cm²) *(2)	Tensile Strength (kgf/cm²) *(3)
TB-1	15.5 - 16.0	Limestone	2.72	0.1	559.7	102.6
TB-1	83.9 - 84.4	Limestone (biomicrite)	2.70	0.3	222.9	49.2
TB-2	112.6 - 113.1	Limestone	2.74	0.4	685.5	74.2
TB-2	144.6 - 145.1	Quartz sandstone	2.59	1.5	388.8	77.7
TB-2	154.5 - 155.0	Sandy limestone	2.77	0.5	536.5	54.5

Note: *(1) ASTM C97-83
       *(2) ASTM D2938-79
       *(3) ASTM D3967-81

Table 7-9   Laboratory Test Results of Drilled Cores at Power Plant Site

Drillhole No.	Depth (m)	Rock Name	*(1)Specific Gravity	*(1)Absorption (%)	*(2)Unconfined Compression Strength (kgf/cm^2)	*(3)Tensile Strength (kgf/cm^2)
PB-1	24.6 – 25.0	Shale	2.71	0.2	77.7	34.1
PB-1	42.0 – 42.5	Shale	2.77	0.8	208.5	74.5
PB-1	55.3 – 55.9	Sandstone	2.73	0.2	528.7	116.7
PB-2	45.4 – 45.8	Limestone	2.72	0.2	408.8	46.8
PB-2	68.8 – 69.2	Limestone	2.73	0.1	273.1	53.8

Note: *(1)   ASTM C97-83
        *(2)   ASTM D2938-79
        *(3)   ASTM D3967-81

PLAN

PROFILE

LEGEND

DRILLING LOGS

Legend of Geological Log

	Alluvium
	Peridotite
	Limestone
	Limestone (Bituminous)
	Sandy limestone
	Dolomitic limestone
	Sandstone

Quaternary
- al — Alluvium
- ym — Slope Wash
- Trv — Travertine

Cretaceous
- Of — Ophiolite (Peridotite)
- Kp — Sandstone, Siltstone, Shale

Jurassic ~ Cretaceous
- Jkr — Limestone

Carboniferous ~ Permian
- Pk — Limestone, Sandstone

Ordovician ~ Devonian
- D — Limestone, Dolomitic limestone, Shale, Sandstone
- O — Shale, Siltstone

Cambrian
- Eo — Limestone
- Eo — Sandstone, Shale, Quartzite, Limestone

- – – – Geologic Boundary
- 20 Strike and Dip of Strata
- 80 Strike and Dip of Joint
- Fault and Direction of Movement
- Overthrust
- Fault (assumed)
- Rock Slide Surface
- Spring through Limestone Cave
- Drillhole

① Depth of Drillhole (m)
② Geological Log
③ R.Q.D = Rock Quality Designation (%)
  C.L. = Core Loss (%)
④ R.C. = Rock Classification
  W: Weathering 1 (Very Fresh)
              5 (Strongly Weathered)
  H: Hardness 1 (Very Hard)
             5 (Soft)
  C: Interval of Cracks
     1 (Over 30cm)
     5 (Under 1cm)
⑤ R.E. = Rock Evaluation
  ⓖ Very Good
  ⓔ Very Bad
⑥ qu = Unconfined Compression Strength of Core (kgf/cm²)
⑦ Lu = Lugeon Value (ℓ/m/min/10kgf/cm²)
  ( ) : Converted Lugeon Value
⑧ W.T.(D) = Water Table in Drillhole during Drilling
⑨ W.T.(F) = Final Water Table (m)

Note: This map is compiled on the basis of data as follows:
1. Geological Map of Dam, Tunnel Route and Powerplant sites (Scale : 1/25,000) DSI, 1988
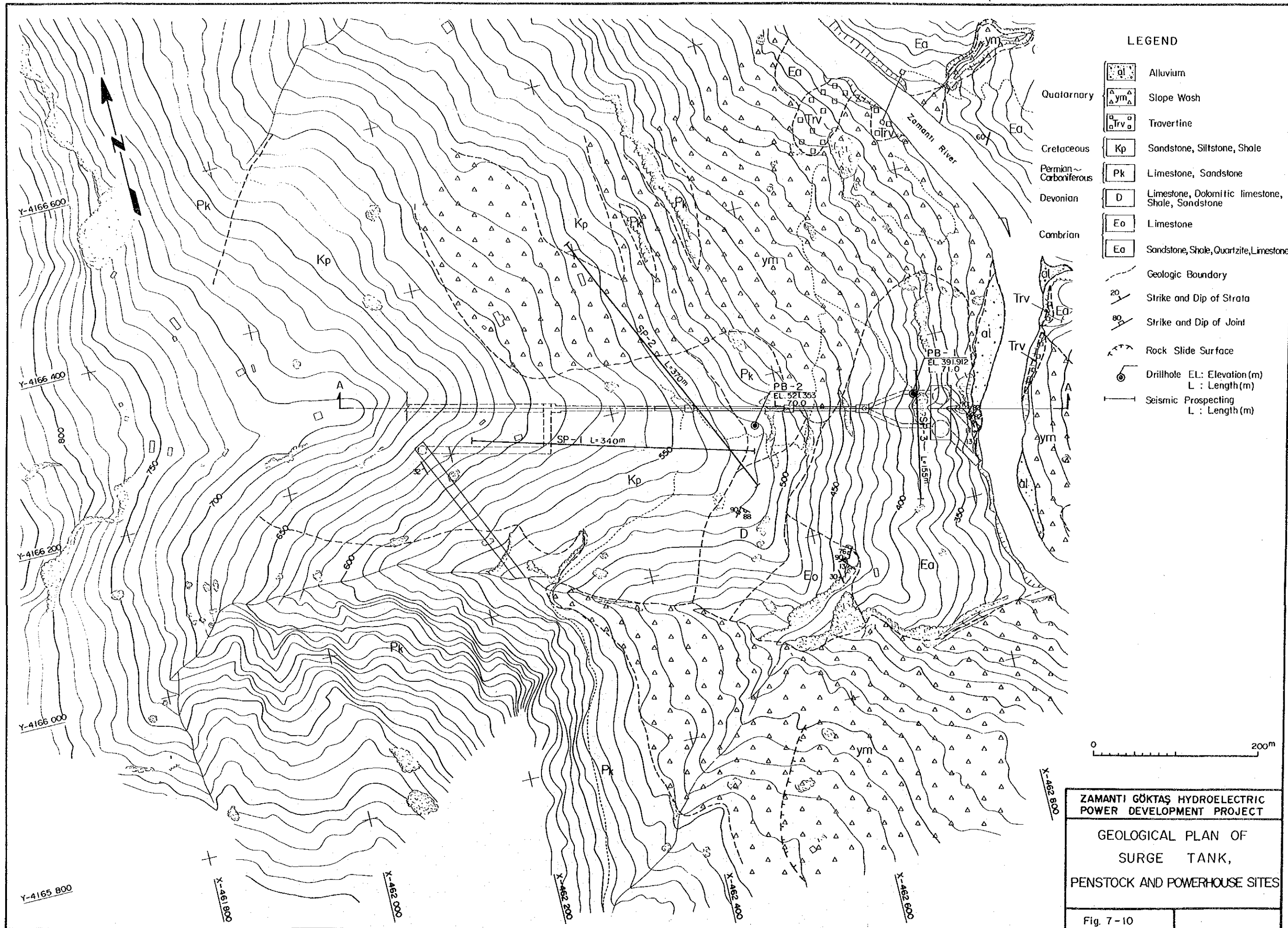2. Results of aerialphoto interpretation (1988) and geological mapping (1987, 1988) by JICA

0 2500m

ZAMANTI GÖKTAŞ HYDROELECTRIC POWER DEVELOPMENT PROJECT

GEOLOGICAL PLAN AND PROFILE
OF HEADRACE TUNNEL ROUTE

Fig. 7 - 9

7 - 59

LEGEND

|		
Quaternary	al	Alluvium
	ym	Slope Wash
	Trv	Travertine
Cretaceous	Kp	Sandstone, Siltstone, Shale
Permian~ Carboniferous	Pk	Limestone, Sandstone
Devonian	D	Limestone, Dolomitic limestone, Shale, Sandstone
Cambrian	Eo	Limestone
	Ea	Sandstone, Shale, Quartzite, Limestone

Geologic Boundary

20 Strike and Dip of Strata

80 Strike and Dip of Joint

Rock Slide Surface

Drillhole EL: Elevation (m) L : Length (m)

Seismic Prospecting L : Length (m)

ZAMANTI GÖKTAŞ HYDROELECTRIC POWER DEVELOPMENT PROJECT

GEOLOGICAL PLAN OF SURGE TANK, PENSTOCK AND POWERHOUSE SITES

Fig. 7-10

7 - 61

A — A

700 m

700 m

600

600

500

500

400

400

300

300

SP-1 Seismic Prospecting, Projection (40m down stream)

0.35km

2.2 km/s

3.7 km/s

Kp

Pk

D

Eo

ym

al

Ea

Zamanti River

ym

PB-2
EL. 521.353
L. 70. 0
Projection
(20m down stream)

PB-1
EL. 391.912
L. 71. 0
Projection
(20m down stream)

LEGEND

Quaternary

| al | Alluvium |
| ym | Slope Wash |

Cretaceous

| Kp | Sandstone, Siltstone, Shale |

Devonian·Permian~ Carboniferous

| Pk | Limestone, Sandstone |
| D | Limestone, Dolomitic limestone, Shale, Sandstone |

Cambrian

| Eo | Sandstone, Shale, Quartzite, Limestone |

Geologic Boundary

Ground Water Level

2.2km/s / 3.7km/s Seismic Primary Wave Velocity and Its Boundary

Drillhole

DRILLING LOGS

① Depth of Drillhole (m)
② Geological Log
③ R.Q.D = Rock Quality Designation (%)
    C.L. = Core Loss (%)
④ R.C. = Rock Classification
    W: Weathering 1 (Very Fresh)
                  5 (Strongly Weathered)
    H: Hardness 1 (Very Hard)
                5 (Soft)
    C: Interval of Cracks
                1 (Over 30cm)
                5 (Under 1 cm)
⑤ R.E. = Rock Evaluation
    Ⓖ Very Good
    Ⓔ Very Bad
⑥ qu = Unconfined Compression Strength of Core (kgf/cm²)
⑦ Lu = Lugeon Value (ℓ/m/min/10kgf/cm²)
    ( ): Converted Lugeon Value
⑧ W.T.(D) = Water Table in Drillhole during Drilling
⑨ W.T.(F) = Final Water Table (m)

Hole No. PB-1

Elevation : 391.912ᵐ
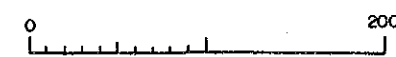Depth of Hole : 71.00ᵐ Angle from Horizontal : Vertical
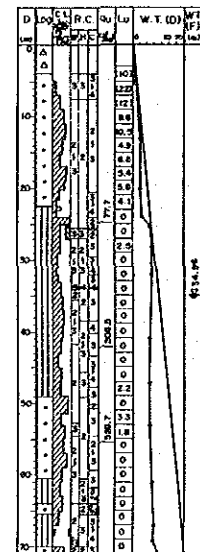
Hole No. PB-2

Elevation : 521.353ᵐ
Depth of Hole : 70.00ᵐ Angle from Horizontal : Vertical
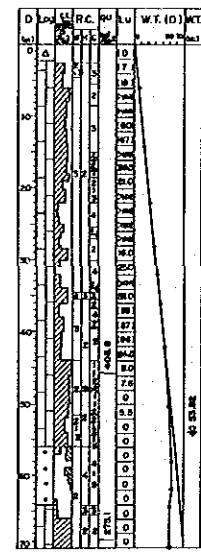
Legend of Geological Log

△	Slope Wash
	Sandstone
	Shale
	Limestone

ZAMANTI GÖKTAŞ HYDROELECTRIC
POWER DEVELOPMENT PROJECT

GEOLOGICAL PROFILE OF

SURGE TANK,

PENSTOCK AND POWERHOUSE SITES

Fig. 7-11

0   200m

7 - 63

7.7 In-situ Rock Tests at Dam Site

7.7.1 Introduction

In-situ tests were conducted with rocks inside exploratory adits at the Goktas dam site. These tests were carried out with the aims of determining various characteristics of bedrock such as coefficients related to deformation, cohesion (C), and angle of internal friction (ϕ).

The test items were ① plate bearing test, ② block shear test, and accessory laboratory compressive strength tests of concrete test pieces.

These tests were carried out by DSI and JICA teams using testing equipment owned by the DSI and based on the methods of testing in technical specifications prepared by the JICA Team. Performance of a part of the tests was carried out by the DSI Team after return of the JICA Team to Japan. Compressive strength tests on concrete test pieces were carried out at the DSI laboratory. The rock in the exploratory adits is ophiolite, which is of rock classifications broadly divided for deeper parts of the adits and parts slightly closer to the ground surface, 2B III and 2B IV.

7.7.2 Plate Bearing Test

(1) Selection of Test Locations

Locations for plate bearing tests were selected at parts deep inside the exploratory adits and at parts close to the ground surface. These tests were conducted at four points in DA-1, the exploratory adit at the right bank of the dam site, and three points at DA-2, the exploratory adit at the left bank. One of the four points at the right bank was selected at a place close to the ground surface which was different from the three other points tested ahead of it. The test locations are listed in Table 7-10).

Table 7-10   Location of Plate Bearing Tests

Test No.	Location (m)	Rock	Rock Classification	Direction of load
DA-1				
P-1	TD20.0	Ophiolite	2BIII: (b)	Vertical
P-2	TD40.5	ditto	2BIV : (c)	ditto
P-3	TD(B)2.1	ditto	2BIII: (b)	Horizontal
P-4	TD(B)4.0	ditto	2BIII: (b)	Vertical
DA-2				
P-1	TD16.3	Ophiolite	2BIV : (c)	Vertical
P-2	TD19.0	ditto	2BIV : (c)	ditto
P-3	TD(B)5.8	ditto	2BIV : (c)	ditto

(B):   Branch of adit.

Locations of the center line on DA-1 and DA-2 branches
are TD 29.0 m and TD 36.0 m from the entrances.

The geological conditions and rock evaluations of the places where
tests were performed are as described below.   The rock at the test
sites was ophiolite.

DA-1, P-1, TD 20.0 m : The rock is extremely dark blue-green and
exists partially calcite in places. Joint
dip is of 90 degrees in the direction from
upstream to downstream of the river, and
joint is observed to be at spacings 30 to
40 cm predominantly.   But as a whole the
rock itself is hard and the overall rock
evaluation is (b).

DA-1, P-2, TD 40.5 m : Part of the joints is of light brown color,
but the rock is a dark green-blue as a
whole, and is hard.   Joints exist at

spacings of 10 to 15 cm, but are tight. The overall rock evaluation is ⓒ.

DA-1, P-3, TD(B) 2.1 m: The rock is an extremely dark green-blue and has partial intercalations of calcite in the form of spots. Joints are developed at 30-cm spacings, but the rock is dense and hard. The overall rock evaluation is ⓑ.

DA-1, P-4, TD(B) 4.0 m: The rock is an extremely dark green-blue and is fresh and hard. Joints dip 90 deg in the direction of the dam axis with those at spacings of 25 to 30 cm predominant, but the rock as a whole is hard. The overall rock evaluation is ⓑ.

DA-2, P-1, TD 16.3 m and P-2, TD 19.0 m : The rock is an extremely dark blue-green in a wet condition, is fresh, and hard. There are tight joints at spacings of 3 to 15 cm distributed, and the overall evaluation of the rock is ⓒ.

DA-2, P-3, TD(B) 5.8 m: The rock is an extremely dark blue-green with partial intercalations of calcite in the form of spots. Joints are distributed at spacings of around 20 cm, but the rock is fresh and hard as a whole. The overall evaluation of the rock is ⓒ.

(2) Method of Testing

Plate bearing tests are conducted to judge coefficients related to deformation of bedrock. The modules of deformation (D), secant modulus of elasticity (E_s), tangential modules of elasticity (E_t), and creep factor (C_f) of the rock were determined by these tests. The tests were performed based on the loading diagram prescribed in the Technical Specifications to a maximum load of 65 kg/cm^2 using loading plates 30 cm in diameter and oil jacks 200 t in capacity.

The duration of the creep test was 6 hr under vertical load of 60 kg/cm^2.

The main pieces of equipment and devices used in the tests are as given in Table 7-11.

Table 7-11   Equipment and Devices for Plate Bearing Test

Equipment and Devices	Description
Oil Jack	Capacity 200t x 1 unit (Ram diameter 15.24 cm stroke 15 cm)
Pump	Hand control type, Max. oil pressure: 1,100kg/cm^2
Dial Gauge	6 sets (used for loading side and reaction side) Min. gauge: 1 x 10^{-3} mm, stroke 13 mm
Loading Plate	Diameter 30 cm x 2 set (used for loading side and reaction side)
Supporting Post	1 set (Steel box type with regulator)

7.7.3   Block Shear Test

(1)   Selection of Test Locations

For carrying out block shear tests, test locations each consisting of one set of four blocks were respectively selected at places of rock conditions considered to be suitable as dam foundations and representative of the geological conditions at the right and left banks.

The test locations were selected in a range of TD 13 to 20 m in DA-1, the *right-bank adit*, and TD 10 to 20 m in DA-2, the left-bank adit. Detailed test locations are as given in Table 7-12.

Table 7.12   Location of Block Shear Tests

Test No.	Location (m)	Rock	Rock Classification	Direction of Horizontal Load
DA-1				
BS-1	TD15.4	Ophiolite	2BIII: ⓑ	
BS-2	TD17.4	ditto	ditto	upstream to
BS-3	TD18.6	ditto	ditto	downstream
BS-4	TD19.9	ditto	ditto	
DA-2				
BS-1	TD10.8	Ophiolite	2BIV : ⓒ	
BS-2	TD12.0	ditto	ditto	upstream to
BS-3	TD13.5	ditto	ditto	downstream
BS-4	TD15.7	ditto	ditto	

(2)   Method of Testing

Block shear tests are performed to obtain the shear strength of rock (τ), and the cohesion (C) and angle of internal friction (ϕ) of the rock are obtained by the tests.

Testing was done based on the loading diagram prescribed in the Technical Specifications with vertical loads of N = 2 kg/cm², N = 4 kg/cm², N = 6 kg/cm², and N = 8 kg/cm² respectively applied by jack pressure through loading plates to four concrete blocks (60 x 60 cm) per set.   Further, in a condition of vertical displacement kept at D < 0.01 mm/20 min, shearing load of 0.5 kg/cm²/min was applied to the center of the bottom surface of the concrete block at a downward angle of 16.7 deg.   Shearing was done on horizontal surfaces of rock of 60 x 60 cm (A = 3,600 cm²) and concrete using this procedure.   The principal pieces of equipment and devices used in the tests are listed in Table 7-13.

In order to obtain the concrete strengths of test blocks, cylindrical specimens of concrete were made, and after curing in the field,

compression tests were performed to match the time of the in-situ tests.

Table 7-13 Equipment and Devices for Block Shear Test

Equipment & Devices	Description
Oil jack for vertical load	– Capacity 200t x 1 unit – Ram diameter 25.35 cm (A = 504.7 cm^2) – Jack stroke 18 cm
Pump of oil jack for vertical load	– Hand control type – Max. oil pressure: 396 kg/cm^2
Oil jack for diagonal	– Capacity 200t x 2 units – Ram diameter: 19.05 cm (A = 285 cm^2) – Jack stroke: 11 cm
Pump of oil jack for diagonal load	– Hand control type – Max. oil pressure 702 kg/cm^2
Dial gauges for measuring vertical and horizontal deformations	– 8 set (for vertical deformation 4 sets; for horizontal deformation 4 sets) – Min. gauge: 1 x 10^{-3} mm
Reaction plate for vertical load	– Dimension: 30 x 25 cm
Cover plate and roller for vertical load	– Dimension: 70 cm x 70 cm
Supporting post for vertical load	– 1 set (steel box type with regulator)

7.7.4 Results of Tests and Evaluations

The results and evaluations of plate bearing tests and block shear tests carried out in exploratory adits at the right- and left-bank of the dam site are as described below.

(1) Bearing Strength of Bedrock

It was ascertained by the load-deformation diagram of the plate bearing tests that rock classifications ⓑ and ⓒ both amply had bearing stress of not less than 65 kgf/cm^2. The relationship between load and deformation is roughly linear, with almost no proper-

ties indicating yielding that could be recognized, showing that the bedrocks in the exploratory adits at the right and left bank of the dam site are sound.

(2) Plate Bearing Tests

The results of plate bearing tests indicating the deformation characteristics of the bedrock are given in Table 7-14. The modulus of deformation (D) of the bedrock was determined for incremental loads of 15, 30, 45, and 60 kgf/cm^2, while secant modulus of elasticity (E_s) and tangential modulus of elasticity (E_t) were determined for the section of maximum load level at 20 to 65 kgf/cm^2. In case of the calculated value for testing being abnormally high in view of the condition of the bedrock seen in field reconnaissances, or when abnormalities were indicated in the relationships of load and deformation as well as of plastic deformation and elastic deformation, the test values were omitted.

Looking at the bedrock characteristic values in test results, the ratios of elastic and plastic deformations were 32 to 67 percent in case of rock classification of ⓑ and 30 to 95 percent in case of c . This indicates the bedrock to be sound and subjected to almost no influence of cracking.

Moduli of deformation were 107,700 to 132,100 kgf/cm^2 for classification of ⓑ and 39,900 to 103,100 kgf/cm^2 for ⓒ with 19,200 kgf/cm^2 of slightly low values, but generally speaking, it was shown that the bedrock had little deformability.

Tangential moduli of elasticity were 189,200 to 239,600 kgf/cm^2 with classification ⓑ and 57,500 to 167,700 kgf/cm^2 with ⓒ, very high moduli of elasticity, for bedrock of hard and favorable characteristics.

Regarding creep characteristics, creep deformation was very small with 0.010 to 0.015 mm for bedrock of classification ⓑ and 0.006 to 0.071 mm for classification ⓒ, and creep factor (C_f) was in a fairly broad range of 8 to 42 percent.

Convergence of the creep curve was generally within 6 hours although with part of classification ⓒ there were test results in which

creep deformation gradually increased continuously during the 6 hours.

(3) Block Shear Tests

The results of block shear tests are shown in Table 7-15.

The shear stresses (τ_r) of four block shear tests performed at the right-bank exploratory adit DA-1 were 35.3 to 52.3 kgf/cm^2. Meanwhile, compressive strengths (σ_c) of block concrete at the time of testing, estimated from the results of compression tests on concrete test pieces made when testing block concrete were 230 to 260 kgf/cm^2.

In case of estimating shear strength (τ_c) of concrete from σ_c, it is generally considered that τ_c is in the range of $\sigma_c/4$ to $\sigma_c/7$. On comparisons of shear strengths of concrete calculated in accordance with the above and shear stresses (τ_r) the results of block shear tests, the relationship of $\sigma_c/4 > \tau_r > \sigma_c/7$ was obtained for all four blocks. It can be considered from this that block shear stress and concrete shear strength were approximately the same.

The block shear stresses (τ_r) in case of tests in DA-2 at the left bank were τ_r = 16.0 - 25.0 kgf/cm^2. The compressive strengths of concrete in corresponding shear tests are estimated to have been σ_c = 345 - 350 kgf/cm^2. Estimating shear strength (τ_c) of concrete from this σ_c in the same manner as for DA-1 at the right bank, the relationship of $\tau_r < \tau_c$ was obtained for all four blocks. It may be considered from this that the bedrock had been sheared by a shear stress (τ_r) lower than the shear strength (τ_c) of the block concrete.

On the other hand, the test results obtained at DA-1 and DA-2 were low as a whole as judged by deformation characteristics of bedrock obtained in plate bearing tests and visual inspections, and it is though that shear strength (τ) of the bedrock is greater than indicated by test results.

Based on the foregoing, since it may be considered that with regard to block shear at DA-1 shear stress (τ_r) and concrete shear strength

(τ_c) are of roughly identical values, it is estimated that shearing had occurred with block concrete that had not attained the required strength.

In case of DA-2, since shear stress (τ_r) is extremely low compared with shear strength (τ_c) of block concrete, it is estimated that successive loosening had occurred in the bedrock for some reason and the bedrock had been sheared as if peeled off on being subjected to shearing load.

In view of the above, the shear strength of the bedrock at the Goktas dam site was estimated employing Fig. 7-12 which was prepared based on the results of many bearing tests and shear tests carried out in the past and shows the relationships the bedrock classifications and the deformation characteristics of the bedrock, and bedrock classification and shear strength characteristics (C, ϕ).

That is at upper part of Fig. 7-12, bedrock classifications are shown on the abscissa, with the relationship of modulus of elasticity (E_t) and modulus of deformation (D) on the ordinate. On plotting the respective average values of tangential moduli of elasticity and moduli of deformation for bedrocks of classifications ⓑ and ⓒ, the bedrock classification location of B for ⓑ, and an intermediate point between C_H and B for ⓒ were obtained.

Plotting these locations respectively at the bedrock classification locations at the lower part of Fig. 7-12, the C and ϕ values for shear strength $\tau = C + \sigma \tan \phi$ were obtained on the ordinate.

As results of the above, values of $\tau = 50 + \sigma \tan 60°$ in case of bedrock classification ⓑ and $\tau = 40 + \sigma \tan 55°$ for classification ⓒ were obtained as shown in Fig. 7-13. These values are judged to be in correspondence with the bedrock as observed visually in the field.

Although various problematic points remain regarding the results of these tests, it may be said that much fundamental data have been obtained for making a comprehensive evaluation of bedrock at the Goktas dam site.
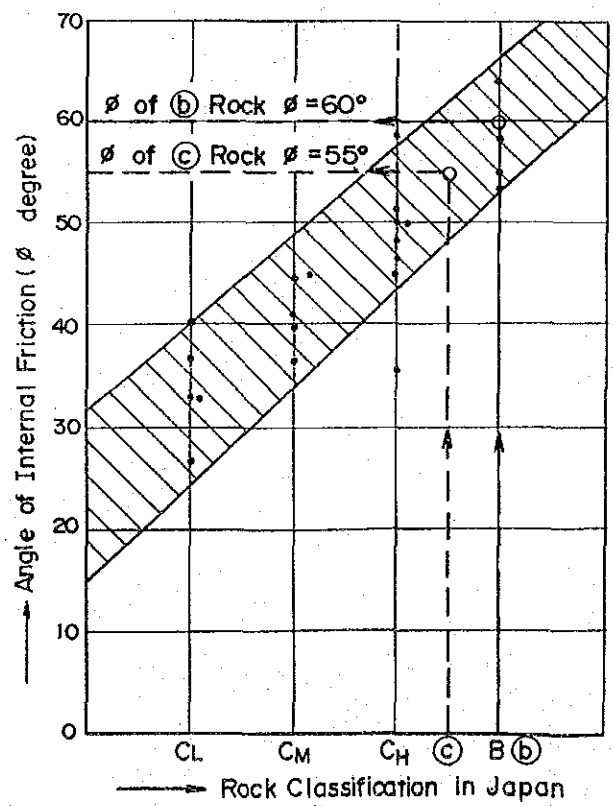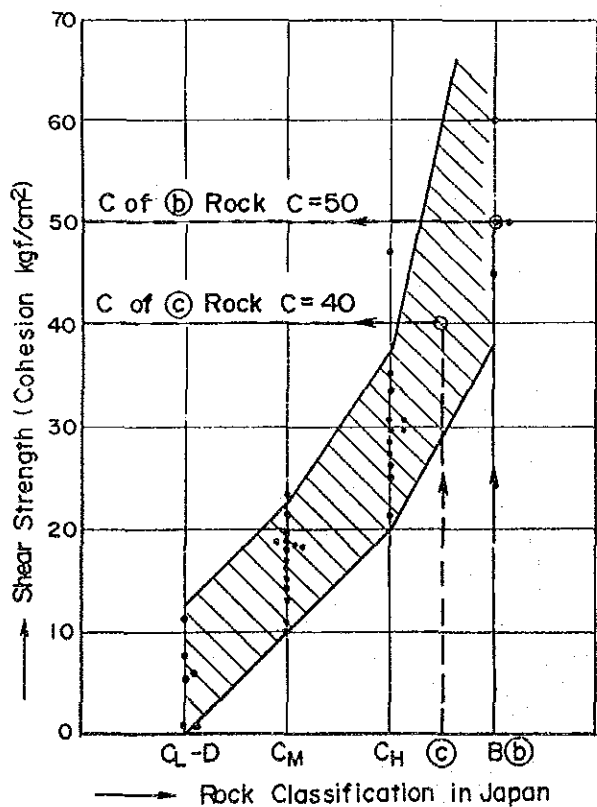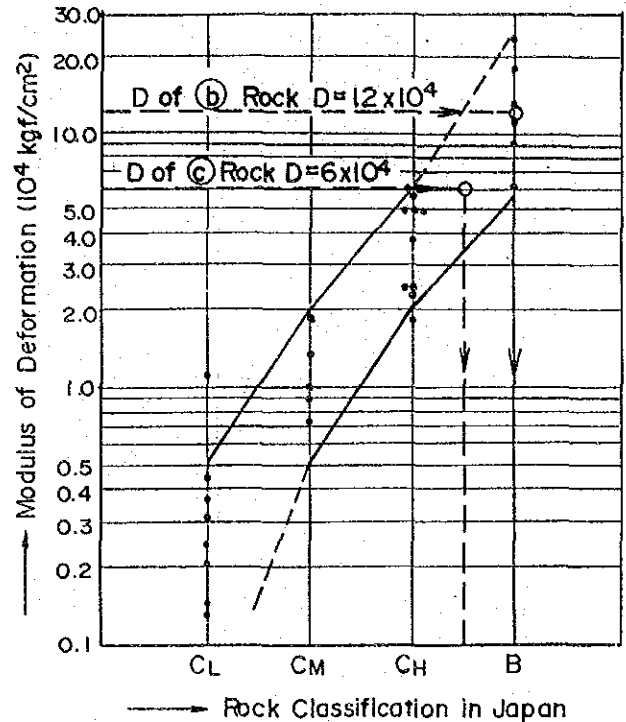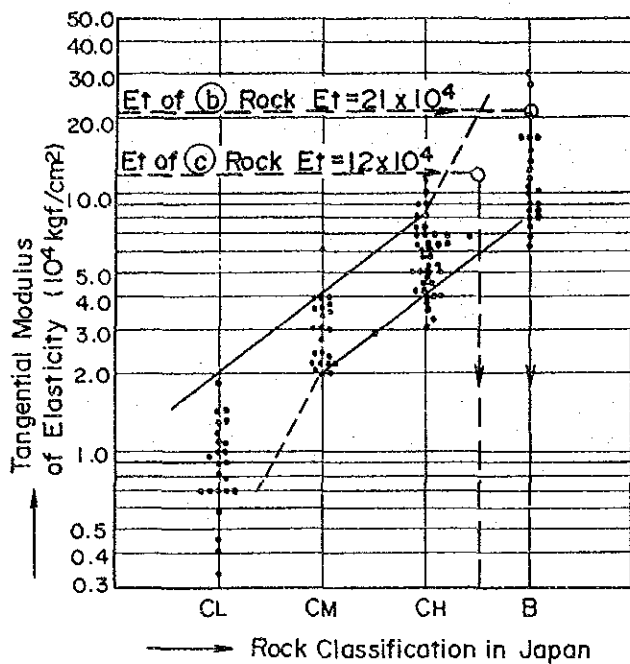
Table 7·14   Results of Plate Bearing Test

Adit	Test No.	Location (m)	Rock Classification	Maximum Deformation ; Σδ (mm)	Final Deformation ; Σδp (mm)	Modulus of Deformation ; D (kgf/cm²)	Secant Modulus of Elasticity ; Es (kgf/cm²)	Tangential Modulus of Elasticity ; Et (kgf/cm²)	Creep Defromation ; δc (mm)	Creep Factor ; Cf (%)
DA-1	P-1	TD. 20.0	Invert	2 BⅢ; ⑤	0.064	0.021	-	-	-	-	-
			Crown	ditto	0.151	0.094	107,700	239,500	189,200	0.010	19
	P-2	TD. 40.5	Invert	2 BⅣ; ○	0.199	0.120	81,200	163,500	137,400	0.006	8
			Crown	ditto	0.052	0.036	-	-	-	-	-
	P-3	TD(B)2.1	Left wall	2 BⅢ; ⑤	0.222	0.164	123,300	207,500	192,000	0.011	18
			Right wall	ditto	0.162	0.094	131,000	216,400	220,600	0.015	26
	P-4	TD(B)4.0	Invert	2 BⅢ; ⑤	0.136	0.094	132,100	306,900	239,600	0.010	25
			Crown	ditto	0.147	0.116	-	-	-	-	-
DA-2	P-1	TD. 16.3	Invert	2 BⅣ; ⓒ	0.432	0.383	-	-	-	-	-
			Crown	ditto	0.320	0.220	56,400	137,200	126,400	0.017	17
	P-2	TD. 19.0	Invert	2 BⅣ; ⓒ	0.156	0.081	103,100	189,800	167,700	0.029	41
			Crown	ditto	0.663	0.525	39,900	92,900	120,700	0.071	42
	P-3	TD(B)5.8	Invert	2 BⅣ; ⓒ	0.883	0.593	19,200	46,400	57,500	0.027	8
		Average ⑤ class rock					120,000	240,000	210,000		
		Average ⓒ class rock					60,000	130,000	120,000		

Table 7-15　Results of Block Shear Test

Adit	Block Number	Location (m)	Rock Classification	① Vertical Load ;N (kgf/cm²)	② Compressive Strength of Concrete Block ;σ_c (kgf/cm²)	③ Vertical Stress of Shear Plane ;σ (kgf/cm²)	④ Shear Stress ;τ_r (kgf/cm²)	⑤ Shear Stress of Concrete ;τ_c (kgf/cm²)	Remarks
DA-1	BS-1	TD 15.4		2	230	12.6	35.3	58 ~ 33	$\frac{\sigma_r}{4} > \tau_r > \frac{\sigma_r}{7}$
	BS-2	TD 17.4	2BⅢ:◎	4	240	14.6	35.3	60 ~ 34	ditto
	BS-3	TD 18.6		6	250	21.7	52.3	63 ~ 36	ditto
	BS-4	TD 19.9		8	260	23.3	51.0	65 ~ 37	ditto
DA-2	BS-1	TD 10.8		2	345	8.2	20.7	86 ~ 49	$\tau_r < \tau_c$
	BS-2	TD 12.0	2BⅣ:◎	4	350	8.8	16.0	88 ~ 50	ditto
	BS-3	TD 13.5		6	350	12.9	23.1	88 ~ 50	ditto
	BS-4	TD 15.7		8	350	15.5	25.0	88 ~ 50	ditto

Fig. 7-12 Relation Between Rock Classification and Deformation or Shear Strength

Tangential Modulus of Elasticity (10^4 kgf/cm²)

Et of ⓑ Rock Et = 21 x 10^4

Et of ⓒ Rock Et = 12 x 10^4

Rock Classification in Japan

Modulus of Deformation (10^4 kgf/cm²)

D of ⓑ Rock D = 12 x 10^4

D of ⓒ Rock D = 6 x 10^4

Rock Classification in Japan

Shear Strength (Cohesion kgf/cm²)

C of ⓑ Rock C = 50

C of ⓒ Rock C = 40

Rock Classification in Japan

Angle of Internal Friction (ø degree)

ø of ⓑ Rock ø = 60°

ø of ⓒ Rock ø = 55°

Rock Classification in Japan

Note: Above figures made by CENTRAL RESEARCH INSTITUTE OF ELECTRIC POWER INDUSTRY in Japan.

Fig. 7-13   Results of Block Shear Test and Estimated Shear Strength
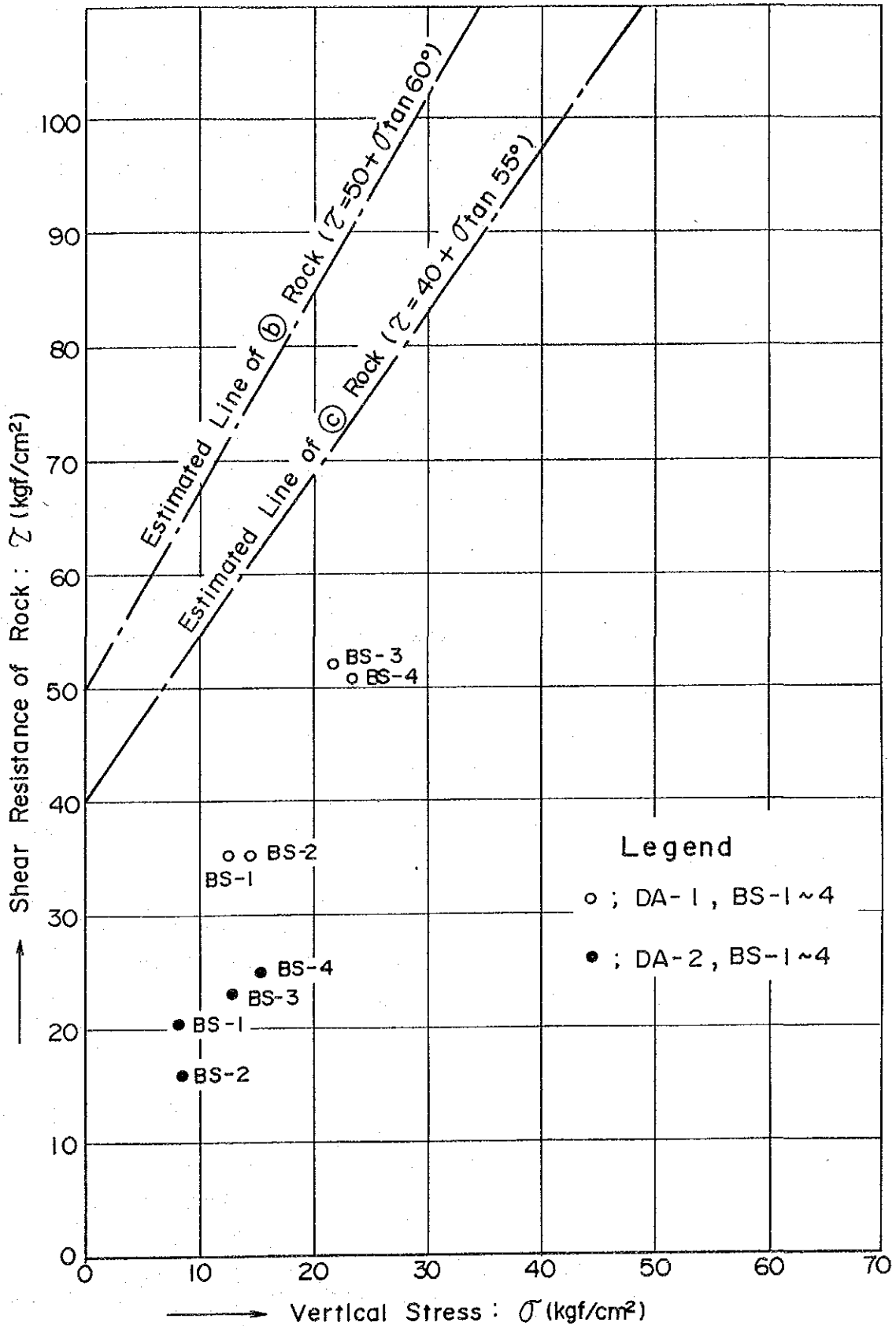
7-8 Geophysical Prospecting of Powerhouse Site

7-8-1 Introduction

Seismic prospecting (refraction method) was carried out by the DSI for the purpose of exploring the geological situation in the vicinity of the powerhouse and penstock line in a range of approximately 50 m deep from the ground surface.

The results of the exploration are described below.

7.8.2 Selection of Prospecting Location

(1) Selection of Prospecting Location

The prospecting location was the right-bank slope of the Zamanti River of gradient of 30 to 50 degrees where the powerhouse and penstock line are planned.

There were three seismic prospecting lines, two of them are along the penstock line and one is in the vicinity of the powerhouse.

PS-1 and PS-2 are prospecting lines along the penstock line laid out at the ridge of comparatively gentle slope spread out above a specific height of approximately 200 m from the bed of the Zamanti River.

PS-3 was laid out at the bottom part of the penstock line and near the powerhouse at a steep slope.

Fig. 7-14 is a location map of the seismic prospecting lines and drillholes, while Table 7-16 gives the coordinates and elevations of the prospecting lines and the drillholes.

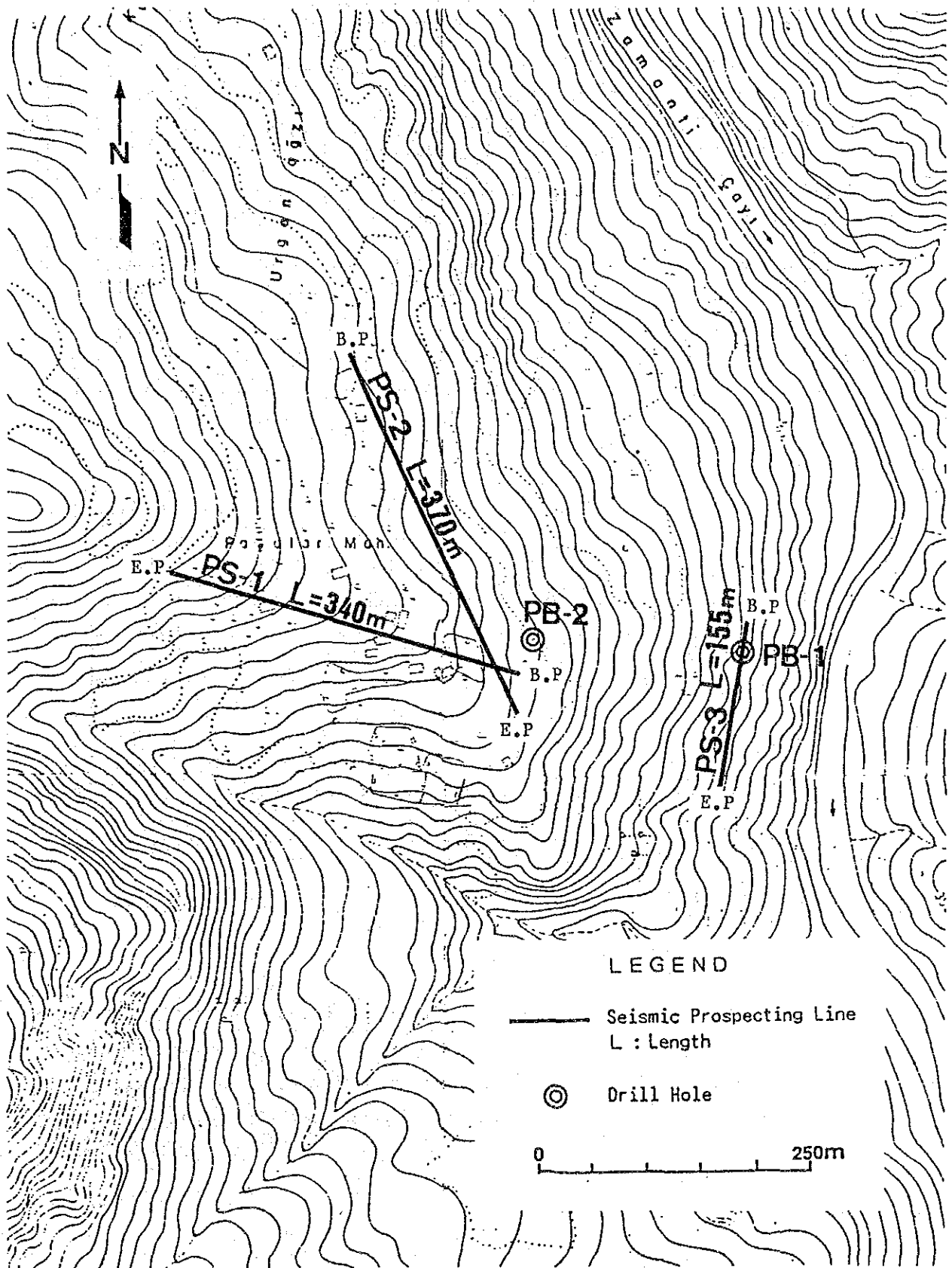Fig. 7-14   Location Map of Seismic Prospecting Line

LEGEND

——— Seismic Prospecting Line
L : Length

◎ Drill Hole

0 ————————— 250m

Table 7-16 List of Location of Seismic Prospecting Line and Drillhole

Line No. and Drillhole No.	Coordinate		Elevation (m)
	X	Y	
PS-1 (B.P.; Beginning Point)	4,166,116.2	462,556.3	520.1
PS-1 (E.P.; Ending Point)	4,166,211.7	462,229.0	615.5
PS-2 (B.P.)	4,166,410.5	462,395.2	555.3
PS-2 (E.P.)	4,166,075.8	462,550.1	520.0
PS-3 (B.P.)	4,166,163.6	462,767.0	391.8
PS-3 (E.P.)	4,166,012.2	462,737.5	389.5
PB-1	4,166,135.9	462,758.6	391.9
PB-2	4,166,145.9	462,565.3	521.4

(2) Quantity of Seismic Prospecting

The quantity of seismic prospecting was the three prospecting lines for a total length of 865 m. The details are given in Table 7-17.

Table 7-17 Quantity of Seismic Prospecting

| Line	Length	Location
PS-1	340 m	Penstock Site
PS-2	370 m	Penstock Site
PS-3	155 m	Penstock and Power Plant Site
Total	865 m	3 Lines

7.8.3 Prospecting Method

(1) Outline of Seismic Prospecting Method

Seismic prospecting is an exploration technique consisting of arti-
ficially generating elastic waves near the ground surface, measuring
the elastic waves at the ground surface, and revealing the
underground geological situation through analyses of the measurement
data.

This prospecting method is frequently used as one of the effective techniques for engineering geologic investigations.

A conceptual drawing of seismic prospecting method is shown in Fig. 7-15.

Fig. 7-15   Diagram of Seismic Prospecting Method

a) Measurement

b) Refraction Paths and Travel Time
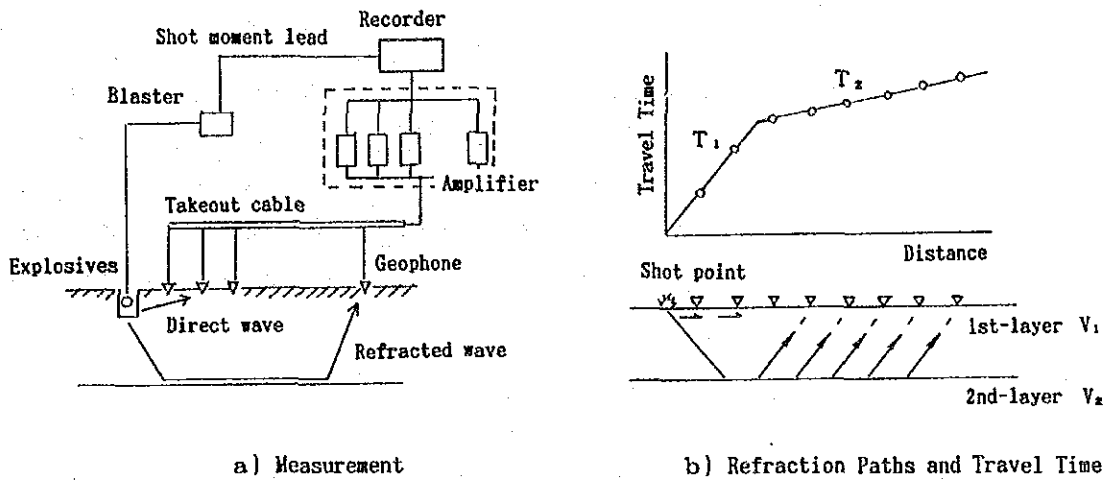
(2) Measurement

Instruments: Measurement was made with the instruments listed in Table 7-18.

Table 7-18   List of Seismic Prospecting Instrument

Name	Specification	Note
Amplifier	No. of channels: 12 Frequency 5-200 Hz	ELECTRO-TECHNICAL LABS. (PRA-2-12)
Recorder	No. of channels: 32	ELECTRO-TECHNICAL LABS. (ER64)
Geophone	Frequency 7.5 Hz	–
Blaster	Capacitor discharge type Shot mark circuit	ELECTRO-TECHNICAL LABS. (BC2-3)
Takeout cable	12 take outs	

o   Receiving Point: Geophones were set underground to attenuate
                       noises such as of wind.

Geophone interval differed depending on the seismic prospecting
line, but was the same on each prospecting line.   The geophone
interval of each prospecting line is given in the table below.

Line Name	PS-1	PS-2	PS-3
Geophone Interval	26 m	28.5 m	26 m

o   Shot Point: There were two shot points to each prospecting line
                  with their locations at the starting and end points
                  of the prospecting line.   Dynamite was used as the
                  seismic energy with blasting conducted at the bot-
                  toms of holes approximately 1 m in depth to generate
                  elastic waves.

(3) Analysis Method

There are various methods for analysis in seismic prospecting, but
in this study Hagiwara's analysis method and its expanded version
which have been used most widely in engineering geologic investiga-
tions were adopted.

However, in case a low-velocity layer exists underground, the depth
of that layer is not detectable with the above-mentioned method
which regards underground structure as discrete velocity-layers.   In
such case, analysis of the travel-time curve assuming a Mirage layer
was done.

Hagiwara's method will be given in an appendix.

7.8.4   Results and Evaluations

(1) Results

Time-distance plots and seismic profiles are shown in Figs. 7-16 to
7-18.

As a result of analyses, the subterranean structure at the investi-
gation site was classified as consisting of 2 to 4 velocity layers.

The velocity-layer classifications for the individual prospecting lines and the velocities for each layer are given in Table 7-19.

Table 7-19   Classification of Velocity Layer

Line	1st Layer	2nd Layer	3rd Layer	Basement
PS-1	0.75 km/s	2.2 km/s	–	3.7 km/s
PS-2	0.85 km/s	2.2 km/s	2.0 km/s	3.7 km/s
PS-3	0.75 km/s	–	–	3.7 km/s

The velocity layers at the respective prospecting lines are described below.

o   PS-1 Line

The velocity structure at this line consists of three layers according to the velocites analyzed.

The velocity of the first layer is 0.75 km/s. The thickness of the layer is 4 to 12 m, being thinner at the middle part of the line and thicker near the beginning and end points.

The velocity of the second layer is 2.2 km/s. The thickness of the layer is 20 to 45 m, being a maximum at the beginning point of the line and decreasing gradually toward the end point.

The third layer is the seismic basement and the velocity is 3.7 km/s.

o   PS-2 Line

There existed the only one unilateral travel-time curve at this line.   Sufficient analysis results could not be expected from this travel-time curve.   Therefore, in determing the velocities and velocity boundaries, the analysis results of PS-1 line, which intersected PS-2 line, were referred to.   Further, since a considerable amount of estimations and assumption were needed in analyzing the whole line from the unilateral travel-time curve, the range of analysis was kept to the vicinity of the shot point.

The velocity structure at this line consists of four layers according to the velocities analyzed.

The velocity of the first layer is 0.85 km/s and the thickness of the layer is from 7 to 11 m.

The velocity of the second layer is 2.2 km/s and the thickness of the layer is from 42 to 49 m.

The third layer was estimated to be of lower velocity than the overlying layer as judged from the seismogram. The distribution of this layer was found at this line only and could not be seen at other lines. This layer ranges near 200 to 300 m in distance from the beginning point of the line.

Since the velocity of low-velocity layer can not be analyzed in the travel-time curve, the velocity is assumed here to be 2 km/s. The depth was analyzed considering the layer to be a Mirage layer, but the depth could be determined for only one point because of the unilateral travel-time curve. Consequently, the velocity boundary which was passing through the calculated depth point was drawn to be roughly parallel to the ground surface. The thickness of the layer is estimated as 38 m from the gap (60 ms) in travel time.

The fourth layer is the seismic basement and the velocity is 3.7 km/s.

o PS-3 Line

The velocity structure at this line consists of the two layers, namely, surface layer and seismic basement.

The intermediate velocity layers seen at the other lines could not be detected at this line.

The velocity of the first layer is 0.75 km/s. The layer thickness varies between 2 and 11 m, with it being extremely thin at gully.

The second layer is the seismic basement and the velocity is 3.7 km/s.

(2) Evaluation

The analysis results of seismic prospecting were examined to ascertain the accuracy through comparisons with surface geological investigations and drilling exploration. A velocity boundary does not necessarily coincide with the geologic boundary. This is because the velocity boundary is analyzed based on differences in physical properties. Besides this, complex geologic structure or measuring condition may also cause incompatibility of the boundary between geology and geophysics.

On comparison of the analysis results in this investigation with drilling data, the depth of the seismic basement coincided roughly with the depth of fresh rock distribution confirmed in drilling. However, a considerable difference was seen in the distribution of the first layer with the geologic boundary according to drilling.

The reason for this is that the geophone interval might be slightly longer, considering the following two phenomena.

o The first layer was analyzed to be thicker than in drilling.
o Its velocity was somewhat high for a talus deposit in dry condition.

Thereupon, assuming that the geophone interval was shorter than it really was, the travel-time curve of the first layer was modified so that the thickness of the first layer would coincide with the drilling data and reanalyses were attempted by using the new travel-time curve.

It is thought that the reanalysis profiles express the velocity structures of the area investigated more accurately. The reanalysis profiles for each line are shown in Fig. 7-19, and comparisons of results of the seismic analysis and drilling data in Tables 7-20 to 7-22.

The velocity layers at the respective lines based on the results of reanalyses are described below.

o PS-1 Line

The drillhole used for comparisons was PB-2, the location of which is at a distance of 31 m from the beginning point of the line.

The velocity of the first layer is 0.35 km/s. The thickness of the layer is from 1 to 4 m.

The velocity of the second layer is 2.2 km/s. The thickness of the layer becomes slightly thicker compared with the analysis results mentioned in (1) and is 23 to 48 m.

The third layer is the seismic basement and the velocity is 3.7 km/s.

o PS-2 Line

The drillhole used for comparisons was PB-2, the location of which is at a distance of 71 m from the end point of the line.

The velocity of the first layer is 0.35 km/s and the thickness of the layer is from 2 to 5 m.

The velocity of the second layer is 2.2 km/s and the thickness of the layer is from 47 to 50 m.

The third layer is low velocity layer and the velocity is assumed as 2.0 km/s. The thickness of the layer is 38 m. If the assumed velocity is made lower, the layer thickness becomes smaller.

The fourth layer is the seismic basement for this line and the velocity is 3.7 km/s.

o PS-3 Line

The drillhole used for comparisons was PB-1, the location of which is on the line.

This line was of a two-layers structure according to analysis of the travel-time curves. However, drilling data indicates a three-layers structure consisting of talus, weathered rock and fresh rock. Thereupon, the reanalysis of three-layers structure including the blind zone was done to coincide with the drilling data.

The velocity of the first layer is 0.4 km/s. The layer thickness is 5 m at maximum with no layer at gully.

The second layer was a blind layer so that an assumption of velocity was necessary. The velocity is assumed in 0.8 km/s to coincide with drilling data. The thickness of the blind zone is calculated in maximum. The thickness of the layer is 5 m at maximum with the layer lacking at gully.

The third layer is the seismic basement and the velocity is 3.7 km/sec.

Table 7-20   PS-1 Seismic Analysis and Drilling Data

Drilling Data PB-2			Seismic Profile (Fig. 7-16)		Reanalysis Profile (Fig. 7-19)	
Layer	Thickness (m)	Geology	Thickness (m)	Velocity (km/s)	Thickness (m)	Velocity (km/s)
1st	2.25	Talus deposit	4 - 12	0.75	1 - 4	0.35
2nd	41.75	Slightly oxidized rock	20 - 45	2.20	23 - 48	2.20
Basement	-	Fresh rock	-	3.70	-	3.70

Table 7-21   PS-2 Seismic Analysis and Drilling Data

Drilling Data PB-2			Seismic Profile (Fig. 7-17)		Reanalysis Profile (Fig. 7-19)	
Layer	Thickness (m)	Geology	Thickness (m)	Velocity (km/s)	Thickness (m)	Velocity (km/s)
1st	2.25	Talus deposit	7 - 11	0.85	2 - 5	0.35
2nd	41.75	Slightly oxidized rock	42 - 49	2.20	47 - 50	2.20
3rd	-	-	38	2.00	38	2.00
Basement	-	Fresh rock	-	3.70	-	3.70

Table 7-22   PS-3 Seismic Analysis and Drilling Data

Drilling Data PB-1			Seismic Profile (Fig. 7-18)		Reanalysis Profile (Fig. 7-19)	
Layer	Thickness (m)	Geology	Thickness (m)	Velocity (km/s)	Thickness (m)	Velocity (km/s)
1st	4.00	Talus deposit	2 - 11	0.75	0 - 5	0.40
2nd	3.50	Weathered rock	-	-	0 - 5	0.80
Basement	-	Fresh rock	-	3.70	-	3.70

(3)   Investigation Results of the DSI

The DSI has carried out analysis work besides field works.   The delay-time and ray-tracing method was used for analysis.   The technique is given in Computer Analysis of Seismic Refraction Data published by the U.S. Department of the Interior, Bureau of Mines. (Report of Investigation 7595, US Dept. of the Interior, Bureau of Mines, 1972).
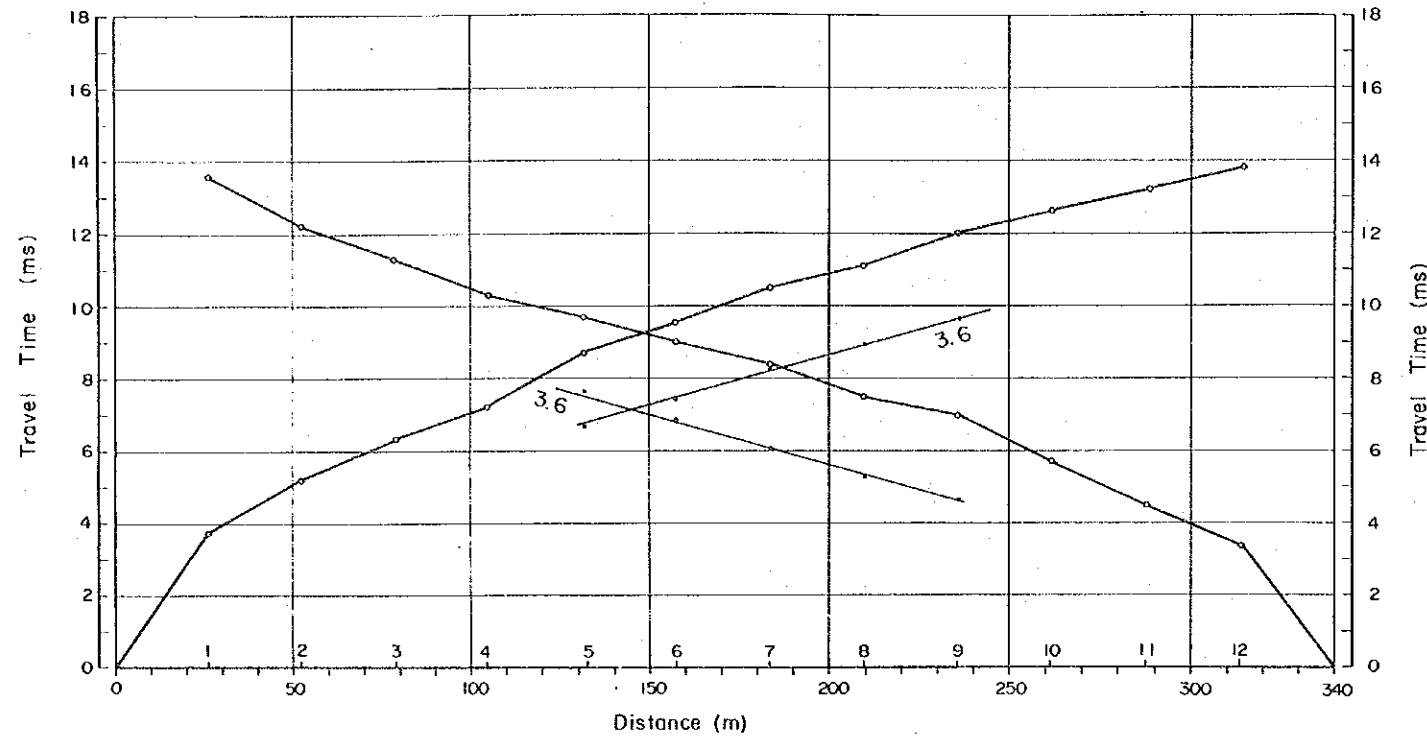
On comparison of the analysis results obtained by the DSI and the JICA Team, although there was a fair degree of agreement, they were not completely the same. This is thought to have been due to the differences in the analysis methods respectively used and in the interpretations by the analyzers.

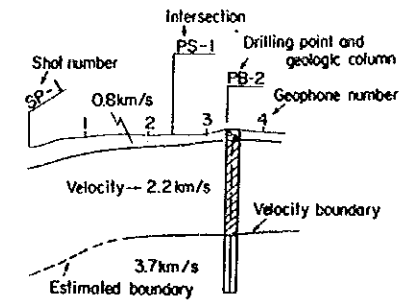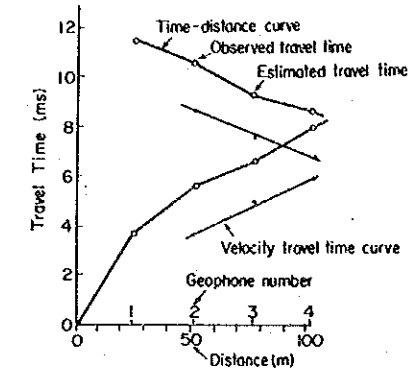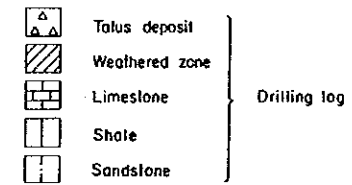The results of the analyses performed by the DSI will be given in an appendix.

PS-I TIME-DISTANCE PLOT

PS-I SEISMIC PROFILE

LEGEND

ZAMANTI GÖKTAŞ HYDROELECTRIC POWER DEVELOPMENT PROJECT

PS-I TIME-DISTANCE PLOT

AND SEISMIC PROFILE

Fig. 7-16

7-91

PS-2   TIME – DISTANCE PLOT

Travel Time (ms) / Distance (m)

(axis values: 22, 20, 18, 16, 14, 12, 10, 8, 6, 4, 2, 0)

Distance (m): 0, 50, 100, 150, 200, 250, 300, 350, 370

Geophone numbers: 1 2 3 4 5 6 7 8 9 10 11 12

LEGEND

Travel Time (ms)

Time-distance curve
Observed travel time
Estimated travel time

Velocity travel time curve

Geophone number

Distance (m)

Intersection

Shot number
PS-1
Drilling point and geologic column

SP-1
0.8km/s
PB-2
Geophone number

1 2 3 4

Velocity—2.2km/s

Velocity boundary

3.7km/s

Estimated boundary

	Talus deposit	
	Weathered zone	
	Limestone	Drilling log
	Shale	
	Sandstone	

PS-2   SEISMIC PROFILE

Elevation (m): 600, 580, 560, 540, 520, 500, 480, 460, 440, 420, 400, 380

SP-1

PB-2
Projection
Offset 43.2ᵐ

PS-1

SP-1

0.85km/s

2.2km/s

2.2km/s

2.0km/s ?

3.7km/s ?

3.7km/s ?

Distance (m): 0, 50, 100, 150, 200, 250, 300, 350, 370

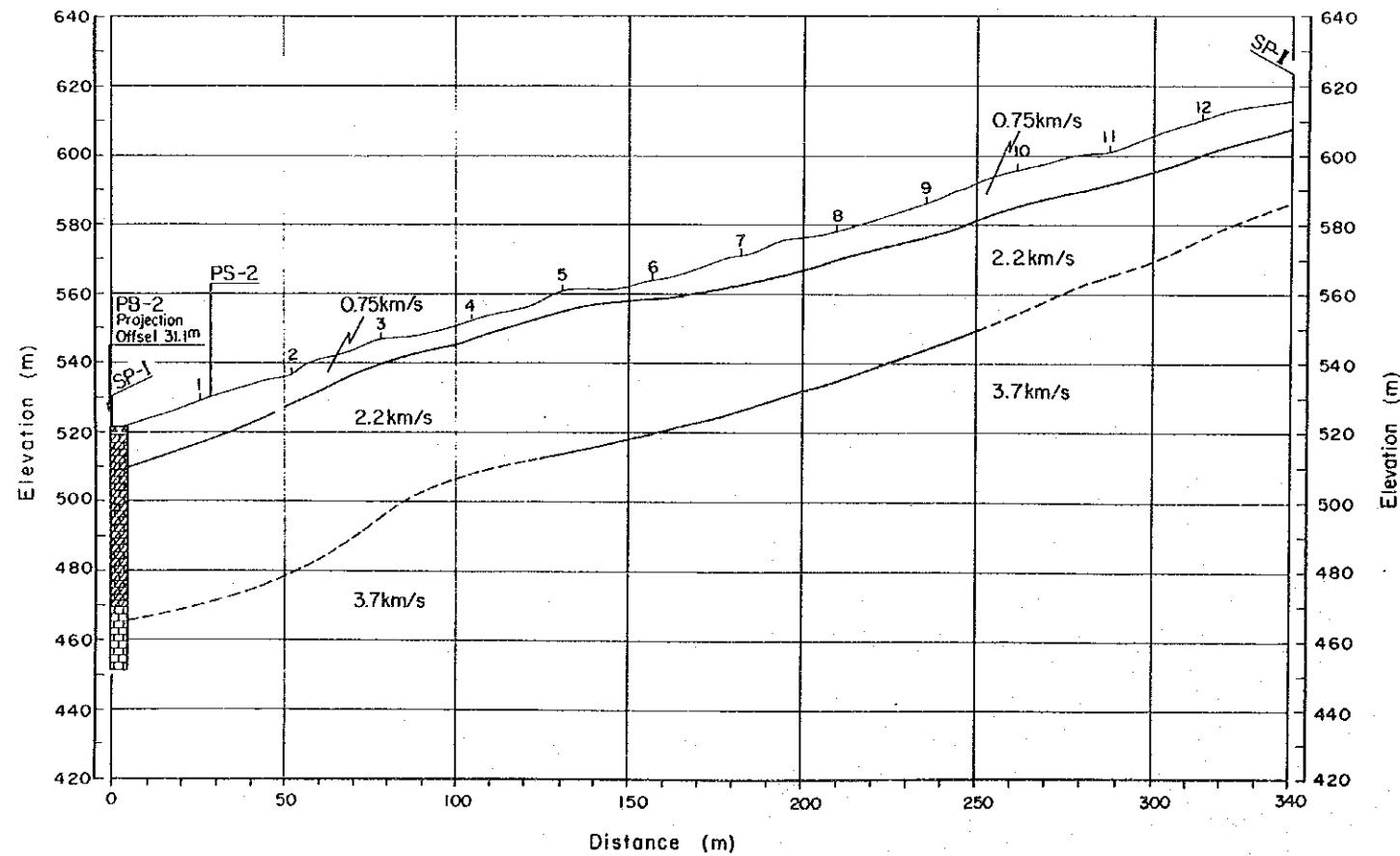Geophone numbers: 1 2 3 4 5 6 7 8 9 10 11 12
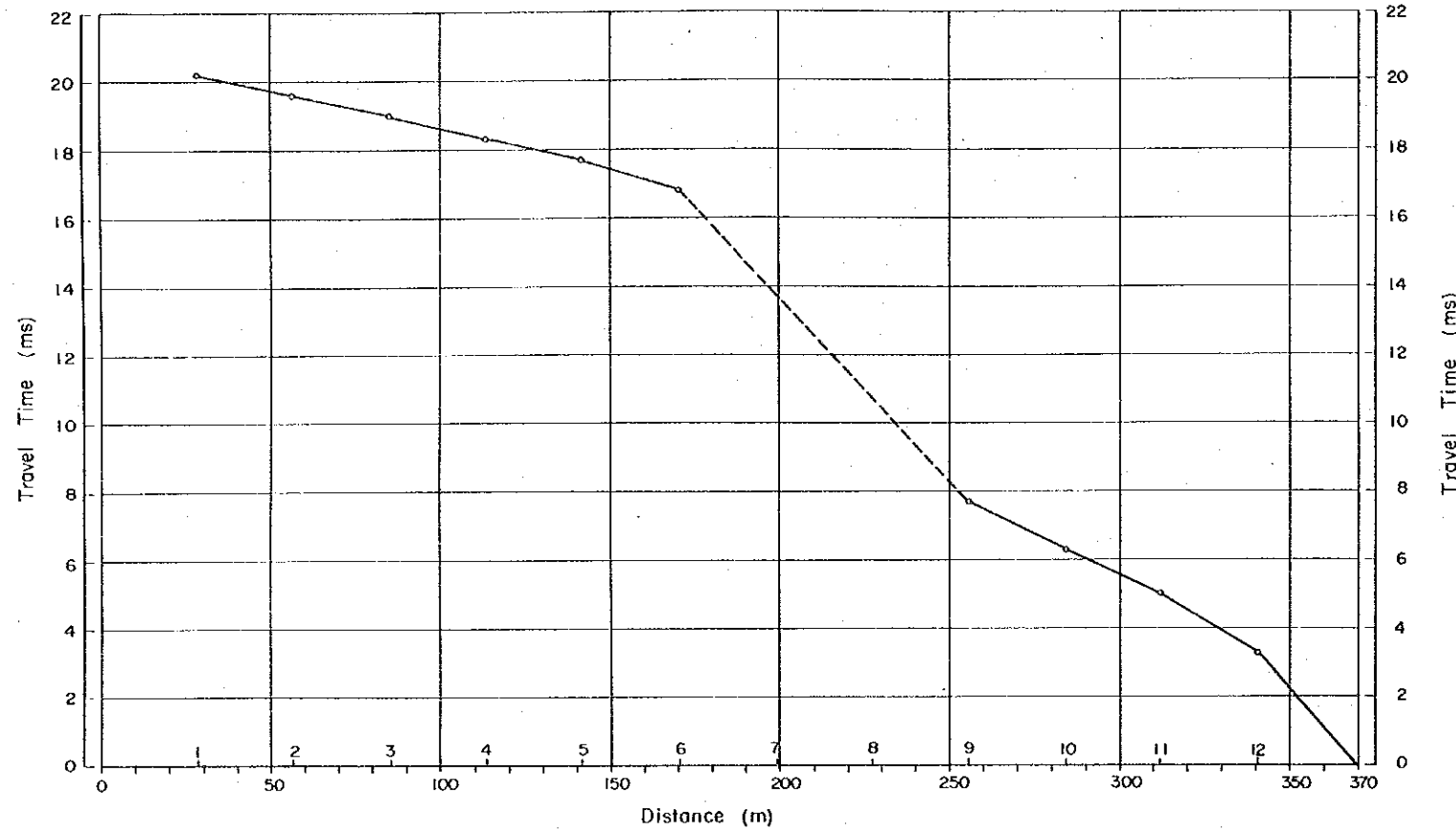
PS-3 TIME-DISTANCE PLOT

PS-3 SEISMIC PROFILE
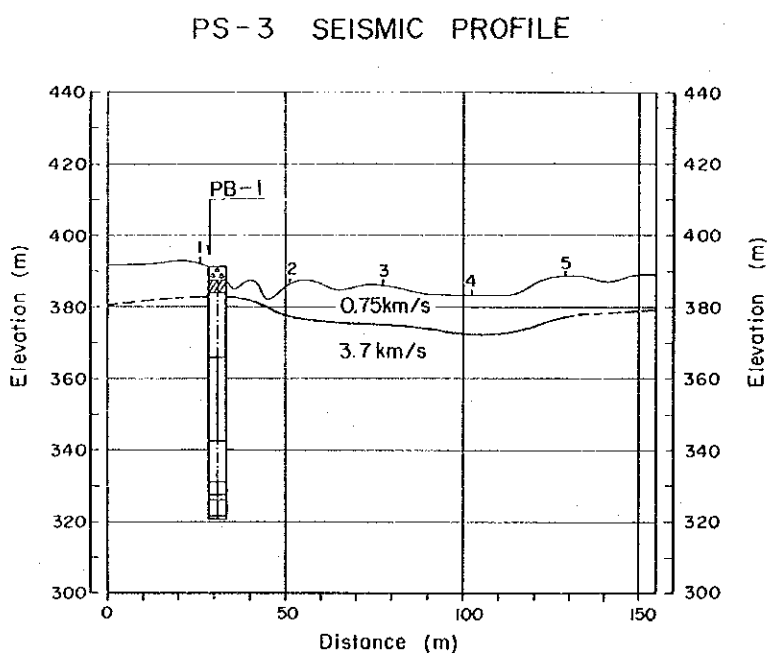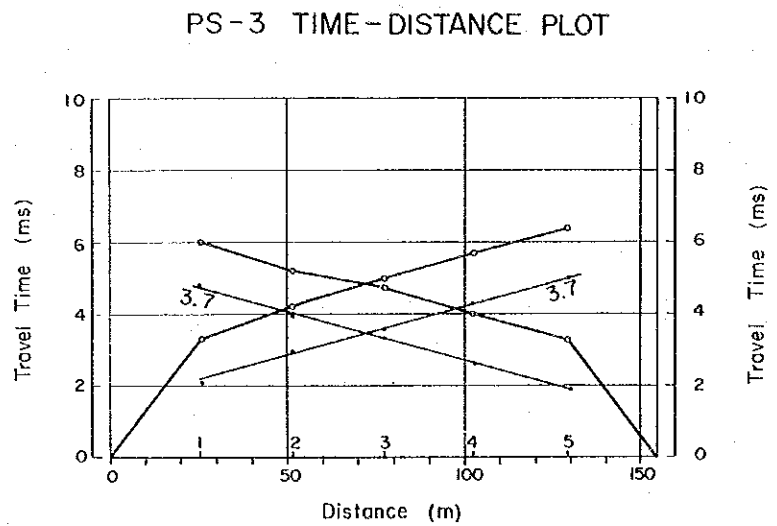
ZAMANTI GÖKTAŞ HYDROELECTRIC
POWER DEVELOPMENT PROJECT

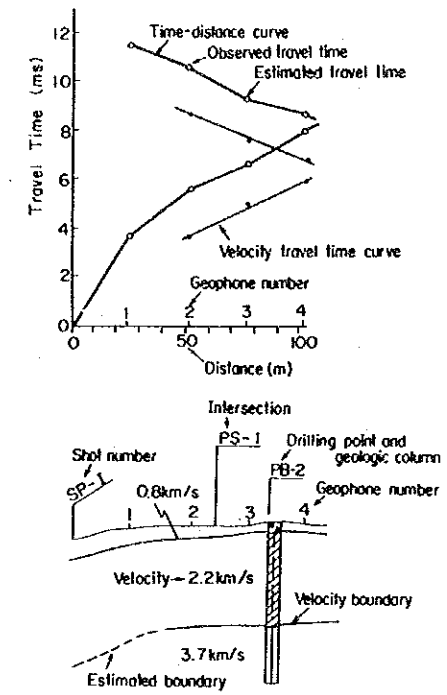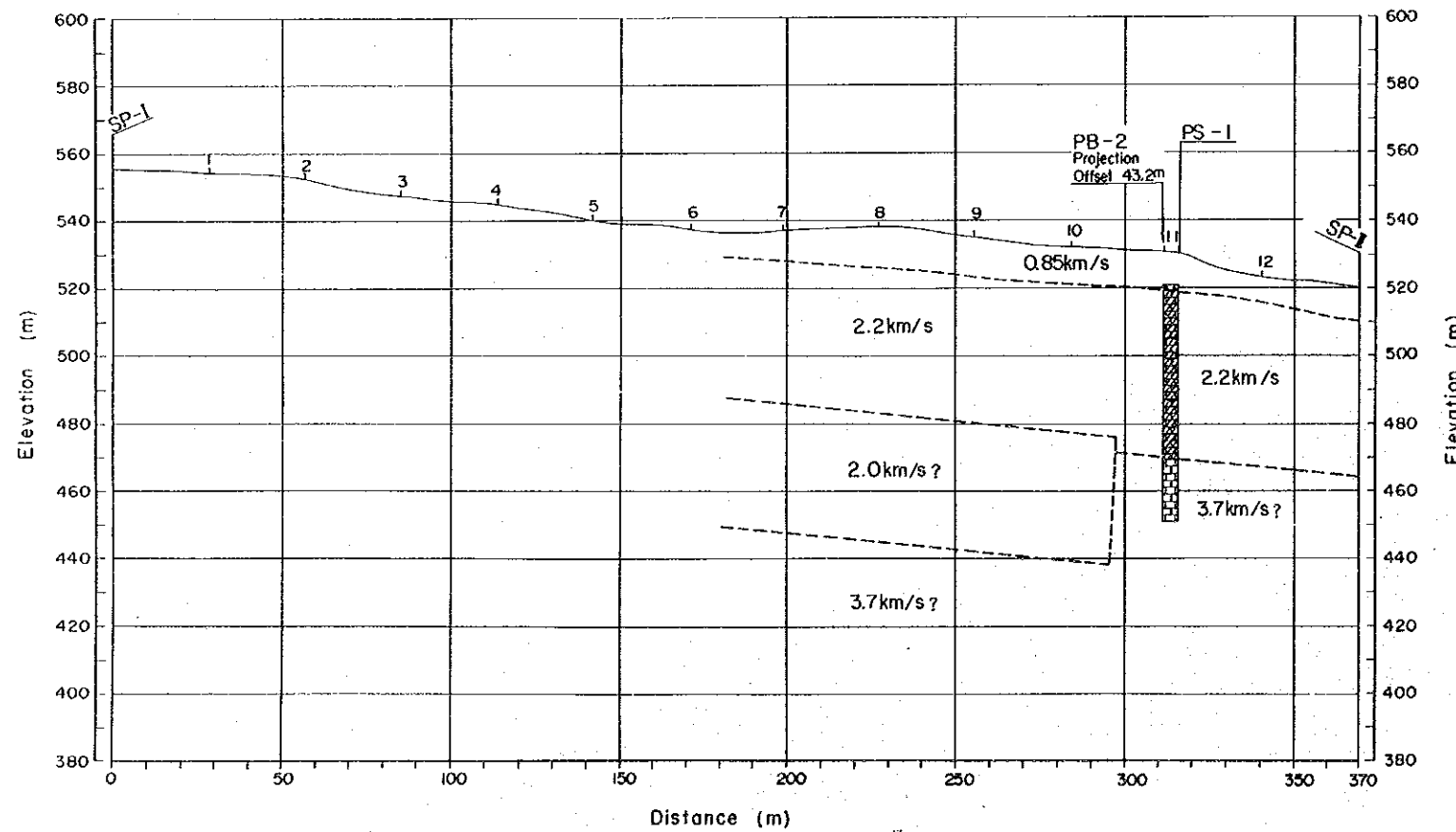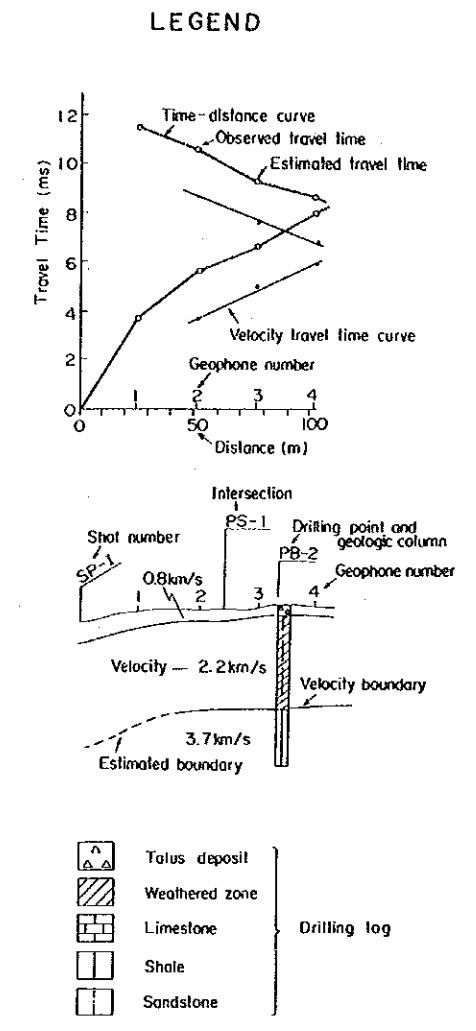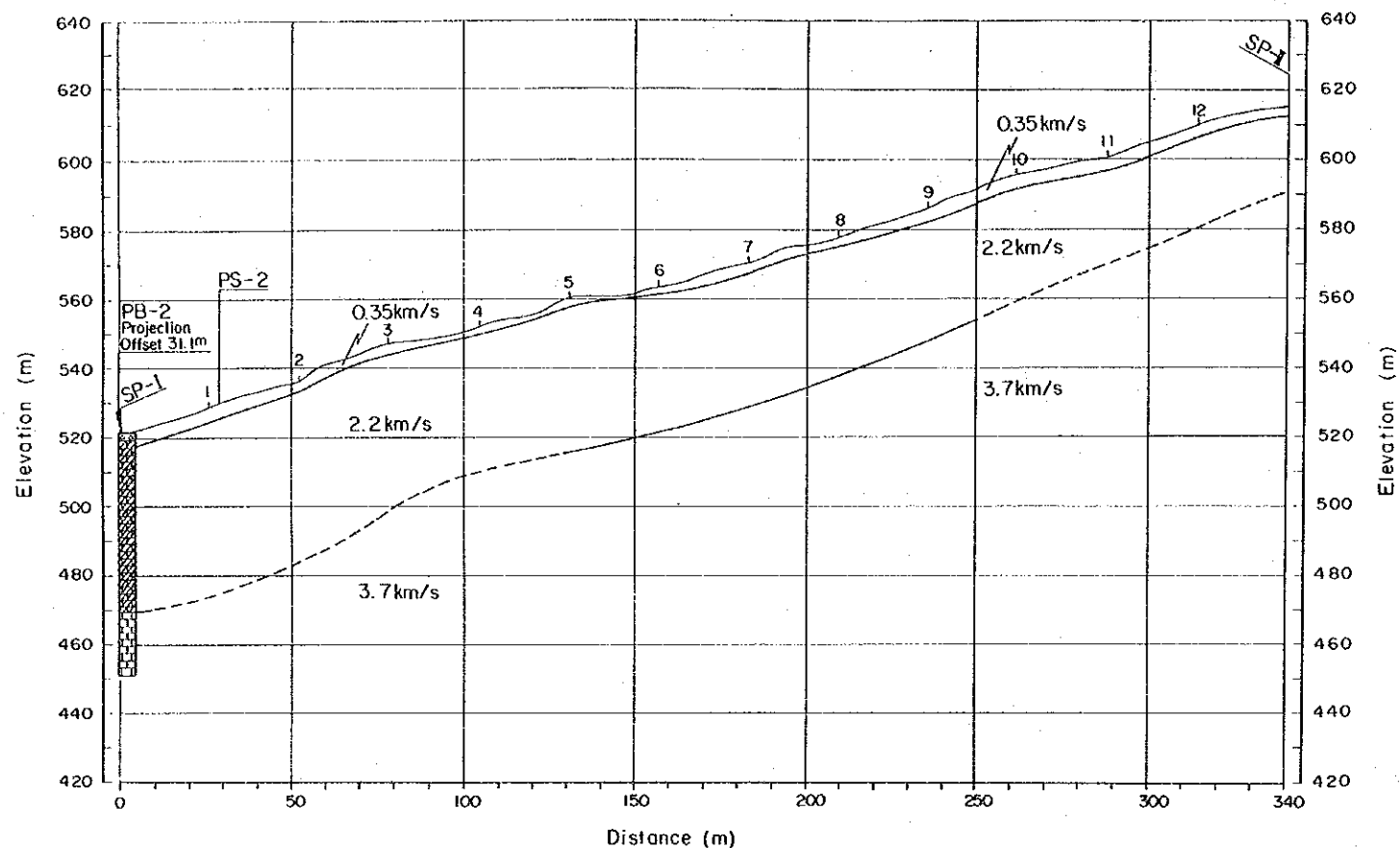PS-3   TIME-DISTANCE PLOT

AND SEISMIC PROFILE

Fig. 7-18

PS-1 REANALYSIS PROFILE

PS-2 REANALYSIS PROFILE

PS-3 REANALYSIS PROFILE
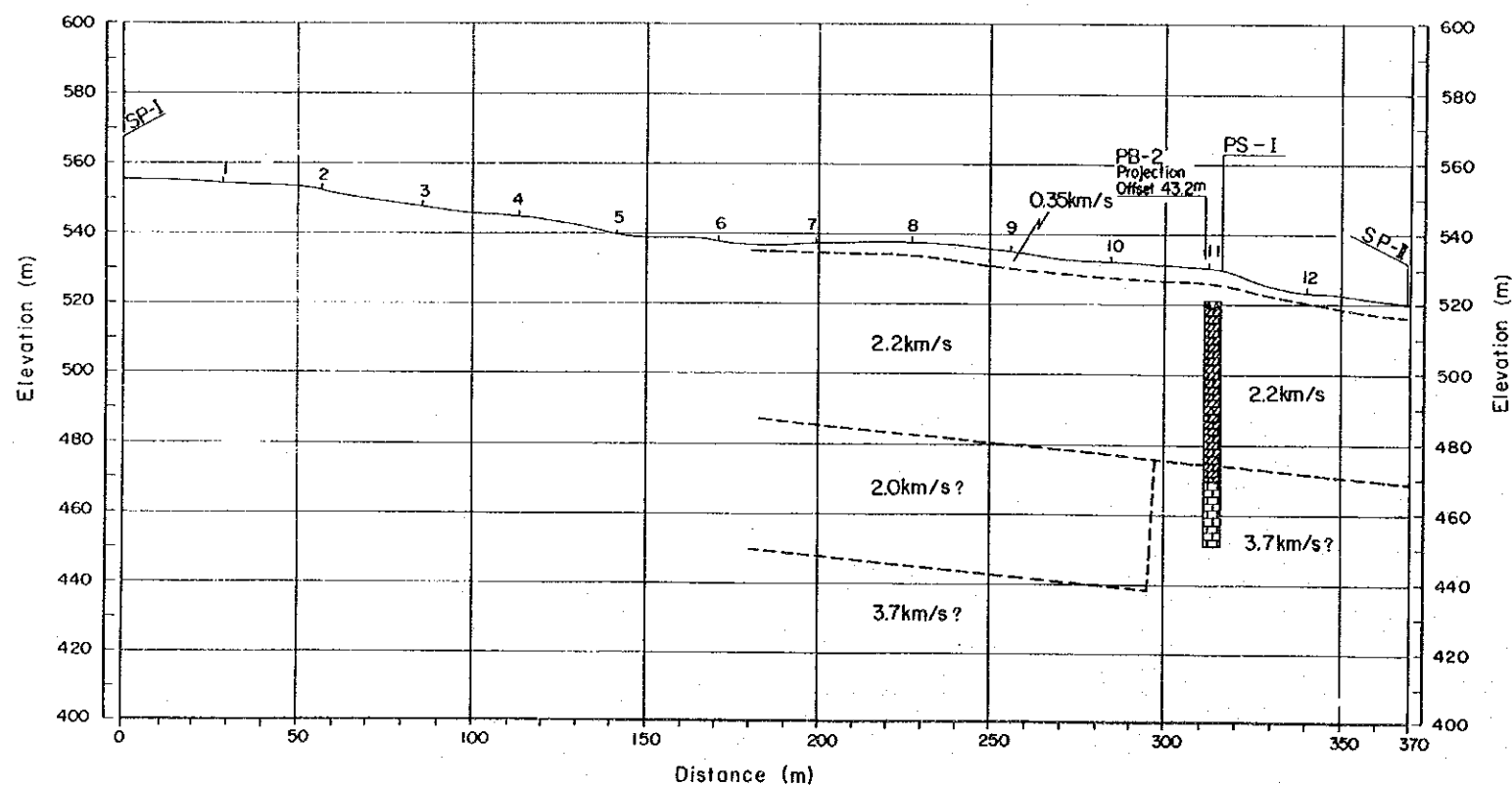
LEGEND
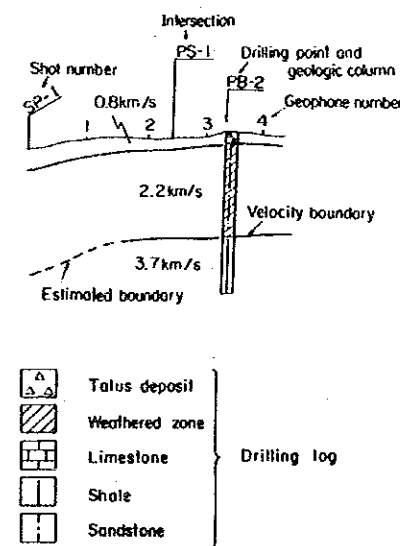
ZAMANTI GÖKTAŞ HYDROELECTRIC
POWER DEVELOPMENT PROJECT

PS-1, PS-2, PS-3

REANALYSIS PROFILES

Fig. 7-19

7 - 97

7.9 Construction Materials

7.9.1 Investigations and Tests

Regarding investigations and tests of construction materials, sur-
face explorations of candidate sites for collection were carried out
by the JICA Survey Team and the DSI, and laboratory tests were con-
ducted by the DSI on samples obtained from the various sites. The
materials tests performed up to this time may be divided into
concrete aggregate tests and soil tests. Of these, the soil tests
were conducted considering the case of a rockfill type being
selected for the dam in this Project.

The locations from which samples were collected for concrete aggre-
gate and soil laboratory tests are shown in Fig. 7-20. The test
quantities and test items of the samples collected are given in
Table 7-23.

Regarding concrete aggregates, as shown in Fig. 7-20, there is a
total of four sites, KAYA-1 to KAYA-4, as quarry candidates for
obtaining crushed stone, while there is one location (RD-C) for
obtaining natural aggregates from alluvial deposits. Other than
these, application of alluvial deposits distributed at the Zamanti
River bed as concrete aggregates can be considered, but the
topography of the Zamanti River basin is rugged, while the river
width is narrow at 40 to 60 m, and it cannot be said that conditions
are favorable for collecting large quantities of concrete aggrega-
tes.

In the event a rockfill type is selected for the dam in this
Project, there will be no place in the neighborhood of the dam site
where a large quantity of soil materials can be collected, and
possibilities are limited to the vicinities of RD-A and RD-B
approximately 20 km in straight-line distance from the projected dam
site as shown in Fig. 7-20. The results of soil tests on samples
collected from the RD-A and RD-B sites are given in an appendix.

7.9.2 Concrete Aggregates

Concrete aggregate tests were performed on samples collected from the four candidate quarry sites of KAYA-1 to KAYA-4 and the one alluvial deposit candidate site of RD-C as mentioned previously. The results of these tests are given in Table 7-24 and 7-25.

The rocks of KAYA-1 to KAYA-4 sampled from the candidate quarry sites in Table 7-24 were as follows:

    KAYA-1, -2, -3 sites: limestone
    KAYA-4 site   :   peridotite

The samples from KAYA-1 to KAYA-4 are all judged to be applicable as concrete aggregates as seen from the criteria in ASTM Standards (American Society for Testing and Materials Standards) and JIS (Japanese Industrial Standards), which are also given in Table 7-24.

On the other hand, with the samples of alluvial deposits listed in Table 7-25, the standard values in ASTM Standards and JIS are exceeded in the soundness and clay lumps tests, and the materials are judged to be unsuitable for use as concrete aggregates.

According to the above test results, concrete aggregates for the Goktas Project are to be collected from the candidate quarry sites of KAYA-1 to KAYA-4 along the Zamanti River. Of KAYA-1 to KAYA-4, it is considered that KAYA-1 is the site which is best from the point of view of stable supply of concrete aggregates to the dam site where the greatest volume of concrete is expected to be used. It is considered necessary for investigations and tests of artificial crushed stone from this site to be carried out hereafter in greater detail.

Table 7-23 Quantity of Laboratory Test for Construction Materials

[for Core Material]

Item / Location	Number of Sampling	Grading	Atterberg limits	Soil classification	Specific gravity	Compaction test	Triaxial shear Strength	Permeability test
RD – A (Doğan Cayi River)	44	44	41	44	44	44	15	8
RD – B (Doğan Cayi River)	21	21	21	21	21	21	5	2
Total	65	65	62	65	65	65	20	10

[for Concrete Aggregate]

Item / Location	Number of sampling	Grading	Specific gravity	Absorption	Soundness	Abrasion loss	Clay lumps (Under #200)	Clay lumps	Unit weight	Organic impurities	Alkali-Aggregate	Porosity	Unconfined compression
RD – C (Doğan Cayi River)	22	22 [1]	22 [1]	22 [1]	22 [1]	19	22 [1]	22 [1]	22 [2]	22	22	—	—
KAYA – 1	4	—	4	4	4	4	—	—	—	—	—	4	12
KAYA – 2	1	—	1	—	—	—	—	—	—	—	—	—	—
KAYA – 3	1	—	1	—	— [3]	—	—	—	—	—	—	—	3
KAYA – 4	2	—	2	—	— [3]	—	—	—	—	—	—	—	3
Total	30	22	30	29	29	26	22	22	25	22	22	6	18

Notes: 1) Carried out "Sand" and "Gravel"
2) 22 tests for "Sand", 17 tests for "Gravel"
3) Carried out "Sand" and "Gravel"

Name of Quarry Site	Sampling No.	Specific Gravity	Absorption (%)	Abrasion loss (%) 100cycle	Abrasion loss (%) 500cycle	Unconfined Compression Strength (kgf/cm²)	Soundness (%) Sand	Soundness (%) Gravel	Porosity (%)	Unit Weight (g/cm³)	Remarks
KAYA-1	T1	2.69	0.29	6.1	25.6	1065,1070,1240	2.1		0.78	—	
	T2	2.67	0.38	10.6	28.7	1100,1070,1285	0.0		1.02	—	
	T3	2.69	0.28	6.2	26.5	805, 925,1055	0.8		0.75	—	
	T4	2.65	0.29	4.9	21.7	1020,1270,1315	0.0		0.77	—	
KAYA-2	T1	2.72	0.36	4.6	17.9	—	1.0		0.97	2.69	Carried out flakiness, elongation tests
KAYA-3	T1	2.73	0.24	4.5	19.9	595, 720, 724	8.7	1.7	0.65	2.69	
KAYA-4	T1	3.32	—	—	—	900, 935, 975	3.5	1.0		3.29	Carried out flakiness, elongation tests
	T2	2.87	0.62	5.8	20.2	—	—		—		
Maximum Allowance for Aggregate	ASTM			less than 50.0			less than 10.0	less than 18.0			
	JIS	more than 2.5	less than 3.0	less than 40.0			less than 10.0	less than 12.0			

Table 7-24(2) Laboratory Test Results for Concrete Aggregate (Quarry Site)

— Flakiness, Elongation Test Results —

Sample No.	Aggregate Size-fraction	Mass of Sample (g)	Passing the gauges (g)	Remaining the gauges (g)	Flakiness index (%)	Elongation index (%)
KAYA – 2 T – 1	1″ ~ 3/4″	4,000	941	651	23.5	16.0
	3/4″ ~ 1/2″	2,000	721	632	36.1	31.6
	1/2″ ~ 3/8″	500	232	230	46.4	46.0
	3/8″ ~ 1/4″	200	86	107	43.0	53.5
KAYA – 4 T – 1	1″ ~ 3/4″	4,000	681	1,163	17.2	29.1
	3/4″ ~ 1/2″	2,000	750	1,002	37.5	50.1
	1/2″ ~ 3/8″	500	205	245	41.0	49.6
	3/8″ ~ 1/4″	200	90	105	45.0	52.5

Note : BS 812/75 Standard.

Table 7-25 Laboratory Test Results for Concrete Aggregate (RD Site)

Item Sample No	Grading (%) Sand	Grading (%) Gravel	Specific gravity Sand	Specific gravity Gravel	Absorption (%) Sand	Absorption (%) Gravel	Unit Weight (kg/m3) Sand	Unit Weight (kg/m3) Gravel	Soundness (%) Sand	Soundness (%) Gravel	Clay lumps (under #200)(%) Sand	Clay lumps (under #200)(%) Gravel	Clay lumps (%) Sand	Clay lumps (%) Gravel	Abration (%) 100cycle	Abration (%) 500cycle	Organic impurities	Alkali-Aggregate Reaction
C-401	40	60	2.558	2.728	5.26	0.93	1.840	1.748	44.8	40.3	5.04	1.13	3.20	0.31	6.22	28.6	Innocuous	Innocuous
402	38	62	2.547	2.668	5.49	2.30	1.853	1.784	45.9	31.9	6.99	0.92	5.71	0.7	5.80	26.2	"	"
403	60	40	2.523	2.656	5.71	2.07	1.705	1.800	41.4	42.9	8.13	1.58	7.98	12.5	7.20	26.6	"	"
404	40	60	2.568	2.679	4.82	2.27	1.831	—	39.4	31.4	7.20	0.55	7.11	0.47	7.20	29.5	"	"
405	50	50	2.584	2.618	5.49	2.58	1.786	1.856	42.9	33.5	7.59	0.61	6.99	0.51	6.00	28.0	"	"
406	36	64	2.555	2.697	5.26	1.44	1.753	—	40.2	37.4	7.33	1.52	6.44	1.11	—	—	"	"
407	48	52	2.526	2.637	5.93	1.86	1.761	1.810	45.7	46.3	7.03	1.26	5.82	0.68	6.20	28.2	"	"
409	84	16	2.525	2.698	4.82	2.21	1.774	—	44.7	44.4	7.06	1.60	5.98	1.46	—	—	"	"
411	37	63	2.579	2.671	5.93	1.46	1.855	1.807	46.6	42.5	8.87	1.15	6.65	0.90	5.76	24.14	"	"
413	53	47	2.579	2.693	5.26	4.38	1.808	1.782	41.6	32.1	7.14	0.70	5.60	0.22	5.9	25.2	"	"
415	41	59	2.544	2.735	4.38	1.76	1.855	—	42.0	39.6	6.50	1.26	6.08	0.82	7.5	29.8	"	"
417	41	59	2.546	2.798	5.49	1.41	1.83	1.832	44.0	40.6	6.19	0.83	4.42	0.12	6.24	27.9	"	"
418	41	59	2.575	2.713	4.82	1.67	1.825	1.829	38.6	28.4	6.83	1.72	6.42	1.47	6.00	23.9	"	"
419	64	36	2.551	2.661	5.49	2.33	1.754	1.758	47.4	42.6	7.29	1.18	6.34	0.71	8.80	31.2	"	"
421	48	52	2.565	2.685	4.82	1.66	1.749	1.844	42.1	37.2	10.3	0.78	8.7	0.62	6.30	25.4	"	"
423	40	60	2.529	2.665	6.61	2.08	1.777	1.749	52.5	38.8	6.64	0.90	5.36	0.80	7.92	30.5	"	"
425	41	59	2.557	2.714	5.26	4.74	1.874	1.746	38.3	40.4	4.95	0.58	3.79	0.23	—	—	"	"
427	49	51	2.594	2.691	4.82	4.85	1.845	—	42.4	30.9	.20	1.50	5.96	0.66	6.00	22.8	"	"
429	40	60	2.609	2.709	4.17	1.80	1.852	1.823	39.2	25.3	10.5	1.25	9.79	1.04	6.20	25.5	"	"
431	44	56	2.589	2.721	4.60	1.97	1.829	1.866	44.9	25.1	9.21	0.96	4.92	0.54	7.14	27.4	"	"
433	38	62	2.590	2.653	4.60	1.42	1.751	1.900	40.5	24.3	9.09	0.69	9.03	0.21	9.40	26.0	"	"
436	37	63	2.584	2.759	4.82	1.36	1.781	1.828	47.1	33.6	9.11	0.26	8.43	0.20	6.50	24.9	"	"
ASTM				more than 2.5		less than 3.0			less than 10.0	less than 18.0			less than 3.0	less than 2.0	less than 50.0			
JIS									less than 10.0	less than 12.0			less than 1.0	less than 0.25				
Allowable Maximum															40.0			

Note: Sand is under 5mm, Gravel is over 5mm.

KAYA-1 AND KAYA-4
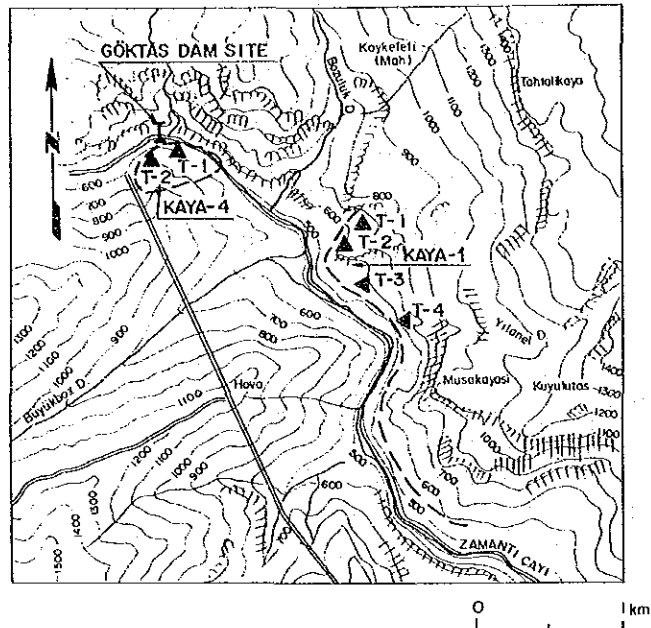
KAYA-2 AND KAYA-3
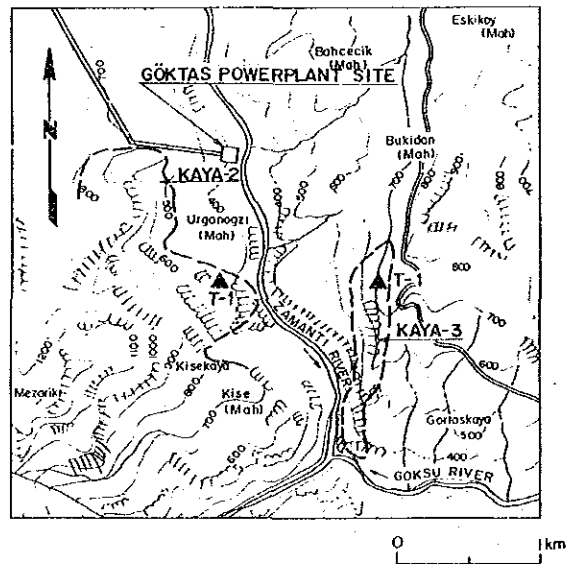
GENERAL LOCATION MAP
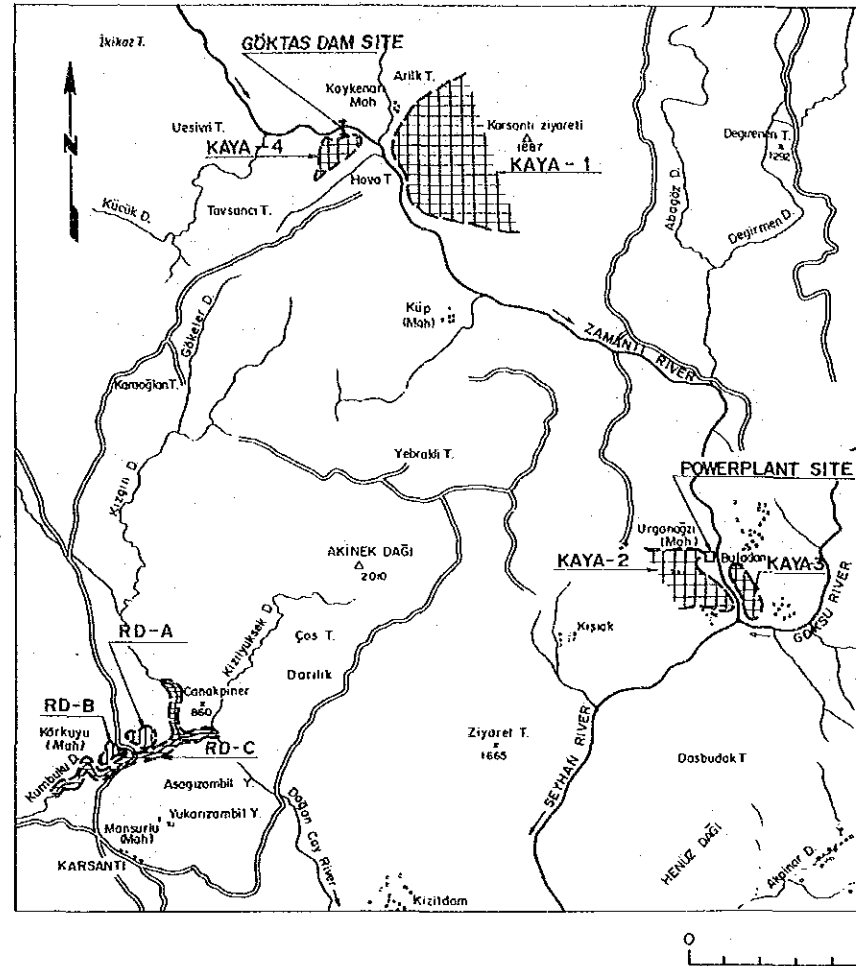
LEGEND

Core Material (RD-A and RD-B)

Concrete Aggregate (RD-C)

Concrete Aggregate (KAYA-1,2,3 and 4)

▲ ■ Sampling Point

RD-C
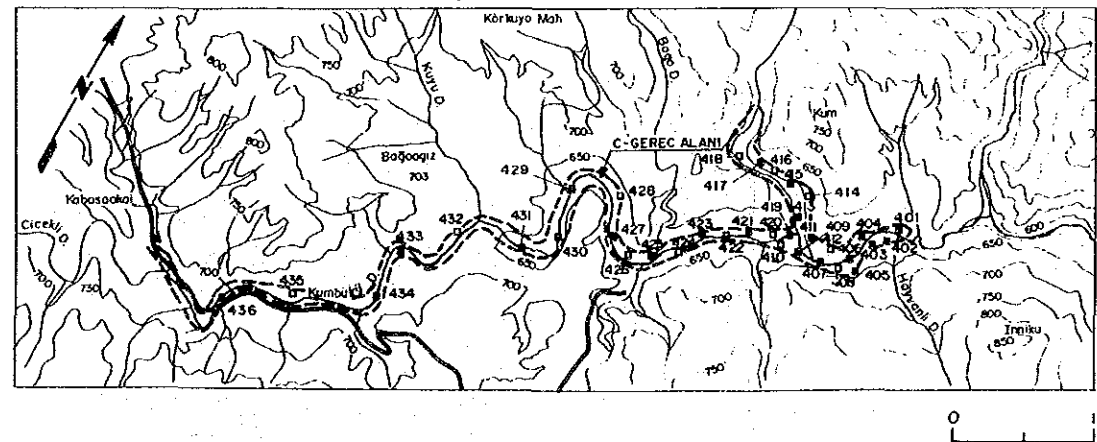
ZAMANTI GÖKTAŞ HYDROELECTRIC
POWER DEVELOPMENT PROJECT

LOCATION MAP OF

QUARRY AND BORROW AREA

Fig. 7-20

CHAPTER 8.   SEISMICITY

CHAPTER 8. SEISMICITY

CONTENTS

List of Figures

List of Tables

CHAPTER 8.   SEISMICITY

8.1   Structural Geology of Turkey

8.1.1   Geological Outline

The Anatolian Peninsula region has been subjected to the repeated organic movements since the beginning of Paleozoic age, and presents a complex geology. Concerning the structural geology of Turkey, it can be classified into four east-west oriented tectonic zones. Namely, they are in order from the north, the Pontids, Anatolids, Taurids, and Border Folds as shown in Fig. 8-1 after Dr. Hirano (1981).

In the Pontids, Cretaceous to Paleogene rhyolitic-basaltic volcanic rocks are predominant, while there is partial distribution of Jurassic to Cretaceous ophiolite. In the Anatolids, strongly deformed Eocene to Miocene marine clastic rocks and Quaternary volcanic rocks are distributed on the basement rocks of Jurassic to Cretaceous ophiolite and slightly metamorphosed rock. The continental deposits of Pliocene to Quaternary are distributed at the mountainland basins. The basement of the Taurids consists mainly of Precambrian to Mesozoic strata and ophiolite, while Eocambrian to Pliocene neritic sedimentary rocks are predominant in the Border Folds.

Fig. 8-1   Tectonic Zone of Turkey (after Hirano, 1981)
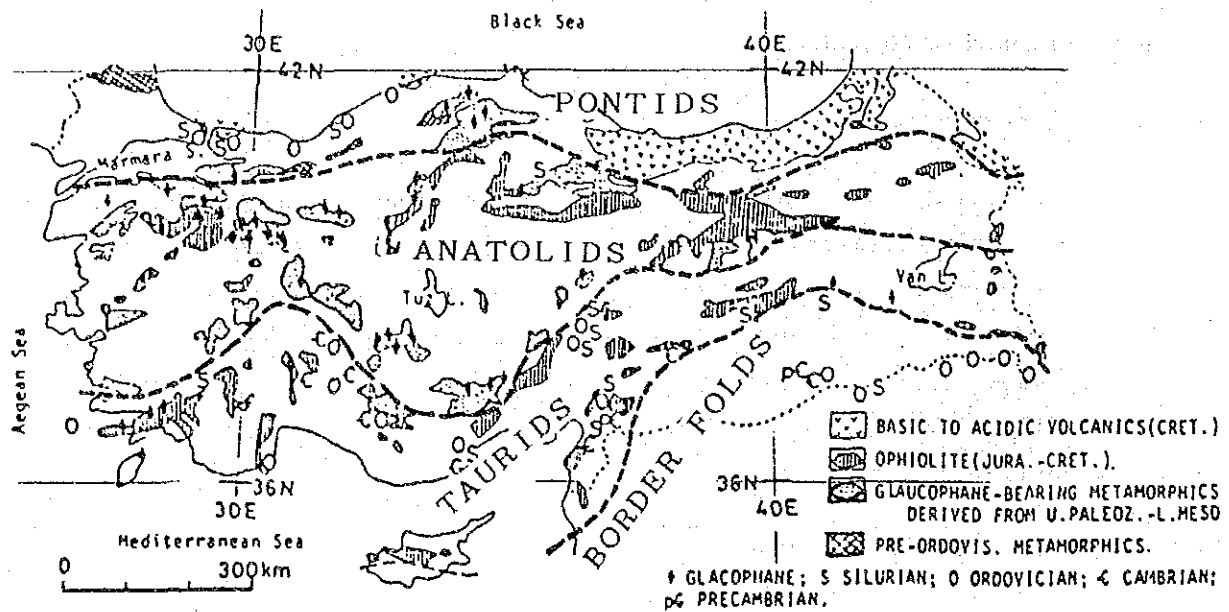
8.1.2   Neotectonics of Turkey

Various plate tectonics models around Turkey have been proposed by McKenzie (1972), Alptekin (1973), Papazachos (1974), Dewey & Sengor (1979), and others.

Turkey is surrounded by three macro-plates, i.e. Eurasian Plate, Arabian Plate and African Plate, as shown in Fig. 8-2. Basically, Arabian and African Plates are drifting toward north relatively against Eurasian Plate causing the tectonic compressive stress field.

Moreover, many micro-plates such as Aegean Plate, Iran Plate, Anatolian Plate (Turkey Plate) and Black Sea Plate are located in Republic of Turkey surrounded by the three macro-plate which mentioned above.

Fig. 8-2 Typical Plate Tectonics Model
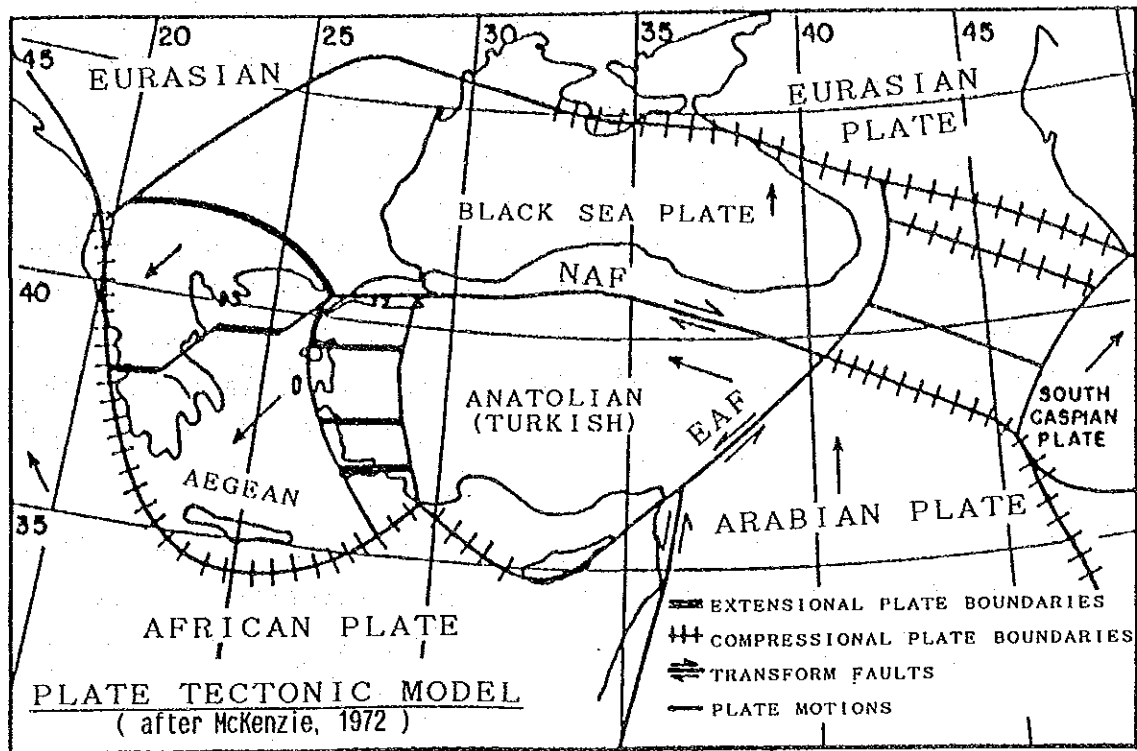
8.1.3 North Anatolian Fault and East Anatolian Fault

The Anatolian Peninsula region is divided by two transform faults named North Anatolian Fault and East Anatolian Fault, which make up the plate boundaries. Particularly, there two transform faults prominently divide the previously-mentioned old tectonic zones.

The North Anatolian Fault extends east-west, presenting a gentle arc bulging northward at the northern part of Turkey and its total length is in excess of approximately 1,000 km. It is a morphologically distinct and seismically active right lateral strike-slip fault. The accumulated horizontal displacement of it was considered to be 70 to 80 km in the past, but recently, some researcher says that it should be 20 to 30 km, and this subject requires further study. The occurrence of the North Anatolian Fault is said to have been 10 to 12 million years ago, but the direction of displacement has not always been consistently right-handed horizontal and it appears there was a time in the middle of Pliocene Epoch when a left-handed horizontal displacement was indicated. Many active faults, earthquake-associated faults and mountainland basins are distributed along this fault, while there have been also volcanic activities, and it may be seen that this is a first-class structure of the Quaternary Period.

The East Anatolian Fault divides the Taurids, and on land it has a length of approximately 560 km with a strike of N60°E - S60°W. It shows a thrust-fault nature at the southwestern part, but a left-handed lateral displacement is prominent on the whole. It is covered by Quaternary volcanic rocks and the displacement topography is not always distinct, while the degree of activity is slightly lower compared with the North Anatolian Fault, but this is also a paramount structure of this region. The fault intersects the North Anatolian Fault east of Karliova to comprise a triple junction. As a consequence, the Anatolian Plate sandwiched by the two faults would apparently shift westward.

As described in the foregoing, the neotectonics of Turkey is made complex reflecting the mutual movements between the plates in the field of tectonic stress from north-south compression caused by the northward-drifting Arabian Plate since the late Miocene Epoch.

8.2 General Seismicity of Turkey

8.2.1 Seismological Outline

It is well known that many earthquakes have been occurred in Turkey, which located in Alpine-Himalayan seismic zone. As explained before, three macro-plates, i.e. Eurasian Plate, Arabian Plate and African Plate, develop the mutual movements around Turkey. And moreover, Micro-Plates such as Aegean Plate, Iran Plate, Anatolian Plate and Black Sea Plate develop the mutual complicated movements, in Turkey.

There micro-places are small, but move more rapidly. The cause of the local increase in Seismic activity of this region is attributed to the existence of these small but rapidly moving micro-plates.

Fig. 8-3 clearly shows the distribution of the major fault systems in Turkey. It can be understood that the major faults are running along the border zone of the micro-plates which mentioned above.

Shortly speaking, earthquakes in Turkey occur as the results of relative movements among the many macro/micro plates i.e. Eurasian

Plate, African Plate, Arabian Plate, Aegean Plate, Iran Plate, Anatolian Plate (Turkey Plate) and Black Sea Plate.

Fig. 8-3   Major Fault Systems in Turkey
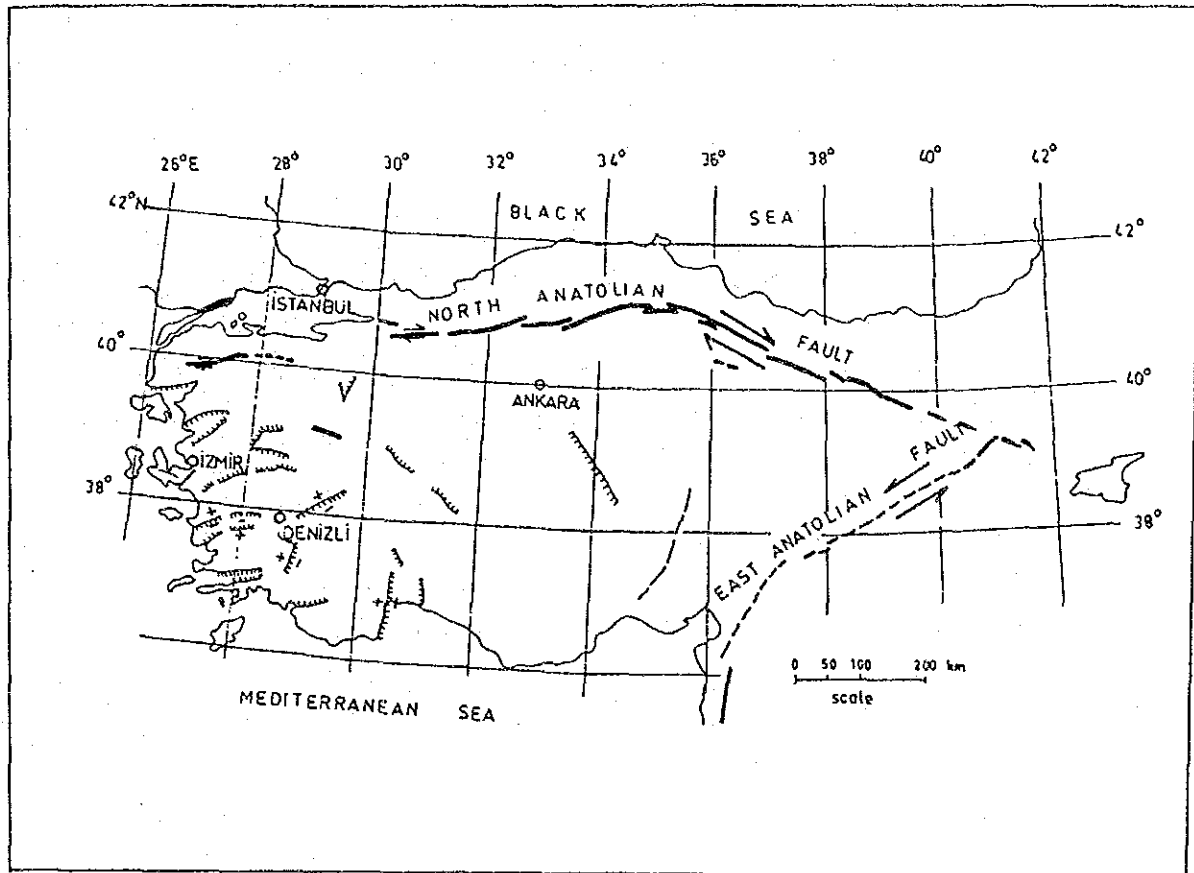
8.2.2   Seismic Activities

Epicenters of 5,980 earthquakes which occur in Turkey during the period 1901 - 1985 are indicated in Fig. 8-4. The location map of the larger earthquakes (Ms $\geq$ 6) of the period 1899 - 1983 is also given in Fig. 8-5.

By the way, the seismic active zone for Turkey can be classified into four groups as follows, taking plate tectonics model, distribution of active faults, occurrence of historical earthquakes into consideration.

(1) North Anatolian Fault Region

The North Anatolian Fault is a transform fault which is situated in
the boundary between the Black Sea Plate and the Anatolian Plate
(Turkey Plate). The number of earthquakes larger than magnitude 5.5
($M \geq 5.5$) in the North Anatolian Fault region exceeds 60 since 1900.
They are the shallow-focal-depth earthquakes conforming to the
right-lateral fault.

Meanwhile, the earthquake which occurred at Erzincan in 1939 at the
eastern part of the North Anatolian Fault registered M 7.9, which is
the strongest in this century in Turkey. Since then, earthquakes in
this region have occurred every several to ten and several years,
and it is well-known that the hypocenters of these earthquakes have
shifted westward in remarkably orderly manner.

According to the investigations thus far, the earthquake faults
which were produced as results of these earthquakes do not strictly
coincide in cases, but approximately, they are produced by repeated
cycles of motion of the active faults running roughly parallel in
the vicinity of the North Anatolian Fault. In view of the cumula-
tive vertical displacement of the active faults and the vertical
displacements of the individual earthquake faults the return period
if of the order of several hundred of several thousand years
($< 5,000$ yr).

The earthquake faults are in a number of multiple echelon arrange-
ments composed of segments made of echelon fissures, the smallest of
which are ten and several centimeters. Small-scale echelon arrange-
ments with segment lengths of less than several hundred meters are
arrayed in correspondence with the lateral displacement of related
transform faults. On the other hand, large-scale echelon arrange-
ments of segment lengths ten and several kilometers do not
necessarily correspond with related transform faults. This is
because they are affected by geological anisotropies near the ground
surface such as existing fissures and volcanic rock mass.

(2) East Anatolian Fault Region

The East Anatolian Fault is a transform fault which is situated in the boundary between the Anatolian Plate (Turkey Plate) and the Arabian Plate. Shallow earthquakes conforming to the left-lateral fault are predominant in the East Anatolian Fault region. Most of them have occurred less than 25 km in focal depth. The recurrence of the earthquakes larger than magnitude 5.5 ($M \geq 5.5$) in this region is around 12 years.

(3) West Anatolian Region

Rather deeper earthquakes conforming to the normal faults along the east-west graben are predominant in the West Anatolian region.

(4) Other Regions

They have relatively low seismic activities in the area except for the regions (1), (2) and (3) in Turkey.

Fig. 8-4 Seismicity of All Data in 1901 — 1985

Total Number of Plots in the Area of $\triangle \leq 1,000.0$ (km) is 5,980.
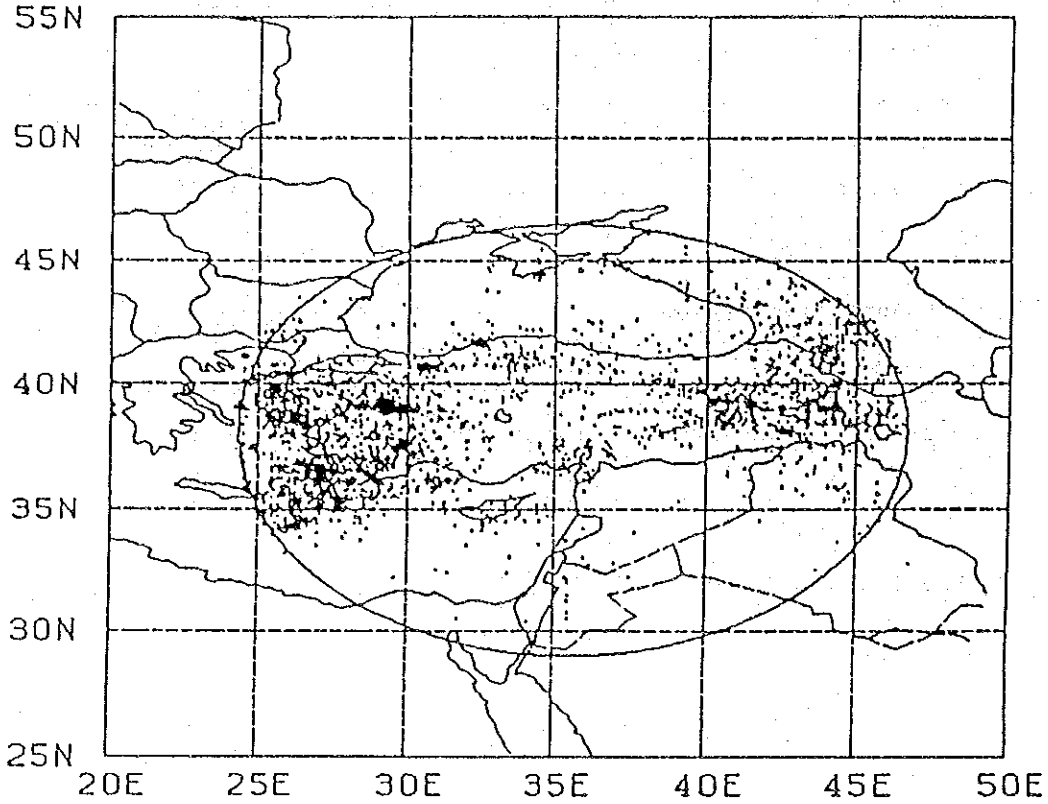
Fig. 8-5 Location of the Larger Earthquakes (Ms $\geqq$ 6)
of the Period 1899 — 1983
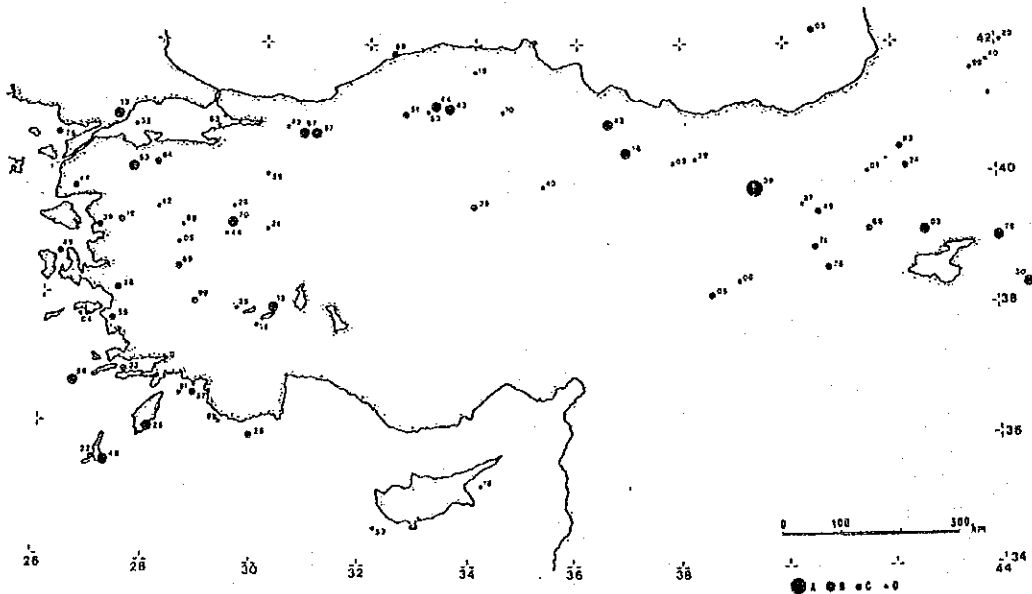
Map of the northeast Mediterranean region under study (34° N to 42° N and 26° E to 44° E), i.e. Turkey, Cyprus, northern Syria, Lebanon, Iraq, frontiers of Iran and the USSR. The map shows the location of the larger earthquakes ($M_s \geqslant 6$) of the period 1899-1983. Numbers refer to the last two figures of the year in which a particular earthquake occurred. A implies $8.0 > M_s \geqslant 7.5$; B: $7.5 > M_s \geqslant 7.0$; C: $7.0 > M_s \geqslant 6.5$; D: $6.5 > M_s \geqslant 6.0$.

8.3 Design Seismic Coefficient

8.3.1 Design Seismic Coefficient for Existing Dams

To determine the design seismic coefficient for the Project, the correlation between seismic risk and adopted design seismic coefficient for the existing and planned dams in Turkey was studied. The design seismic coefficients (horizontal ground level seismic coefficients) for the 45 dam sites were in hand out of 74 dam sites (ICOLD World Register of Dams, 1982).

Available Seismic Risk Map for Turkey was prepared in 1972 by the Government of Turkey (İMAR ve İSKÂN BAKANLIĞI). Then, the correlation between seismic risk and the design seismic coefficient was studied by comparing the risk map with the dam location. The Seismic Risk Map for Turkey which shows the 5 zones relating to the degree of risk covering the whole of Turkey is given in Fig. 8-6. The result of the survey is also given in Fig. 8-7.

Consequently, the results can be summarized by item as follows;

o The maximum value of adopted design seismic coefficient was 0.18,

o The minimum value of adopted design seismic coefficient was 0.15,

o The value 0.18 as design seismic coefficient was adopted for 1 site out of 45 sites, similarly 0.15 for 18 sites, 0.12 for 4 sites, 0.10 for 16 sites and 0.05 for 6 sites,

o The coefficient 0.15 is noticeable in 1st degree zone given in Fig. 8.3-1,

o The coefficient 0.12 or 0.10 is noticeable in 2nd degree zone,

o The coefficient 0.15 or 0.10 is noticeable in 3rd degree zone, and,

o The coefficient 0.05 is noticeable in 4th degree zone.

In this study, the reasonable results are obtained, that is the high coefficient was adopted for the hazardous zone, and on the contrary the low coefficient for the safer zone.

Considering above-mentioned tendency, it can be standardized as follows from the viewpoint of aseismic design for dams in Turkey.

o The design seismic coefficient 0.15 can be applied for the 1st degree zone,

o The coefficient 0.15 - 0.12 for the 2nd degree zone,

o The coefficient 0.12 - 0.10 for the 3rd degree zone, and,

o The coefficient 0.10 - 0.05 for the 4th degree zone.

Fig. 8-6   Seismic Risk Map for Turkey (1972)
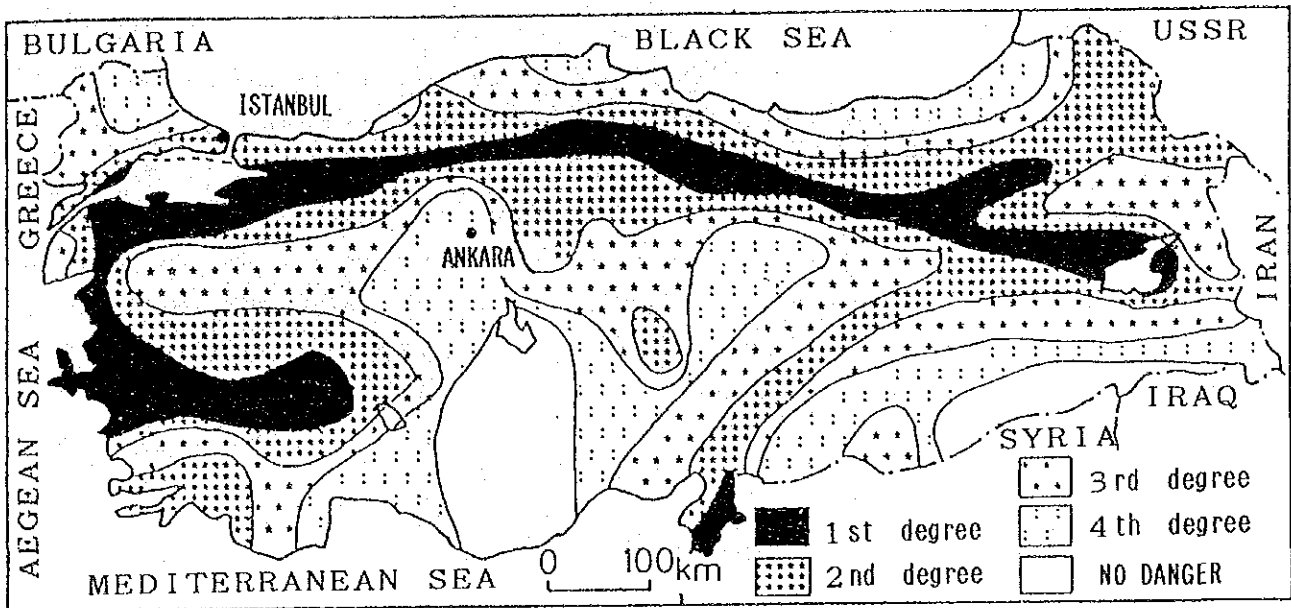
Fig. 8-7   Design Seismic Coefficient used for Dams in Turkey

Seismic Risk Zone	Design Herizontal Ground Seismic Coefficient			
	0.05	0.10	0.15	
I			0.12	0.18
II				
III				
IV				
V				

8.3.2 Maximum Acceleration at Goktas Site

The estimation of the maximum ground acceleration at Goktas site by probability analysis was performed to determine the design seismic coefficient. The seismicity data used in this study are those compiled by NOAA (National Oceanic and Atmospheric Administration Environmental Data Service) and are 5980 in number during the period 1901-1985. Of previously proposed attenuation models which express peak ground acceleration A (gal), in terms of earthquake magnitude M, and hypocentral distance R (km), or epicentral distance D (km), five models shown below are used in this study.

$$\text{Log } A = 3.090 + 0.347 \ M - 2 \ \text{Log } (R+25) \qquad (1)$$
proposed by C. Oliveira

$$\text{Log } A = 2.674 + 0.278 \ M - 1.301 \ \text{Log } (R+25) \qquad (2)$$
proposed by R.K.McGire

$$\text{Log } A = 2.041 + 0.347 \ M - 1.6 \ \text{Log } R \qquad (3)$$
proposed by L. Esteva and E. Rosenblueth

$$\text{Log } A = 2.308 + 0.411 \ M - 1.637 \ \text{Log } (R+30) \qquad (4)$$
proposed by T. Katayama

$$\text{Log}(A/640) = (D+40)(-7.6+1.724 \ M - 0.1036 \ M^2)/100 \qquad (5)$$
proposed by S. Okamoto

A probabilistic model based on the "Theory of Extreme Values" can be established by taking an equal time interval of one year. Although a probability function of the maximum ground acceleration expected at a certain particular dam site is not known, it is reasonable to suppose that the function should be associated with the third-type asymptotic distribution.

The seismicity data used are shown in Fig. 8-4 and the results obtained in this probabilistic analysis are given in the Table 8-1, Table 8-2 and Table 8-3.

Table 8-1   Distribution of Magnitude and Epicentral Distance of the
Seismicity Data

M \ △	0≦△<50	<100	<200	<300	<400	<500	<600	<700	<800	≦1000	Total
2.5≦M<4.0	0	0	0	1	3	15	28	17	56	167	297
4.0≦M<4.5	0	7	12	11	30	79	125	85	159	306	813
4.5≦M<5.0	2	6	16	20	41	143	257	147	224	465	1321
5.0≦M<5.5	3	9	27	27	71	247	335	259	370	427	1775
5.5≦M<6.0	0	13	26	34	94	163	189	191	282	315	1307
6.0≦M<6.5	3	3	10	14	30	37	44	58	71	67	340
6.5≦M<7.0	0	0	0	4	9	9	11	17	29	17	93
7.0≦M<7.5	0	0	0	0	3	5	2	1	14	6	31
7.5≦M<8.0	0	0	0	0	1	1	0	0	0	0	2
8.0≦M<8.5	0	0	0	0	0	0	0	0	0	1	1
Total	8	38	90	111	282	699	994	785	1205	1768	5980

△ : Epicentral Distance (km)
M : Magnitude

Table 8-2 Maximum Accelerations during a year from 1901 to 1985

Year	Oliveira, C. Eq. (1)	McGuire, R. K. Eq. (2)	Esteva, L. & Rosenblueth, E. Eq. (3)	Katayama, T. Eq. (4)	Okamoto, S. Eq. (5)
1901	.8	8.2	.9	2.7	.0
1902	.6	6.3	.6	2.0	.0
1903	2.9	17.2	2.7	6.3	1.9
1904	.6	7.5	.8	2.7	.0
1905	.9	8.7	.9	3.3	.0
1906	.4	4.9	.5	1.4	.0
1907	4.8	27.4	4.5	13.4	10.4
1908	2.6	16.9	2.5	6.6	1.7
1909	.7	7.7	.8	2.6	.0
1910	3.3	19.6	3.1	7.8	3.1
1911	1.7	14.0	2.2	5.7	1.4
1912	1.1	10.5	1.2	4.7	.1
1913	.3	4.7	.4	1.6	.0
1914	6.3	35.4	6.6	20.1	24.7
1915	2.0	14.7	2.0	5.8	.9
1916	1.0	10.9	1.3	4.7	.2
1917	.4	5.0	.5	1.4	.0
1918	3.9	24.6	3.8	12.1	7.6
1919	2.2	15.8	2.2	6.3	1.3
1920	2.0	14.5	2.0	5.5	.8
1921	2.7	17.9	2.6	7.4	2.2
1922	7.3	33.0	7.0	14.7	17.0
1923	1.1	9.9	1.2	3.3	.1
1924	8.3	36.9	8.0	17.5	23.2
1925	2.3	16.7	2.3	6.9	1.6
1926	3.0	19.9	2.9	9.8	3.4
1927	3.8	22.5	4.4	10.4	10.0
1928	2.0	13.3	1.9	5.1	.6
1929	2.7	17.2	2.6	6.6	1.8
1930	4.2	24.8	4.0	11.5	7.6
1931	3.3	21.1	3.2	9.5	4.3
1932	2.6	17.0	2.7	6.5	2.1
1933	1.6	12.5	1.6	4.6	.4
1934	3.1	19.5	3.0	7.9	3.0
1935	.7	8.3	.9	3.3	.0
1936	2.7	17.4	5.3	6.8	10.7
1937	2.3	15.6	2.7	5.9	2.3
1938	2.1	16.7	2.2	7.6	1.7
1939	2.5	16.9	2.4	7.8	1.7
1940	5.7	29.4	5.5	13.6	13.1
1941	4.1	25.8	4.7	12.9	12.5
1942	1.1	11.8	1.4	5.2	.3

unit : gal

Table 8-2 (continued)

Year	Oliveira, C. Eq. (1)	McGuire, R. K. Eq. (2)	Esteva, L. & Rosenblueth, E. Eq. (3)	Katayama, T. Eq. (4)	Okamoto, S. Eq. (5)
1943	2.5	20.0	2.8	10.4	3.3
1944	16.7	57.5	20.1	29.5	62.2
1945	27.5	84.7	35.3	51.3	114.1
1946	1.5	12.2	1.5	4.6	.3
1947	8.1	37.2	7.7	18.3	23.7
1948	.8	7.6	.8	2.7	.0
1949	12.3	46.1	13.7	21.9	40.0
1950	3.0	18.0	2.8	6.8	2.3
1951	9.2	38.3	9.4	17.5	25.7
1952	11.7	46.7	21.2	24.0	72.7
1953	3.8	22.1	3.5	9.3	4.6
1954	.8	8.3	.9	3.0	.0
1955	.5	7.2	.7	2.7	.0
1956	1.1	9.6	1.3	3.4	.1
1957	1.1	11.7	1.4	5.1	.3
1958	.6	6.6	.7	2.0	.0
1959	4.3	22.0	4.3	8.3	5.5
1960	4.0	21.6	4.4	8.4	6.6
1961	5.5	27.6	5.8	11.9	11.4
1962	2.3	14.7	2.1	5.1	.8
1963	1.1	9.3	1.1	3.1	.1
1964	5.4	26.6	4.8	10.9	7.9
1965	5.7	27.3	6.4	11.2	13.0
1966	4.7	24.4	5.1	10.1	9.4
1967	8.6	36.1	9.4	16.2	23.6
1968	2.3	14.8	2.2	5.2	1.1
1969	10.0	37.7	65.6	15.5	82.8
1970	3.1	18.5	2.9	7.0	2.5
1971	9.8	38.4	10.7	16.7	25.9
1972	1.3	10.2	1.2	3.3	.1
1973	1.2	10.1	1.2	3.3	.1
1974	8.2	33.9	8.5	14.1	18.8
1975	3.0	18.5	2.8	7.2	2.4
1976	6.9	28.5	8.2	10.5	13.9
1977	4.8	22.4	4.9	7.9	6.1
1978	1.8	12.4	1.7	5.9	.4
1979	10.0	38.1	15.3	16.0	34.9
1980	4.6	20.7	5.5	6.5	5.9
1981	1.2	8.7	1.1	2.4	.0
1982	3.9	18.9	3.6	6.0	2.7
1983	3.6	18.6	3.3	6.3	2.7
1984	2.6	14.6	2.9	4.4	1.4
1985	1.3	9.2	1.1	2.6	.1

unit : gal

Table 8-3　Maximum Accelerations for Six Return Periods (gal)

Model (Eq. No.)	Proposer(s)	Return Period (Year)					
		50	100	200	500	1000	10000
(1)	C. Oliveira	22	27	32	38	43	54
(2)	R. K. McGuire	73	84	94	105	112	129
(3)	L. Esteva & E. Rosenblueth	51	63	74	86	93	108
(4)	T. Katayama	43	51	58	67	72	86
(5)	S. Okamoto	84	110	133	160	176	208

8.3.3 Design Seismic Coefficient

The Zamanti, Goktas Project site is located in the 4th degree zone, but near the 3rd degree zone delineated in the Seismic Risk Map for Turkey (İMAR ve İSKÃN BAKANLIĞI, 1972). Based on the survey result in 8.3.1, the design seismic coefficient 0.10 can be applied for the Project.

However, it is necessary that the long return period expectancy (Table 8-3) should be checked, taking the uncertainties of the earthquake occurrence into account.

Therefore, 0.12 is to be adopted as the design seismic coefficient of Goktas site in the light of the probabilistic analysis results.

On the otherhand, it is also expected that the further study on whether the design seismic coefficient 0.10 could be applied or not will be continued.

CHAPTER 9.   THE DEVELOPMENT PLAN

CHAPTER 9. THE DEVELOPMENT PLAN

CONTENTS

List of Figures

List of Tables

CHAPTER 9. THE DEVELOPMENT PLAN

9.1 Comparative Study of the Development Plan

9.1.1 Review of Existing Master Plans

(1) Outline of Hydroelectric Power Development Plans for the Seyhan River Basin

The Zamanti and Goksu Rivers rising from the East Toros Mountain Range in the southeastern part of Turkey run roughly parallel to each other in a south-southwest direction until they merge at a point approximately 70 km north-northwest of Adana City to become the Seyhan River, which empties into the Mediterranean Sea in the vicinity of Adana City. The Seyhan River has a catchment area of approximately 20,730 km, a length of approximately 506 km, and an annual discharge of approximately $7,100*10^6$ m^3 to constitute the third largest river in Turkey.

DSI, to facilitate development of the Seyhan River Basin, set up the Lower Seyhan Basin Master Plan in 1981, and the Upper Seyhan Basin Master Plan in 1984. The location of each projects is shown in Fig. 9-1, the outline of the Lower Seyhan Basin Master Plan is shown in Table 9-1 and that of the Upper Seyhan Basin Master Plan are shown in Table 9-2.

According to the latter plan, the hydroelectric power development program is an integrated river development scheme in which twenty sites (total output 1,849.5 MW) on the Seyhan River would be developed in series. This scheme consists of constructing nine power projects on the Zamanti River for a total output of 593.5 MW, six power projects on the Goksu River for a total output of 564.0 MW, and five power projects on the Seyhan River mainstream for a total output of 692.0 MW. This latter figure includes 54 MW of the existing Seyhan Power Plant and 156 MW of the under-construction Catalan Power Plant.

Besides these hydroelectric power projects, the Bahcelic Project, the purpose of which is irrigation only, is planned for the farthest upstream portion of the Zamanti River.

9 – 1

The gradient of the Zamanti River is gentle at 1/700 to 1/1,000
upstream, but it steepens suddenly 1/40 to 1/100 downstream of the
Camlica I intake dam. The gradient diminishes to 1/500 to 1/1,000
after the Zamanti River and the Goksu River combine to form the
Seyhan River.

The Goktas Project encompasses the downstream portion of the Zamanti
River, where both the river's gradient and the banks' slopes are
steep. For this reason, the topological condition of the project
area is favorable for the construction of a dam-waterway project
with a medium-sized reservoir and a tunnel, but not suitable for
constructing a large reservoir.

(2) Review of Master Plans

The Goktas Project will develop the head between the reservoir water
level of the Goktas Dam that is constructed in the downstream por-
tion of the Zamanti River, and the high-water level of the Kavsak
Reservoir planned immediately downstream of the confluence of the
Zamanti and Goksu Rivers.

The Goktas Project is studied in both the Lower Seyhan Basin Master
Plan and the Upper Seyhan Basin Master Plan. The high-water level
of the Goktas Dam in the former plan is 650 m. In the latter plan,
consideration was given to the possibility of leakage from the
calcareous rock zone proximal to the reservoir's backwater end, and
the high-water level was modified to 630 m accordingly. The Goktas
Project as proposed in the Upper Seyhan Basin Master Plan utilizes a
maximum discharge of 125.5 m^3/sec, which is conducted through a
headrace tunnel 16.4 km in length and 5.5 m in diameter to develop
263.5 MW of generating capacity. The characteristics of the project
in the Upper Seyhan Basin Master Plan are shown in Table 9-3.

A review of the master plan was made based on the field studies. As
a result, the principal modifications are as follows.

o Dam axis I (downstream axis) and axis II (upstream axis) are
   proposed in the master plans. Axis A and axis B, which are
   located between the above two axes, are proposed by DSI. As a
   result of surface reconnaissance, photogeological interpretation,

and studies of 1/1,000-scale topological maps, the vicinity of axis A (slightly upstream of axis A) was selected as the dam axis from the engineering geological and economical standpoints (refer to 7.5.3 Consideration from the Viewpoint of Engineering Geology).

o   Landslides can be expected on the slope where the penstock and powerhouse were planned to be installed in the master plans. Therefore, from the point of view of topology and geology, it is necessary for the power plant site to be changed to a location 500 m upstream from the site in the master plans.

o   Because it was clarified by the power plant site's 1/1,000 topological map that the elevation of the riverbed in front of the powerhouse is higher than the 318.0 m high-water level of the Kavsak Reservoir, the tail-water level was calculated by a water level-discharge curve.

o   Because the loss of head of 80 m in the master plan is excessive against a gross head of 312.00 m and a net head of 231.54 m, the economical tunnel diameter was reexamined.

Table 9-1 Projects Planned in the Lower Seyhan Basin Master Plan

Project	River	Purpose	Catchment Area (Km2)	Reservoir		Dam		Maximum Discharge (m2/s)	Power Plant			Note
				H.W.L. (m)	Gross Volume (x106 m3)	Type	Height (m)		Effective Head (m)	Installed Capacity (MW)	Energy (GWh)	
GOKTAS	ZAMANTI	Energy	8,400	650	211.0	C.G	170.0	116.0	263.0	244.0	1,108.0	
MENGE	GOKSU	"	3,600	525	304.0	R	98.0	166.0	74.4	89.0	247.0	
KOPRU	"	"	4,300	445	260.0	R	135.0	186.0	118.1	189.0	480.9	
KAVSAK	SEYHAN	"	13,000	318	7.4	C.G	36.0	272.8	55.3	120.0	563.8	
YEDIGOZE	"	"	13,830	235	655.0	R	121.0	221.0	93.0	315.0 (300.0)	950.5 (968.8)	
IMAMOGLU	"	Irrigation & Energy	13,922	135	80.0	C.G	43.0	385.0	13.0	40.0 (62.0)	148.0 (196.0)	
CATALAN	"	Flood Control & Energy	15,387	125	2,100.0	R	75.0	310.0	57.4	155.0 (156.0)	508.8 (491.1)	

Note) Dam Type R : Rockfill Dam
       CG: Concrete Gravity Dam

Numbers in the parentheses show the value given in the Upper Seyhan Basin Master Plan Report.

Table 9-2 Projects Planned in the Upper Seyhan Basin Master Plan

Project	River	Purpose	Catchment Area (Km²)	Reservoir		Dam		Power Plant				Note
				H.W.L. (m)	Gross Volume (x10⁶ m³)	Type	Height (m)	Maximum Discharge (m³/s)	Effective Head (m)	Installed Capacity (MW)	Energy (GWh)	
BAHCELIK	ZAMANTI	Irrigation	2,732	1,500	218.0	R	63.0	-	-	-	-	
GUMUSOREN	"	Irrigation & Energy	6,325	1,292	138.9	R	34.0	30.0	20.0	5.0	23.8	
GICIK	"	Energy	6,325	1,270	-	C.G	9.7	30.0	4.0	1.0	-	
CAMLICA I	"	"	7,399	1,190	-	C.G	29.5	58.0	289.2	140.0	524.6	
CAMLICA II	"	"	7,663	860	-	C.G	28.0	67.4	53.4	30.0	132.9	
CAMLICA III	"	"	7,769	795	-	C.G	30.0	62.5	48.0	25.0	123.0	
TATLAR	"	"	7,796	740	-	C.G	39.5	80.1	89.83	60.0	290.8	
INDERE	"	"	146	1,410	60.3	R	47.0	11.2	663.15	62.0	236.3	
TOPAKTAS	"	"	374	670	-	C.G	49.0	22.1	38.0	7.0	344.0	
GOKTAS	"	"	8,400	630	133.3	C.G	139.0	125.5	231.5	263.5	1,186.5	
YAMANLI I	GOKSU	"	602	1,330	-	C.G	23.0	25.0	105.37	22.0	100.6	
YAMANLI II	"	"	1,696	1,170	-	C.G	28.5	43.7	329.31	120.0	393.0	
YAMANLI III	"	"	2,055	760	-	C.G	25.5	29.3	122.66	30.0	175.3	
FEKE	"	"	3,530	610	507.9	R	144.0	159.3	128.0	170.0	426.3	
MENGE	"	"	3,743	480	41.3	C.G	45.0	51.6	33.0	33.0	113.4	

Note) Dam Type R : Rockfill Dam
CG: Concrete Gravity Dam

Table 9-3 Development Scale of Goktas Project in the Upper Seyhan Basin Master Plan

Item	Unit	Development Scale
Catchment Area	km^2	8,400
Reservoir		
High-Water level	m	630
Gross Storage Capacity	$10^6 m^3$	133.34
Effective Storage Capacity	$10^6 m^3$	48.81
Available Drowdown	m	17.69
Power Generating		
Gross Head	m	312.00
Effective Head	m	231.54
Maximum Discharge	m^3/s	125.5
Installed Capacity	MW	263.5
Annual Energy Production	GWh	1,186.5
Dam		
Type	-	Concrete Gravity
Height x Width	m x m	139 x 262
Volume	$10^3 m^3$	914
Waterway		
Tunnel (D x L x n)	mxmxn	5.5 x 16,400 x 1
Penstock (D x L x n)	mxmxn	(4.5 4.0) x 480.0 x 1
Spillway		
Design Flood Discharge	m^3/s	4,078
Powerhouse		
Type	-	Vertical Shaft, Francis
No. of Unit	unit	3

Note: The characteristics above reflect the condition with natural flows

DEVELOPMENT PLAN IN THE SEYHAN RIVER BASIN

LEGEND

IRRIGATION AREA

RESERVOIR

ZAMANTI GÖKTAŞ HYDROELECTRIC POWER DEVELOPMENT PROJECT

DEVELOPMENT PLAN

IN THE SEYHAN RIVER BASIN

Fig. 9-1

9 - 7
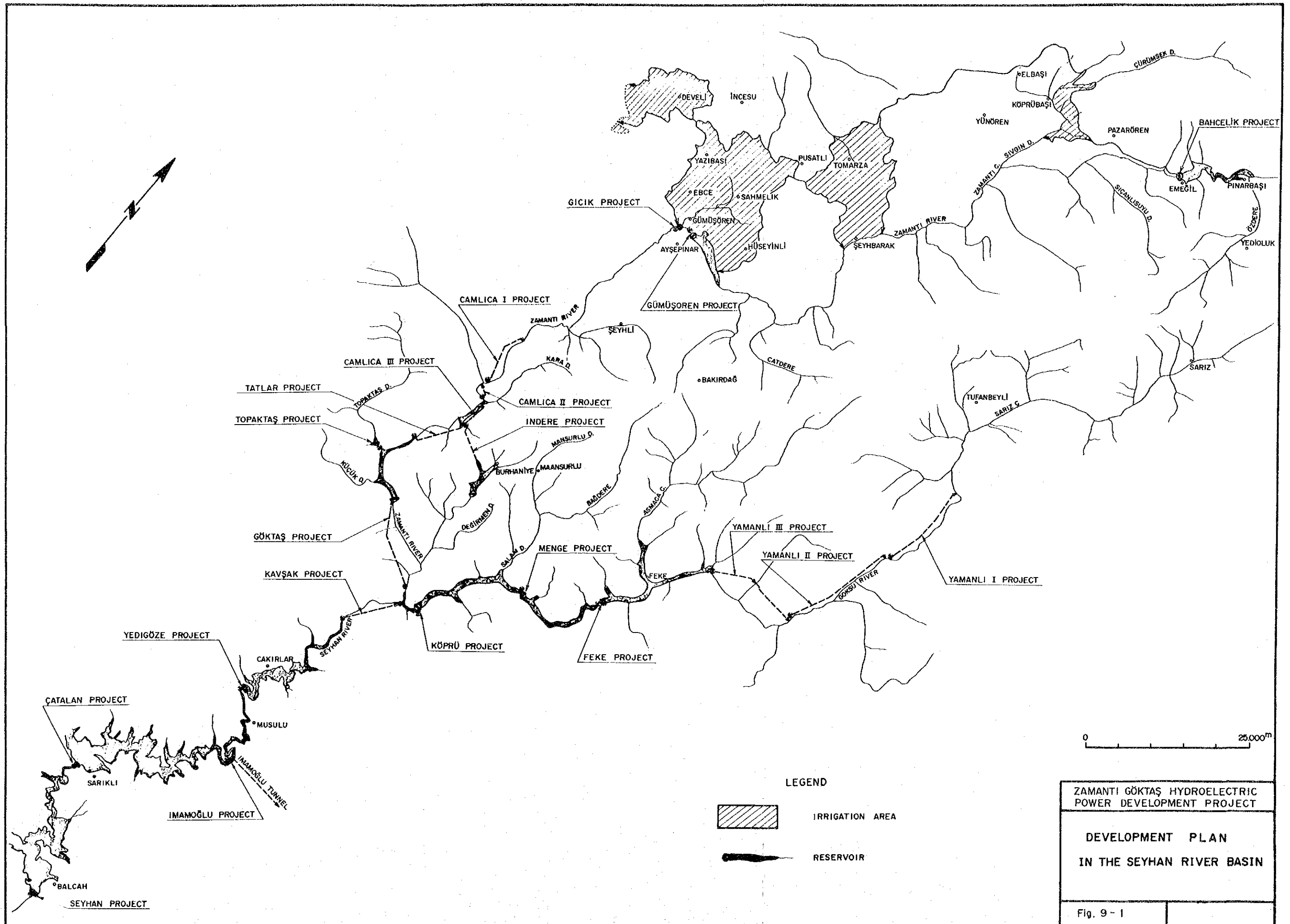
9.1.2 Basic Concept for the Study

Nine power and/or irrigation projects are planned in the Zamanti River upstream of the Goktas Project. Upstream, the Bahcelik and Gumusoren Projects will exert direct effects upon the Goktas scheme, because they have relatively large reservoirs for controlling river discharge and irrigation systems. The Indere Project that is planned for the river of that name will also effect the Goktas Project, because water from the Indere River is scheduled to be discharged upstream of the Goktas Reservoir.

The other projects will have no direct effects upon the Goktas Project, because they are run-of-river projects with very small ponds.

Development is divided into the following three stages in the Upper Seyhan Basin Master Plan.

(1) First Stage

No projects are considered in the river. River discharge continues under natural flow conditions.

(2) Second Stage

The Gumusoren and Indere Projects are in operation but irrigation water is not yet taken from the Gumusoren Reservoir.

(3) Third Stage

The Bahcelik Project is in operation and irrigation water is taken from the Gumusoren and Bahcelik Reservoir.

Because the study on the Bahcelik, the Gumusoren and the Indere Projects are under preparation and their development time is not clear, both the development type and scale will be studied under natural flow conditions (First Stage).

The economic condition of the project that is selected by the above study will be studied under Second and Third Stage Condition.

The basic values — such as the high-water level, reservoir storage capacity, maximum discharge, irrigation water etc., that are deter-

mined in the "Upper Seyhan Basin Master Plan" -- are adopted in this study.

The regulated outflow from the Gumusoren Reservoir at second stage is shown in Table 9-4, the inflow to the Gumusoren Reservoir at third stage is shown in Table 9-5, the regulated outflow from the Gumusoren Reservoir at third stage is shown Table 9-6, and the power discharge through the Indere Powerhouse at second stage and third stage is shown in Table 9-7.

A study was made using 1/5,000 maps, and a study for selected fundamental plan was made using 1/1,000 map.

Table 9-4 Regulated Monthly Outflow from the Gumusoren Reservoir (Stage II)

(Unit: 10^6 m^3)

YEAR	JAN	FEB	MAR	APR	MAY	JUN	JUL	AUG	SEP	OCT	NOV	DEC	TOTAL
1940	35.84	36.16	55.99	74.68	77.17	52.41	40.40	40.40	39.10	40.40	39.10	40.40	572.05
1941	40.40	47.40	90.87	87.93	87.97	44.30	39.62	39.62	38.34	39.62	38.34	39.62	634.05
1942	39.62	35.79	67.47	90.59	93.61	41.50	37.99	37.99	36.77	37.99	36.77	37.99	594.09
1943	37.99	34.32	37.99	75.98	78.52	45.14	33.69	33.49	32.61	33.69	32.61	33.69	509.94
1944	33.69	31.52	41.35	40.01	41.35	36.93	31.79	31.79	30.77	31.79	30.77	31.79	413.54
1945	31.79	28.72	31.79	30.77	31.79	30.68	28.51	28.51	27.59	28.51	27.59	28.51	354.73
1946	28.51	25.75	28.51	27.59	28.51	27.59	28.51	28.51	27.59	28.51	27.59	28.51	335.66
1947	28.51	25.75	28.51	27.59	28.51	27.59	28.51	28.51	27.59	28.51	27.59	28.51	335.66
1948	33.09	26.67	28.51	55.47	57.32	50.81	33.09	33.09	32.02	33.09	32.02	33.09	443.70
1949	30.06	29.09	33.09	32.02	33.09	29.09	30.06	30.06	29.09	30.06	29.09	30.06	360.68
1950	27.40	27.15	31.12	35.14	36.31	26.52	27.40	27.40	26.52	27.40	26.52	27.40	348.95
1951	27.40	24.75	27.40	26.52	27.40	26.52	27.40	27.40	26.52	27.40	26.52	27.40	322.64
1952	31.79	31.23	57.44	69.29	69.40	37.04	31.79	31.79	30.76	31.79	30.76	31.79	400.47
1953	35.20	20.71	31.79	64.42	66.57	49.37	35.20	35.20	34.07	35.20	34.07	35.20	481.59
1954	48.27	31.80	76.84	125.34	129.52	71.31	52.04	48.27	46.71	48.27	46.71	48.27	760.27
1955	34.43	43.60	48.27	46.71	48.27	33.32	34.43	34.43	33.32	34.43	33.32	34.43	472.70
1956	34.29	32.21	43.56	58.13	60.06	41.14	34.29	34.29	33.18	34.29	33.18	34.29	473.03
1957	28.76	30.97	37.09	35.90	37.09	35.90	28.76	28.76	27.83	20.76	27.83	20.76	301.94
1958	36.75	25.90	38.46	56.90	58.80	56.90	36.75	36.75	35.56	36.75	35.56	36.75	483.90
1959	34.53	33.19	45.29	43.83	45.29	43.03	34.53	34.53	33.42	34.53	33.42	34.53	453.15
1960	29.81	39.51	42.23	75.78	78.31	42.69	33.88	32.06	29.63	29.81	28.84	29.81	497.02
1961	24.97	26.92	29.81	28.84	29.81	28.84	24.97	24.97	24.17	24.97	24.17	24.97	322.26
1962	40.61	22.56	45.29	43.83	45.29	33.06	34.16	34.16	33.06	34.16	33.06	34.16	417.76
1963	47.99	36.60	59.11	79.43	82.08	79.43	57.36	47.99	46.44	47.99	46.44	47.99	671.56
1964	33.64	44.89	57.02	55.18	57.02	43.53	33.64	33.64	32.56	33.64	32.56	33.64	505.32
1965	49.91	30.39	83.09	80.41	83.09	51.96	46.25	46.25	44.76	46.25	44.76	46.25	637.10
1966	45.67	51.09	73.09	70.73	73.09	47.49	45.67	45.67	44.20	45.67	44.20	45.67	636.46
1967	55.04	41.25	54.58	128.16	132.43	66.44	55.49	55.04	53.27	55.04	53.27	55.04	795.67
1968	62.01	51.49	137.15	210.73	147.35	93.20	62.01	62.01	60.01	62.01	60.01	62.01	1063.01
1969	60.76	56.01	157.59	158.88	164.18	101.13	66.79	60.76	58.80	60.76	58.80	60.76	1066.49
1970	44.16	62.94	84.73	81.99	84.73	58.10	44.16	44.16	42.73	44.16	42.73	44.16	695.36
1971	34.72	39.09	48.72	47.15	48.72	44.21	34.72	34.72	33.60	34.72	33.60	34.72	478.96
1972	39.66	32.48	49.51	60.94	62.97	60.94	39.66	39.66	38.38	39.66	38.38	39.66	536.96
1973	30.70	35.82	39.66	38.38	39.66	30.20	28.16	28.16	27.26	28.16	27.26	28.16	390.55
1974	27.48	28.07	39.56	38.28	39.56	26.17	27.04	27.04	26.17	27.04	26.17	27.04	362.83
1975	37.48	24.42	69.41	120.77	133.06	70.04	39.59	37.48	36.27	37.48	36.27	37.48	677.33
1976	40.87	35.07	58.66	111.03	114.73	66.80	40.87	40.87	39.56	40.87	39.56	40.87	666.38
1977	40.71	54.92	92.04	109.67	113.33	61.65	40.71	40.71	39.40	40.71	39.40	40.71	714.13
1978	54.59	51.63	77.28	88.11	91.04	60.33	43.78	43.78	42.37	43.78	42.37	43.99	669.19
1979	44.76	59.46	65.83	63.71	65.03	63.71	43.44	43.44	42.04	43.44	42.04	43.44	630.95
1980	54.18	43.27	96.66	178.14	184.07	96.34	54.18	54.18	52.43	54.18	52.43	54.18	964.81
1981	62.98	48.93	113.18	109.53	113.18	109.53	53.35	53.35	51.63	53.35	51.63	62.98	1074.02
1982	62.98	58.03	64.25	122.56	126.65	67.37	44.32	44.32	42.89	44.32	42.89	44.32	764.91
TOTAL	1669.10	1607.26	2519.77	3215.06	3246.73	2211.03	1669.00	1645.44	1590.96	1643.18	1590.18	1653.02	24260.74
MEAN	38.82	37.38	58.60	74.77	75.51	51.42	38.81	38.27	37.00	38.21	36.98	38.44	564.20
MAX	62.98	62.94	157.59	210.73	184.07	109.53	66.79	62.01	60.01	62.01	60.01	62.98	1066.49
MIN	24.97	22.56	27.40	26.52	27.40	26.17	24.97	24.97	24.17	24.97	24.17	24.97	322.26

Table 9.5　Monthly Inflow to the Gumusoren Reservoir (Stage III)

(Unit: 10^6 m^3)

YEAR	JAN	FEB	MAR	APR	MAY	JUN	JUL	AUG	SEP	OCT	NOV	DEC	TOTAL
1940	14.93	15.54	26.97	75.71	41.65	25.84	13.79	10.51	9.08	7.97	11.36	13.01	267.16
1941	11.13	18.96	45.75	84.10	46.01	17.09	12.42	10.81	9.60	10.16	9.77	6.93	263.53
1942	4.36	6.85	26.06	81.27	50.75	14.91	7.92	6.76	6.72	8.38	16.58	13.87	244.44
1943	8.99	5.07	6.16	60.58	56.69	19.57	5.88	4.58	4.71	4.84	4.05	6.14	105.05
1944	6.43	4.06	16.65	32.98	34.60	10.18	2.89	3.03	3.30	5.39	5.33	5.39	130.23
1945	5.94	5.36	6.59	30.65	24.59	9.43	5.15	4.23	3.06	4.01	3.96	4.44	108.22
1946	3.90	4.04	7.66	18.03	18.40	5.54	4.34	3.69	3.62	4.82	3.06	3.96	81.05
1947	3.93	4.09	18.01	15.86	6.07	9.11	5.29	3.61	3.88	3.88	5.14	5.69	84.56
1948	5.94	4.07	6.10	40.18	47.34	21.45	9.08	6.54	5.46	5.15	4.72	5.04	161.87
1949	5.23	5.04	12.39	26.54	25.67	5.77	3.05	3.63	3.62	3.80	3.80	4.26	103.61
1950	4.69	4.53	8.70	24.16	38.58	6.99	3.36	2.69	2.47	2.69	2.55	2.69	104.09
1951	2.77	2.53	16.73	8.87	14.22	10.87	3.88	2.66	2.55	2.77	2.55	2.82	73.21
1952	4.23	9.37	24.29	71.90	32.01	13.20	7.93	5.53	5.14	4.50	4.07	4.36	186.49
1953	4.72	4.60	5.58	60.65	30.26	20.58	9.60	6.70	5.93	5.75	5.56	5.45	173.47
1954	5.39	8.05	35.99	104.66	71.75	33.06	22.17	17.14	16.54	17.08	17.61	17.62	360.67
1955	19.22	17.19	19.20	31.51	38.95	13.96	10.67	10.97	9.83	9.45	9.07	11.31	201.34
1956	9.00	13.30	19.96	49.41	34.05	18.22	10.93	7.94	6.45	14.13	13.67	10.97	200.14
1957	9.37	9.37	34.60	24.64	23.87	19.50	8.63	6.10	7.02	7.10	6.52	6.51	163.33
1958	6.40	0.20	17.18	58.01	35.98	28.88	13.65	13.57	12.13	12.31	11.19	11.31	228.81
1959	10.82	6.99	30.44	41.40	28.10	21.19	11.49	9.63	9.18	10.23	9.97	8.93	190.30
1960	9.04	18.57	18.63	74.70	41.66	20.40	15.43	14.28	12.08	10.79	10.33	9.11	255.82
1961	9.15	9.27	14.02	20.18	12.24	14.00	7.63	4.43	4.29	4.13	4.29	5.88	109.51
1962	3.69	4.74	38.73	34.82	26.73	13.21	9.41	9.00	8.10	8.33	7.81	12.46	177.03
1963	18.66	16.12	28.88	61.43	54.74	45.79	28.84	21.78	19.54	19.26	17.63	16.69	349.37
1964	13.02	12.00	49.47	40.28	30.22	20.87	11.60	9.78	10.91	10.12	8.96	10.34	227.57
1965	8.69	7.46	54.22	63.08	46.79	25.68	18.11	15.24	13.31	14.91	14.72	17.29	299.71
1966	23.61	24.78	38.25	44.09	44.93	23.17	18.44	15.54	17.02	16.69	15.62	18.96	321.09
1967	16.04	13.43	26.28	96.49	80.68	33.88	27.62	23.31	19.68	20.30	20.15	22.60	401.26
1968	18.63	22.71	73.62	153.23	80.05	49.24	29.88	27.84	23.74	24.35	23.89	29.43	556.61
1969	26.75	22.53	78.40	86.13	134.49	54.78	33.50	25.63	21.62	18.03	13.55	23.33	540.74
1970	22.31	31.24	54.52	72.57	54.75	33.96	16.93	11.80	11.15	17.34	10.12	17.49	362.19
1971	17.69	11.51	24.77	46.35	47.22	21.58	6.53	6.97	7.54	8.53	9.96	13.62	222.20
1972	10.47	10.63	24.17	41.19	38.61	33.86	14.13	4.25	8.80	13.09	12.54	17.12	228.07
1973	22.56	12.06	22.54	41.08	30.11	11.43	2.85	1.75	3.05	3.84	5.51	9.48	175.07
1974	17.49	15.78	26.00	20.98	27.49	3.70	1.61	1.92	4.98	7.88	8.10	8.07	144.00
1975	10.95	9.61	39.54	57.79	50.55	35.62	11.63	7.73	11.07	8.09	9.80	10.24	262.62
1976	10.90	8.71	37.58	74.49	80.56	32.27	5.11	3.01	6.29	11.56	17.12	22.46	310.08
1977	16.74	22.07	49.96	78.16	80.22	32.33	12.52	8.79	8.30	6.44	12.60	15.33	343.44
1978	18.14	19.65	30.60	59.73	78.19	34.75	11.08	8.00	11.66	10.66	14.88	21.28	318.63
1979	31.07	26.04	34.88	52.33	46.93	40.58	11.42	3.15	6.25	5.20	23.47	20.96	303.10
1980	27.70	24.68	46.38	94.85	139.63	59.80	25.14	12.39	15.70	25.05	16.93	21.41	509.65
1981	16.03	17.29	75.49	80.78	87.18	69.65	22.30	11.02	7.00	12.06	16.17	42.83	457.00
1982	23.89	40.72	23.61	88.38	88.25	35.21	11.93	6.11	15.02	12.24	14.83	4.06	364.27
TOTAL	541.66	560.60	1295.55	2446.99	2118.58	1071.89	526.58	394.07	399.78	434.17	469.12	541.15	10800.15
MEAN	12.60	13.04	30.13	56.91	49.27	24.93	12.25	9.16	9.30	10.10	10.91	12.58	251.17
MAX	31.07	40.72	78.40	153.23	139.63	69.65	33.50	27.84	23.74	25.05	23.89	42.83	556.61
MIN	2.77	2.53	5.58	8.87	6.07	3.70	1.61	1.75	2.47	2.69	2.55	2.69	73.21

Table 9-6 Regulated Monthly Outflow from the Gumusoren Reservoir (Stage III)

(Unit: 10^6 m^3)

YEAR	JAN	FEB	MAR	APR	MAY	JUN	JUL	AUG	SEP	OCT	NOV	DEC	TOTAL
1940	12.68	11.86	12.68	12.27	12.68	12.27	12.68	12.68	12.27	12.68	12.27	12.68	149.72
1941	12.68	16.04	18.65	18.05	18.65	9.40	9.71	9.71	9.40	9.71	9.40	9.71	151.91
1942	9.71	8.77	11.76	11.38	11.76	7.16	7.40	7.40	7.16	7.40	7.16	7.40	104.45
1943	7.40	6.60	7.40	7.16	7.40	0.0	0.0	0.0	0.0	0.0	1.60	1.65	47.41
1944	1.65	1.54	1.65	1.60	1.65	0.0	0.0	0.0	0.0	0.0	0.0	0.0	8.09
1945	0.0	0.0	0.0	0.0	0.0	0.0	0.0	0.0	0.0	0.0	0.0	0.0	0.0
1946	0.0	0.0	0.0	0.0	0.0	0.0	0.0	0.0	0.0	0.0	0.0	0.0	0.0
1947	0.0	0.0	0.0	0.0	0.0	0.0	0.0	0.0	0.0	0.0	0.0	0.0	0.0
1948	0.0	0.0	0.0	0.0	0.0	0.0	0.0	0.0	0.0	0.0	0.0	0.0	0.0
1949	0.0	0.0	0.0	0.0	0.0	0.0	0.0	0.0	0.0	0.0	0.0	0.0	0.0
1950	0.0	0.0	0.0	0.0	0.0	0.0	0.0	0.0	0.0	0.0	0.0	0.0	0.0
1951	0.0	0.0	0.0	0.0	0.0	0.0	0.0	0.0	0.0	0.0	2.42	2.82	5.24
1952	4.23	4.22	4.51	4.36	4.51	4.36	4.51	4.51	4.36	4.51	4.36	4.51	52.97
1953	4.51	4.07	4.51	4.36	4.51	4.36	4.51	4.51	4.36	4.51	5.35	5.53	55.11
1954	5.53	8.05	30.14	29.16	30.14	11.81	12.20	12.20	11.81	12.20	11.81	12.20	107.24
1955	12.20	11.02	12.20	10.93	11.29	5.98	6.31	6.31	6.11	6.31	6.11	6.31	101.21
1956	6.31	5.90	6.31	6.11	6.31	5.98	6.18	6.18	5.98	6.18	5.98	6.18	73.62
1957	6.18	5.58	6.18	5.98	6.18	5.98	6.18	6.18	5.98	6.18	5.98	6.18	72.78
1958	6.18	5.58	6.18	5.98	6.18	5.98	6.18	6.18	5.98	6.18	5.98	6.18	72.78
1959	6.18	5.58	6.18	5.98	9.36	9.06	9.36	9.36	9.06	9.36	9.06	9.36	97.93
1960	9.36	8.76	9.36	9.06	9.36	4.70	4.85	4.85	4.70	4.85	4.70	4.85	79.41
1961	4.05	4.30	4.85	2.22	2.29	2.22	2.29	2.29	2.22	2.29	3.20	3.31	36.43
1962	3.31	2.99	3.31	3.20	3.31	3.20	3.31	3.31	3.20	4.05	7.40	12.46	53.02
1963	15.38	13.09	15.38	14.88	15.38	14.88	15.38	15.38	14.88	15.38	14.88	15.38	181.07
1964	15.38	14.39	15.38	14.88	10.27	9.94	10.27	10.27	9.94	10.27	9.94	10.27	141.23
1965	10.27	9.28	15.92	15.40	15.92	15.40	15.92	15.92	15.40	15.92	15.40	16.39	177.15
1966	16.39	14.01	16.39	15.86	16.39	15.86	16.39	16.39	15.86	16.39	15.86	16.96	193.56
1967	16.96	15.32	26.28	26.74	27.63	22.59	23.34	23.34	22.59	23.34	22.59	23.34	274.04
1968	23.34	22.71	65.87	63.74	54.09	28.09	29.03	29.03	28.09	29.03	28.09	29.03	430.15
1969	29.03	26.22	60.08	58.15	60.08	29.92	25.04	25.04	24.23	25.04	24.23	25.04	412.11
1970	25.04	22.62	25.04	24.23	25.04	12.20	12.69	12.69	12.28	12.69	12.28	12.69	209.59
1971	12.69	11.46	12.69	12.20	12.69	7.83	8.09	8.09	7.83	8.09	7.83	8.09	117.65
1972	8.09	7.56	8.09	7.83	8.09	7.83	8.09	8.09	7.83	8.09	7.83	8.09	95.48
1973	8.09	7.30	8.09	7.03	8.09	2.16	2.23	2.23	2.16	2.23	2.16	2.23	54.77
1974	2.23	2.01	2.23	2.16	2.23	2.16	2.23	2.23	2.16	3.49	7.89	8.15	39.14
1975	10.80	9.76	11.57	11.19	11.57	11.19	11.57	11.57	11.19	11.57	11.19	11.57	134.72
1976	11.57	10.62	23.55	22.79	23.55	11.07	11.43	11.43	11.07	11.43	16.89	19.60	185.20
1977	19.60	22.07	28.00	27.07	28.00	12.94	13.37	13.37	12.94	13.37	12.94	15.33	221.41
1978	17.08	15.43	17.08	16.53	17.08	14.47	14.96	14.96	14.47	14.96	14.88	15.51	107.42
1979	15.51	14.01	15.51	15.01	15.51	15.01	12.18	12.18	11.78	12.18	21.71	22.44	103.00
1980	27.06	25.32	46.38	54.07	56.70	34.94	21.98	21.98	21.27	21.98	21.27	21.98	375.72
1981	21.98	19.05	42.08	40.72	42.00	40.72	18.41	18.41	17.81	18.41	17.01	31.45	329.71
1982	31.45	28.41	31.45	30.44	31.45	12.27	12.68	12.68	12.27	12.68	12.27	12.68	240.74
TOTAL	450.90	425.00	633.72	621.20	628.22	415.74	382.59	382.59	370.25	384.59	400.73	437.54	5533.16
MEAN	10.49	9.89	14.74	14.45	14.61	9.67	8.90	8.90	8.61	8.94	9.32	10.18	128.68
MAX	31.45	28.41	65.87	63.74	60.08	40.72	29.03	29.03	28.09	29.03	28.09	31.45	430.15
MIN	0.0	0.0	0.0	0.0	0.0	0.0	0.0	0.0	0.0	0.0	0.0	0.0	0.0

Table 9-7 Monthly Power Discharge from the Indere Powerhouse (Stage II, III)

(Unit: 10^6 m^3)

YEAR	JAN	FEB	MAR	APR	MAY	JUN	JUL	AUG	SEP	OCT	NOV	DEC	TOTAL
1940	11.88	13.22	14.13	13.68	14.13	13.68	14.13	14.13	13.68	14.13	13.68	14.13	164.61
1941	14.13	12.77	14.13	13.68	14.13	13.68	14.13	14.13	13.68	14.13	13.68	14.13	166.41
1942	14.13	12.77	15.96	15.44	15.96	15.44	15.96	15.96	15.44	15.96	15.44	15.96	184.43
1943	15.96	14.41	15.96	15.44	15.96	15.75	15.96	15.96	15.44	15.96	15.44	15.96	187.90
1944	15.96	16.35	17.48	16.92	17.48	15.75	13.48	13.48	13.05	13.48	13.05	13.48	179.97
1945	13.48	12.10	13.48	13.05	13.48	13.05	13.48	13.48	13.05	13.48	13.05	13.48	150.77
1946	13.48	12.10	13.48	13.05	13.48	13.05	13.48	13.48	13.05	13.48	13.05	13.48	150.77
1947	13.48	12.10	13.48	13.05	13.48	13.05	13.48	13.48	13.05	13.48	15.64	16.17	164.04
1948	16.17	15.12	16.17	15.64	16.17	15.64	12.72	11.86	11.47	11.86	11.47	11.86	166.15
1949	11.86	10.71	11.86	11.47	11.86	11.26	11.31	11.31	10.94	11.31	10.94	12.31	136.13
1950	11.31	10.21	11.31	10.94	11.31	10.94	11.31	11.31	10.94	11.31	10.94	11.31	133.14
1951	11.31	10.21	11.31	10.94	11.31	10.94	11.31	11.31	10.94	11.31	10.94	11.31	133.14
1952	11.31	13.52	15.01	15.30	15.01	15.30	15.81	15.81	15.30	15.01	15.30	15.81	100.91
1953	16.92	17.95	19.07	19.23	19.07	19.23	16.06	16.06	15.54	16.06	15.54	16.06	200.36
1954	16.06	14.50	16.06	15.54	16.06	15.13	12.97	12.97	12.55	12.97	12.55	12.97	170.35
1955	12.97	11.72	12.97	12.55	12.97	11.61	11.98	11.90	11.60	11.98	11.60	11.90	145.92
1956	11.98	11.21	11.98	11.60	11.98	11.60	11.98	11.98	11.60	11.98	11.60	11.98	141.47
1957	11.98	10.82	11.98	11.60	11.98	11.60	11.98	11.98	11.60	11.98	11.60	14.58	143.69
1958	14.58	13.17	14.58	14.11	14.58	12.01	12.19	12.19	11.79	12.19	11.79	12.19	155.37
1959	12.19	11.01	12.19	11.79	12.19	11.79	12.19	12.19	11.79	11.91	11.79	11.91	143.48
1960	12.19	11.40	12.19	11.79	12.19	11.64	11.91	11.91	11.52	11.91	11.52	11.91	142.06
1961	11.91	10.75	11.91	11.52	11.91	11.52	11.91	11.91	11.52	11.91	11.52	11.91	140.18
1962	11.91	12.45	13.78	13.34	13.78	13.34	13.78	13.78	13.34	13.78	13.34	14.78	161.40
1963	14.78	13.35	14.78	14.30	14.78	14.30	14.62	12.91	12.49	12.91	12.49	12.91	164.62
1964	12.91	12.08	12.91	12.49	12.91	12.49	12.91	12.91	12.49	12.91	12.49	12.91	152.43
1965	12.91	11.91	15.88	15.36	15.88	15.36	15.88	15.88	15.36	16.18	15.36	15.80	181.53
1966	16.18	14.61	16.18	15.66	16.18	15.66	16.18	16.18	15.66	16.18	15.66	16.18	190.51
1967	16.18	14.61	16.77	16.23	16.77	16.23	16.77	16.77	16.23	16.77	16.23	16.77	196.33
1968	16.77	15.49	17.06	16.51	17.06	16.51	17.06	17.06	16.51	17.06	16.51	17.06	200.03
1969	17.06	15.41	17.06	16.51	17.06	14.67	12.78	12.58	12.17	12.58	12.17	12.58	172.62
1970	12.58	11.36	12.58	11.06	11.43	11.06	11.43	11.43	11.06	11.43	11.06	11.43	137.91
1971	11.43	10.32	11.43	11.06	11.43	11.06	11.43	10.54	10.20	10.54	10.20	10.54	130.16
1972	10.54	9.86	10.54	10.20	10.54	10.20	10.54	10.06	9.73	10.06	9.73	10.06	122.52
1973	10.06	9.09	10.06	9.73	10.06	9.73	10.06	10.06	9.73	10.06	9.73	10.06	118.43
1974	10.06	9.09	10.06	9.73	10.06	9.73	10.06	10.06	9.73	10.06	9.73	10.43	118.00
1975	10.43	9.42	12.36	11.96	12.36	11.96	12.36	12.36	11.96	12.36	11.96	12.36	141.81
1976	12.36	11.56	12.36	11.96	12.36	11.96	12.36	12.36	11.96	12.36	11.96	12.36	145.80
1977	12.36	11.16	12.36	11.96	12.36	11.96	12.36	12.36	11.96	12.36	11.96	12.36	145.48
1978	12.36	11.16	12.36	11.96	12.36	11.96	12.36	12.36	11.96	12.36	11.96	12.36	145.48
1979	12.36	11.16	12.36	11.96	12.36	11.96	12.36	12.36	11.96	12.36	11.96	12.77	145.09
1980	12.77	11.94	12.77	12.36	12.77	12.36	12.77	12.77	12.36	12.77	12.36	12.77	150.74
1981	13.09	12.55	13.89	12.96	11.97	11.58	11.97	11.97	11.58	11.97	11.58	11.97	147.90
1982	11.97	10.81	11.97	11.58	11.97	11.58	11.97	11.97	11.58	11.97	11.58	11.97	140.94
TOTAL	567.07	527.95	587.78	567.21	584.70	559.02	561.72	558.05	539.59	557.57	542.18	564.63	6717.49
MEAN	13.19	12.28	13.67	13.19	13.60	13.00	13.06	12.98	12.55	12.97	12.61	13.13	156.22
MAX	17.06	17.95	19.87	19.23	19.87	19.23	17.06	17.06	16.51	17.06	16.51	17.06	200.36
MIN	10.06	9.09	10.06	9.73	10.06	9.73	10.06	10.06	9.73	10.06	9.73	10.06	118.43

9.1.3 Basic Condition for the Study

(1) Fundamental View

The cost of the alternative thermal power plant (which would be built if the Goktas Project is not constructed) is used as the benefit of the Goktas Project, in judging the development type and scale of the project.

An imported coal-fired thermal power plant, which will be supposed to be the future main electric power plant, is adopted as the alternative thermal power plant to be installed in Yumurtalik (located 40 km southeast of Adana City) with an installed capacity of 300 MW.

The annual surplus benefit (B-C) and benefit cost ratio (B/C) obtained from equalized annual costs (C) for the project life (50 years) of the hydropower facility, and the equalized annual cost (B) of the alternative thermal facilities having a capacity equivalent to the hydropower facilities are used in the study as the indices. Market prices without import taxes are used in the comparisons.

Parameters of the alternative thermal plant are as shown in Table 9-8.

With regard to construction cost and fuel cost, they were decided from standard international prices taking into account the situation in Turkey.

The costs of the transmission line between the Goktas Powerhouse and Adana City and the transmission line between the alternative thermal power plant and Adana City are omitted since their influence on the evaluation of the project is small.

(2) Equalized Annual Cost

The equalized annual cost of a hydropower facility consists of depreciation and operation-maintenance cost. This is estimated by multiplying the annual cost factor by the investment cost.

Equalized Annual Cost = Annual Cost Factor x Investment Cost
= Depreciation + Interest
+ Operation and Maintenance Cost

Depreciation + Interest = Investment Cost x
Capital Recovery Factor

° Capital Recovery Factor $= \dfrac{i(1+i)^n}{(1+i)^n - 1}$

- n: Service Life

Civil Facility	50 years
Hydro-mechanical Facility	35 years
Electro-mechanical Facility	35 years

- i: Discount Rate   9.5%

Civil Facility	9.6%
Hydro-mechanical Facility	9.9%
Electro-mechanical Facility	9.9%

° Operation and Maintenance Cost (Rate to Direct Cost)

Civil Facility	0.5%
Hydro-mechanical Facility	1.5%
Electro-mechanical Facility	1.5%

The Goktas Dam is planned as a concrete arch gravity dam in this study.

(3) Benefit

The benefit of the project is summarized according to the project cost, maintenance and operation costs, and the fuel cost of an alternative thermal-power plant. The effective power output and effective energy that are used to calculate the advantages of the project are given according to the below conditions.

(a) The effective power output at the receiving end is expressed by the below equation. This equation reduces the station service rate by 0.3%, the forced outage rate by 0.3%, the scheduled outage rate by 2.0%, and the transmission loss rate by 2.1% from the firm peak output. The firm peak output is defined as the average of 12 monthly minimum power outputs for a study period. This is because a 95% output figure gives too small a firm output under Turkish

river discharge conditions where the wet season is different in each area.

Effective power output = (1 - 0.003) * (1 - 0.003) *
                         (1 - 0.02) * (1 - 0.021) *
                         Firm peak output

(b) The effective energy at the receiving end is expressed by the below equation that reduces the station service rate by 0.3% and transmission loss rate by 1.4% from the average energy for the 43-year period.

Effective Energy = (1 - 0.003) * (1 - 0.014) *
                   Average annual energy

Table 9-8 Alternative Thermal Power Plant for Optimization Study

Interest Rate = 9.5%

Item	Unit	Description
Type		Coal Fired Power Plant
Installed Capacity	MW	300
Annual Plant Factor	%	70
Thermal Efficiency	%	38.3
Annual Energy Production	GWh	1,839.6
Investment Cost	10^6 TL	429,000
Service Life	Years	25
Construction Period	Years	4
Capital Recovery Factor		0.10596
Coal Calorific Value	Kcal/kg	6,500
Coal Surface Moisture	%	7
Oil Calorific Value	Kcal/kg	10,500
Fuel Consumption Rate (Coal 95%)	kg/kWh	0.353
Fuel Consumption Rate (Oil 5%)	kg/kWh	0.011
O & M Cost, Administration Cost	%	3.0
Unit Fuel Cost (Coal)	TL/kg	58.5
Unit Fuel Cost (Oil)	TL/kg	139.1

Annual Cost		Fixed Cost	Variable Cost
Capital Recovery	10^6 TL	45,456.8	—
O & M Cost, Administration Cost	10^6 TL	11,583.0	1,287.0
Fuel Cost	10^6 TL	—	40,803.4
Total	10^6 TL	57,039.8	42,090.4

Annual Cost at Receiving End
  kW   Cost
  kWh Cost
	
	TL/kW
	TL/kWh
		1)
		241,850
			
			2)
			24.69

1) $\dfrac{57,039.8 \times 10^6 \text{ TL}}{300,000 \text{ kW}} \times 1.272 \overset{3)}{} = 241,850$

2) $\dfrac{42,090.4 \times 10^6 \text{ TL}}{1,839.6 \times 10^6 \text{ kWh}} \times 1.079 \overset{3)}{} = 24.69$

3) Adjustment Factor for kW & kWh

Item	kW	kWh
Transmission Loss Rate (%)	1.4	1.1
Station Service Rate (%)	5.6	6.3
Forced Outage Rate (%)	4.0	—
Scheduled Outage Rate (%)	12.0	—

$$\text{kW Adjustment Factor} = \frac{1}{(1 - 0.014) \times (1 - 0.056) \times (1 - 0.04) \times (1 - 0.12)}$$

$$= 1.272$$

$$\text{kWh Adjustment Factor} = \frac{1}{(1 - 0.011) \times (1 - 0.063)} = 1.079$$

9.1.4 Reservoir Operation Plan

The mean annual discharge at Goktas Dam Site is 54 m^3/s. Forty-two percent of this annual discharge is concentrated in the three months from March to May, the season of snow-melting and rain. The total discharge during the dry season, from August to October, is 15% of the annual total discharge; thus, the seasonal variation in the river discharge is relatively small. Because the topographical condition of the project area is very steep and the valley is narrow, it is difficult to construct a large reservoir. But, because the flow regime is good, inflow control effect can be expected with a small reservoir.

The reservoir operational calculation is performed by computer, based on the monthly average discharge, for the period of 43 years from January 1940 to December 1982.

The firm discharge is defined as the minimum discharge available for power generation for 43 years. The firm discharge is obtained by making the power discharge the largest using the discharge mass curve. The discharge mass curve and relationship between the effective storage capacity and the firm discharge are shown in Figs. 9-2 and 9-3.

The efficiency variation of turbine and generator will be taken into account, in the energy calculation, depending on the variation of the reservoir surface level. The mean reservoir water level (high-water level - 1/3 available drawdown) is adopted as the standard intake water level used to design the turbine and generator.

The procedure of the power and energy calculation is shown in Fig. 9-4. The rule adopted for comparison of the development type and scale is the mass curve rule, which delineates ideal reservoir operation. Evaporation from the reservoir surface is ignored in these calculations.

Fig.9-2   MASS CURVE AT GOKTAS DAM SITE

Fig.9-3   Firm Discharge and Effective Storage Capacity
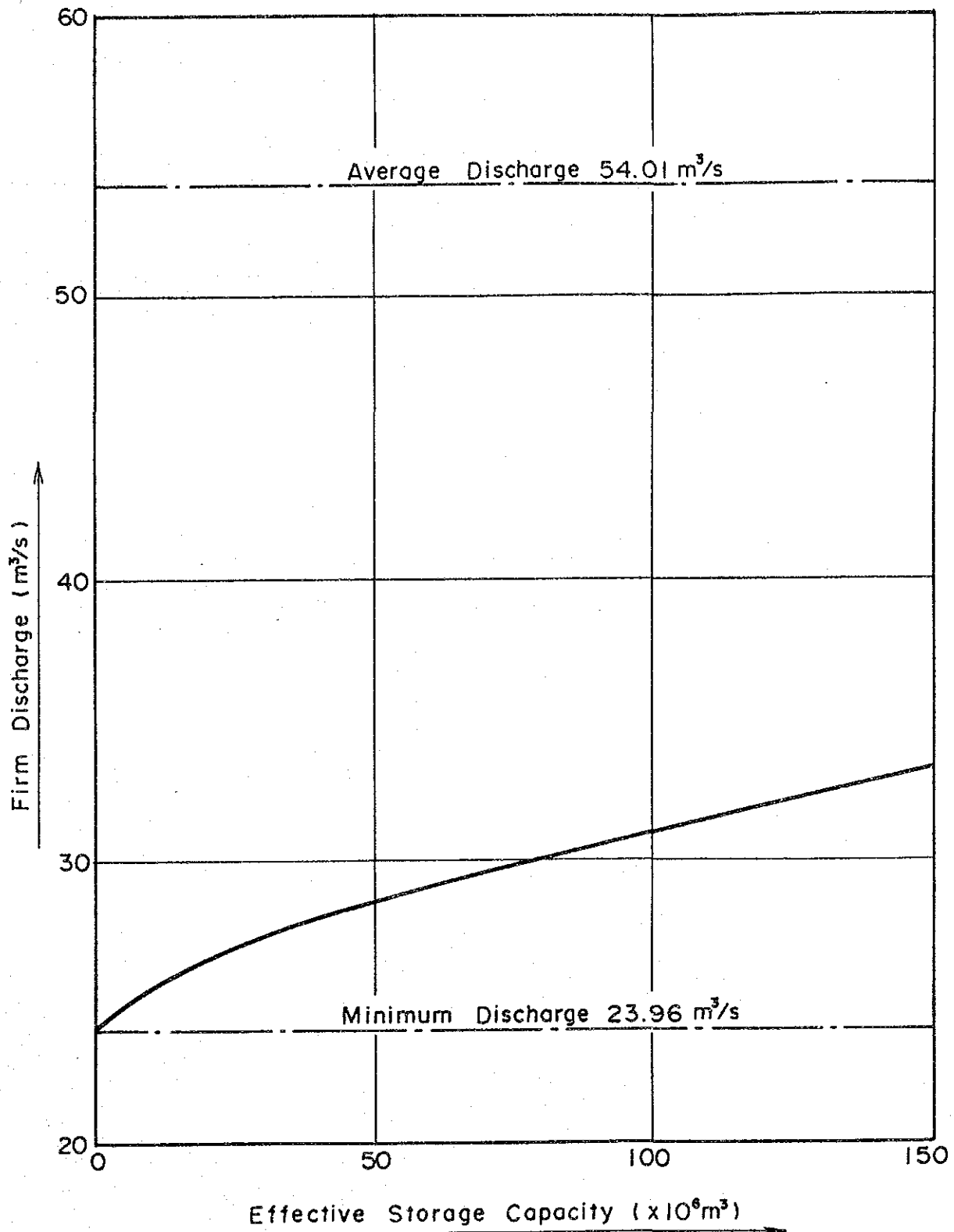
Fig. 9-4 Flow Chart of Power and Energy Calculation

```
                    ┌─────────────────┐
                    │   Runoff Data   │
                    └────────┬────────┘
                             │       ┌──────────────────────────────────┐
                             │◄──────│ Plan of Reservoir & Power Plant  │
                             │       └──────────────────────────────────┘
                    ┌────────┴────────┐
                    │ Storage Volume  │
                    └────────┬────────┘
                             │       ┌──────────────────────────────────┐
                             │◄──────│ Reservoir Storage Capacity       │
                             │       │ & Area Curve                     │
                    ┌────────┴──────────────┐    └──────────────────────┘
                    │ Water Surface Level & Area │
                    └────────┬───────────────┘
                             │       ┌──────────────────────────────────┐
                             │◄──────│ Operation Rule of                │
                             │       │ Reservoir                        │
                    ┌────────┴────────┐    └──────────────────────┘
                    │ Available Discharge for │
                    │ Power           │
                    └────────┬────────┘
                    ┌────────┴────────┐
                    │ Storage Volume  │
                    └────────┬────────┘
                             │
                    ┌────────┴────────┐
                    │ Water Surface Level │
                    └────────┬────────┘
                             │       ┌──────────────────────┐
                             │◄──────│   Tail Water Level   │
                    ┌────────┴────────┐    └──────────────────────┘
                    │  Loss of Head   │
                    └────────┬────────┘
                    ┌────────┴────────┐
                    │ Effective Head  │    ┌──────────────────────────────┐
                    └────────┬────────┘◄───│ Water Level-Discharge Curve │
    ┌───────────────┐        │             └──────────────────────────────┘
    │  Peak Hours   ├───────►│
    └───────────────┘        │
                    ┌────────┴────────┐
                    │ Maximum Discharge │
                    │ for Power       │
                    └────────┬────────┘
                    ┌────────┴────────┐
                    │ Efficiency of Turbine │
                    │ & Generator     │
                    └────────┬────────┘
                    ┌────────┴────────┐
                    │ Power & Energy  │
                    └─────────────────┘
```

9.1.5 Comparative Study of Development Plans

(1) Comparative Study of Alternative Layouts

Four alternative plans including single-stage development, which is proposed in the Upper Seyhan Basin Master Plan to develop a head between the Goktas Reservoir and the Kavsak Reservoir are planned as shown in Fig. 9-5 and Fig. 9-6. The plans have taken into consideration the topological and geological condition of the project area based on the field survey.

Plan I, which is proposed in both the Lower Seyhan Basin Master Plan and the Upper Seyhan Basin Master Plan, is to develop a head in one stage connecting the Goktas Reservoir and the Kavsak Reservoir by a pressure tunnel. Because only one powerhouse is constructed in this plan, the project cost is the lowest. But because the tunnel length of 15.7 km is very long, an economical construction method and construction period must be carefully studied.

Plan II is to develop a head between the Goktas Reservoir and the Kavsak Reservoir dividing it into two stages. The Goktas Reservoir and the No. 1 Powerhouse that is installed 1.0 km downstream of Bozkoy Village is connected by an 11.9 km pressure tunnel. The discharged water from the No. 1 Powerhouse and the river runoff is inducted into an intake that is installed downstream of the No. 1 Powerhouse. The discharge is conducted to the No. 2 Powerhouse through a 5.4 km pressureless headrace tunnel. In this plan, stage development is possible and the project cost of each power plant is minimized by dividing one power plant into two power plants. The total project cost of this plan, however, is higher than that of Plan I.

Plan III is to develop a head between the Goktas Reservoir and the Kavsak Reservoir, divided into three stages. The No. 1 Powerhouse is connected to the Goktas Reservoir by a short 950 m pressure tunnel. The discharged water from the No. 1 Powerhouse is directly inducted and conducted to the No. 2 Powerhouse through a 10.6 km pressureless tunnel. The discharged water from No. 2 Powerhouse and the river runoff is inducted into an intake and conducted to the No.

3 Powerhouse through a pressureless tunnel. In this plan the project cost of each power plan is smaller than that of Plan II, but the total project cost will be higher.

Plan IV is to develop a head dividing into three stages, as in Plan III. In this plan, an intake dam for the No. 3 Powerhouse is installed downstream of the confluence of the Zamanti River and the Indere River to utilize runoff from the Indere River, which has a relatively large catchment area (CA = 146 km). The regulating pondage is prepared by constructing an intake dam for the No. 3 Powerhouse to regulate the runoff of the Indere River. The dam cannot be planned as a large dam for the following reasons.

o The foundation of the dam and the reservoir consists of a calcareous zone and the permeability of the foundation is doubtful.

o There is a widely-distributing slope wash upstream of the dam's right bank slope, and the stability of the slope is doubtful if a high water level is incorporated into the design.

o Moreover, because of the large amount of sediments deposited by the Indere River, the reservoir's effective storage capacity will be quickly dissipated if the reservoir is to be extensive.

A study was carried out for the case of a high-water level of 630 m, an effective storage capacity of $24.70*10^6$ m, and a maximum discharge of 108 m^3/s. The maximum discharge, however, of the No. 2 Powerhouse of Plan II and the No. 3 Powerhouse of Plan III, is set at 111 m^3/s to utilize river runoff downstream of the Goktas Dam. Furthermore, the maximum discharge of the No. 3 Powerhouse of Plan IV is set at 132 m^3/s to utilize the regulated runoff of the Indere River.

(2) Fundamental Development Concept

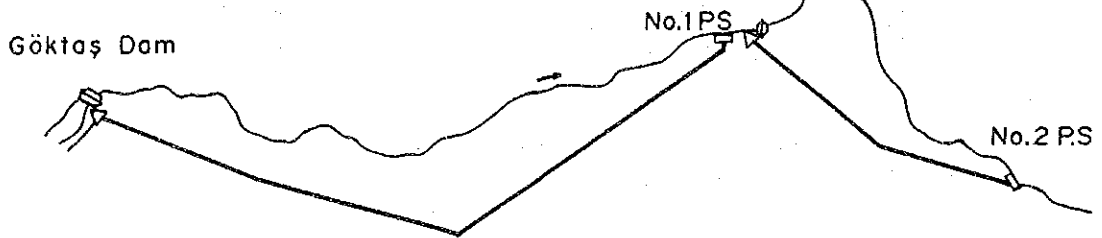The main features and economic comparison results of each plan are shown in Table 9-9. Plan I, which is the most economical plan, is selected as the fundamental development plan by the above study. A further study will be conducted for the selected fundamental plan.

Plan III, which is selected as alternatives considering economic condition and development flexibility, will be studied in Chapter 17's Study on Alternative Plans.

PLAN I

Göktaş Dam

P.S

PLAN II

Göktaş Dam

No.1 P.S

No.2 P.S

PLAN III

Göktaş Dam   No.1 P.S

No.2 P.S

No.3 P.S

PLAN IV

Göktaş Dam   No.1 P.S

No.2 P.S

No.3 P.S

ZAMATI GÖKTAŞ
HYDROELECTRIC POWER
DEVELOPMENT PROJECT

ALTERNATIVE LAYOUT

Fig. 9-5

PLAN II NO.I PS
PLAN III & IV NO.2 PS

PLAN IV
NO.3 PS

PLAN III & IV
NO.I PS

PLAN I PS
PLAN II NO.2 PS
PLAN III NO.3 PS

GÖKTAŞ DAM

L=3600 m

L=5410 m

L=10,180 m

L=4870 m

L=15,680 m

L=950 m

0   2500 m
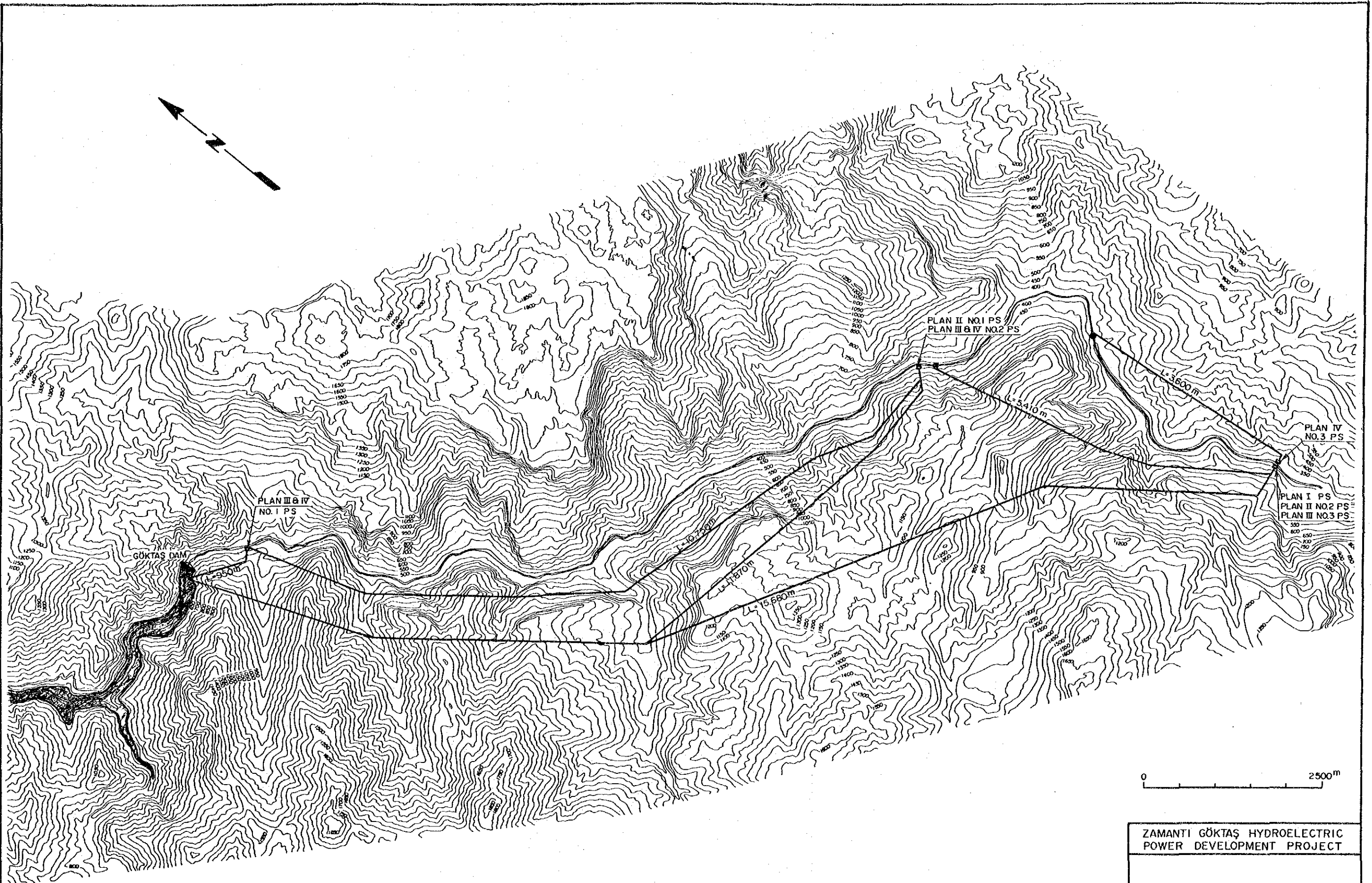
ZAMANTI GÖKTAŞ HYDROELECTRIC
POWER DEVELOPMENT PROJECT

ALTERNATIVE   PLAN

Fig. 9 - 6

9 - 29

Table 9-9 Alternative Study

Item	Unit	Plan I	Plan II No. 1 PS	Plan II No. 2 PS	Plan II Total	Plan III No. 1 PS	Plan III No. 2 PS	Plan III No. 3 PS	Plan III Total	Plan IV No. 1 PS	Plan IV No. 2 PS	Plan IV No. 3 PS	Plan IV Total
High Water Level	m	630.0	630.0	378.0		630.0	496.0	378.0		630.0	496.0	358.0	
Low Water Level	m	620.0	620.0			620.0				620.0		351.0	
Available Drawdown	m	10.0	10.0			10.0				10.0		7.0	
Gross Storage Capacity	10^6 m^3	109.3	109.3			109.3				109.3			
Effective Storage Capacity	10^6 m^3	24.7	24.7			24.7				24.7			
Tunnel Length	m	15,600	11,870	5,410		950	10,750	5,410		950	10,750	3,600	
Tunnel Diameter	m	6.8	6.8	6.9		6.8	6.8	6.9		6.8	6.8	7.5	
Tunnel Type		Pressure	Pressure	Pressure-less		Pressure	Pressure-less	Pressure-less		Pressure	Pressure-less	Pressure	
Maximum Discharge	m^3/s	108	108	111		108	108	111		108	108	132	
Standard Intake Water Level	m	626.7	626.7	374.3		626.7	488.7	374.3		626.7	488.7	354.5	
Tail Water Level	m	321.8	378.0	321.8		496.0	378.0	321.8		496.0	378.0	321.9	
Gross Head	m	304.9	248.7	52.5		130.7	110.7	52.5		130.7	110.7	32.6	
Effective Head	m	284.4	232.7	48.2	280.9	124.9	105.9	48.2	279.0	124.9	105.9	25.7	256.5
Installed Capacity	MW	270.0	220.9	45.0	265.9	119.0	100.5	45.0	264.5	119.0	100.5	28.5	248.0
Firm Peak Power	MW	265.2	216.1	44.7	260.8	114.1	99.3	44.6	258.0	114.1	99.3	28.0	241.4
Annual Energy Production	Gwh	1,147.0	936.8	193.1	1,129.9	499.8	430.7	193.5	1,124.0	499.8	430.7	124.3	1,054.8
Plant Factor	%	48.5	48.4	49.0	48.5	47.9	48.9	49.1	48.5	47.9	48.9	49.8	48.6
Investment Cost	10^6 TL	523,030	453,640	133,380	587,020	260,260	201,870	133,390	595,520	261,570	204,100	121,200	586,870
Annual Cost (C)	10^6 TL	54,395	47,179	13,872	61,051	27,067	20,994	13,873	61,934	27,203	21,226	12,605	61,034
Annual Benefit (B)		89,007	72,590	14,997	87,587	38,440	33,367	14,974	86,781	38,440	33,367	9,479	81,286
Benefit Cost Ratio (B/C)		1.64	1.54	1.08	1.44	1.42	1.59	1.08	1.40	1.41	1.57	0.75	1.33
Surplus Benefit (B-C)	10^6 TL	34,612	25,411	1,125	26,536	11,373	12,373	1,101	24,847	11,237	12,141	3,126	20,252
Unit Cost of Energy	TL/kWh	48.2	51.2	73.1	55.0	55.1	49.6	72.9	56.1	55.4	50.1	103.2	58.9

9.2 Study on Development Scale

9.2.1 Study on Reservoir Capacity

The seasonal and yearly variation of the monthly mean inflow to the Goktas Reservoir, for a period of 43 years, is indicated by the mass curve in Fig. 9-2. From the seasonal point of view, the discharge is generally large in the half-year period from January to June, and small in the period from July to December. The mean annual discharge for the period of 43 years is $1,704 \times 10^6$ m^3 (54 m^3/s). The discharge from January to June is $1,119 \times 10^6$ m^3 (71 m^3/s), which is about two times the discharge of 585×10^6 m^3 (37 m^3/s) from July to December. The annual discharge in the wettest year (1969) of 43 years is $2,616 \times 10^6$ m^3, which is 2.4 times the discharge of $1,114 \times 10^6$ m^3 in the driest year (1973). Thus, the seasonal and annual variation in the inflow to the reservoir is relatively small.

When the effective storage capacity is planned to be large to control the natural inflow, the firm discharge will also become large and the spilled water will decrease. But the available drawdown of the reservoir will increase and the mean effective head will decrease. On the other hand, when the effective storage capacity is planned to be small in scale, the available drawdown will decrease, the mean effective head will increase, and the spilled water will also increase. Therefore, the optimum storage capacity must be determined considering the flow regime and the characteristics of the reservoir.

The basement complex of the reservoir area consists of ophiolite. There is, however, a calcareous zone upstream from the upstream end of the reservoir, and because of the problem of possible leakage through that zone to other river basins, the high-water level of the reservoir is limited to the 630.0 m that was proposed in the Upper Seyhan Basin Master Plan. The sediment volume for fifty years is estimated to be 57.8×10^6 m without the Gumusoren Dam, and 22.0×10^6 m with the dam according to the study in Chapter 6's Meteorology and Hydrology. The sediment elevations against the above volume is 607 m and 580 m, respectively.

In a study of high-water levels, three cases have been compared, having elevations of 630, 620, and 610 meters. To compare reservoir effective storage capacity, five cases of available drawdown — 40, 30, 20, 10, and zero meters — have been taken for each high-water level mentioned above. The effective storage capacities for all the study-case combinations are given in the Table below. The reservoir area-storage-capacity curve given by 1/5,000 topographical map is shown in Fig. 9-7.

(Unit: 10^6 m^3)

| High Water	Available Drawdown (m)				
Level (m)	40	30	20	10	0
630	76.39	62.85	45.59	24.70	2.30
620	–	51.69	38.15	20.89	2.30
610	–	–	30.80	17.26	2.30

The following conditions will be assumed for comparison study purposes.

(1) The minimum peak hour of the Goktas Power Plant is determined to be six hours by the study in "5.2 Supply Program".

(2) The maximum power discharge is determined to maintain the minimum peak-demand period of six hours with the firm discharge, which is derived from the river discharge and effective storage capacity.

(3) The low water level is limited to 590 meters' elevation, based on the sediment surface elevation.

The study results are shown in Fig. 9-8 and Table 9-10. The economics improve with higher dam height. The economic advantages diminish with greater reservoir storage capacity, because the drawdown of the reservoir surface increases and the effective head is lost.

As a result of the above study, the high-water level is set at 630 m, the available drawdown 10 m, and the effective storage capacity 24.7$*10^6$ m for the Goktas Reservoir.

Fig. 9-7 Area-Capacity Curve of Goktas Reservoir
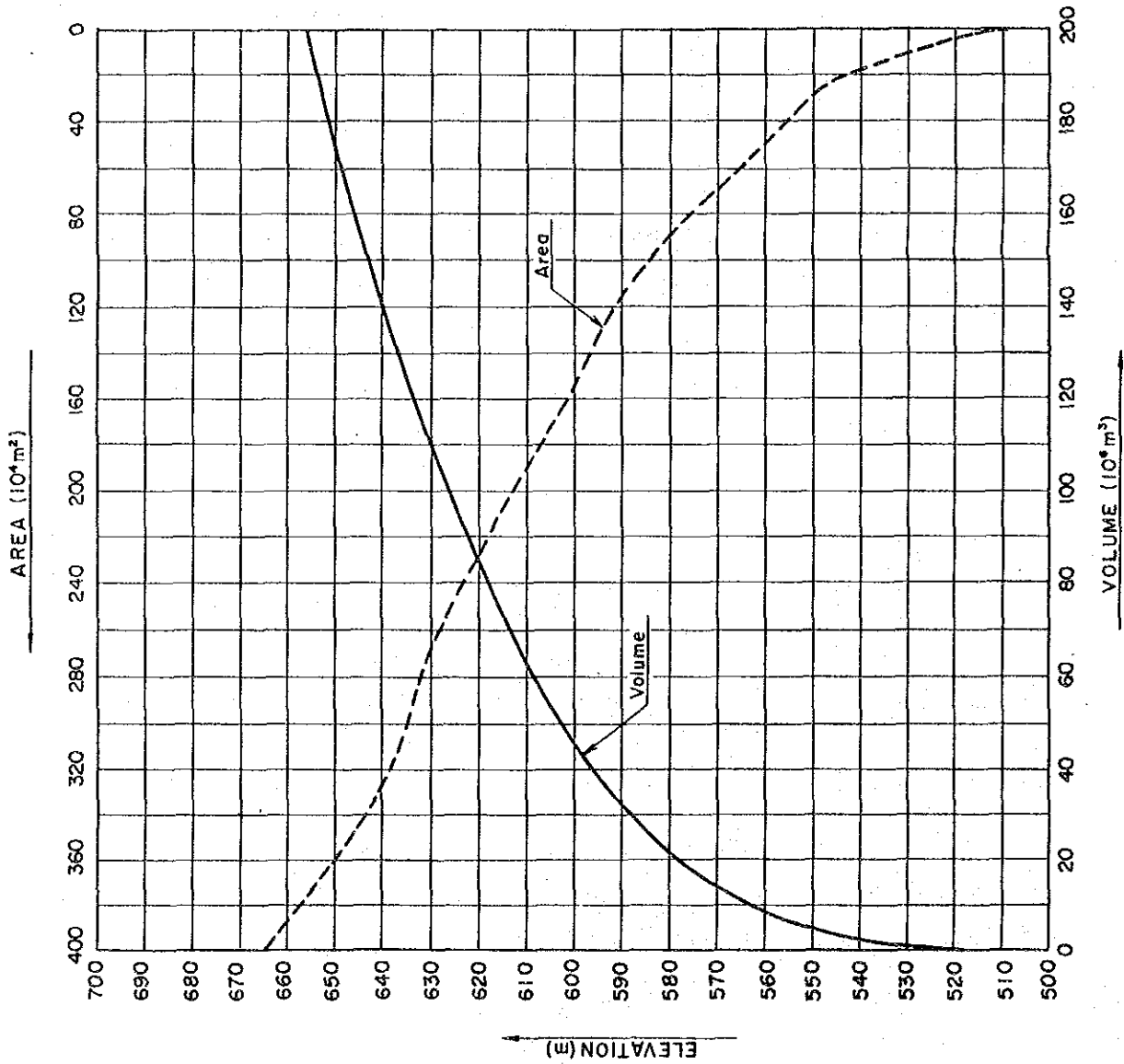
ELEVATION (m)	AREA (10^4 m²)	VOLUME (10^6 m³)
500	0.00	0.00
510	1.82	0.09
520	4.67	0.41
530	11.69	1.23
540	17.86	2.71
550	28.35	5.02
560	49.94	8.93
570	68.30	14.84
580	88.63	22.69
590	116.38	32.94
600	154.46	46.48
610	190.64	63.74
620	227.11	84.63
630	266.98	109.33
640	328.21	139.09
650	360.47	173.52

9 - 34

Table 9-10 Study on High Water Level and Effective Storage Capacity of Reservoir

Item	Unit	A-1	A-2	A-3	A-4	A-5	B-1	B-2	B-3	B-4	C-1	C-2	C-3
High Water Level	m			630.0					620.0			610.0	
Low Water Level	m	590.0	600.0	610.0	620.0	630.0	590.0	600.0	610.0	620.0	590.0	600.0	610.0
Available Drawdown	m	40.0	30.0	20.0	10.0	0.0	30.0	20.0	10.0	0.0	20.0	10.0	0.0
Gross Storage Capacity	10⁶ m³			109.3					84.6			63.7	
Effective Storage Capacity	10⁶ m³	76.4	62.9	45.6	24.7	2.3	51.7	38.2	20.9	2.3	30.8	17.3	2.3
Annual Inflow	10⁶ m³					1,744.4	321.8						
Annual Power Discharge	10⁶ m³	1,734.6	1,729.1	1,719.7	1,705.2	1,669.6	1,723.7	1,715.7	1,701.8	1,669.6	1,710.1	1,698.0	1,669.5
Annual Spill	10⁶ m³	9.8	15.3	24.7	39.2	74.8	20.7	28.7	42.6	74.8	34.3	46.4	74.9
Firm Discharge	m³/s	29.9	29.2	28.3	27.0	24.5	28.7	27.9	26.7	24.5	27.4	26.4	24.5
Maximum Discharge	m³/s	120.0	117.0	113.0	108.0	98.0	115.0	112.0	107.0	98.0	110.0	106.0	98.0
Standard Intake Water Level	m	616.7	620.0	623.3	626.7	630.0	610.0	613.3	616.7	620.0	603.3	606.7	610.0
Tail Water Level	m												
Gross head	m	294.9	298.2	301.5	304.9	308.2	288.2	291.5	294.9	298.2	281.5	284.9	288.2
Effective Head	m	274.4	277.7	281.0	284.4	287.7	267.7	271.0	274.4	277.7	261.0	264.4	267.7
Installed Capacity	MW	289.5	285.6	279.1	270.0	247.8	270.6	266.8	258.1	239.2	252.4	246.4	230.6
Firm Peak Power	MW	270.5	271.0	269.2	265.2	247.1	256.0	256.9	253.4	238.5	242.8	241.7	229.7
Annual Energy Production	GWh	1,100.3	1,118.2	1,133.8	1,147.0	1,143.1	1,073.8	1,090.6	1,104.2	1,103.1	1,046.6	1,061.5	1,063.0
Plant Factor	%	43.4	44.7	46.4	48.5	52.7	45.3	46.7	48.8	52.6	47.3	49.2	52.6
Investment Cost	10⁶ TL	564,560	554,330	539,880	523,030	449,140	536,240	525,780	510,620	489,090	508,840	496,930	479,120
Annual Cost (C)	10⁶ TL	58,714	57,650	56,148	54,395	51,911	55,769	54,681	53,104	50,865	52,919	51,681	49,828
Annual Benefit (B)	10⁶ TL	89,095	89,646	89,609	89,007	84,738	85,108	85,724	85,247	81,783	81,404	81,512	78,780
Benefit Cost Ratio (B/C)		1.52	1.56	1.60	1.64	1.63	1.53	1.57	1.61	1.61	1.54	1.58	1.58
Surplus Benefit (B-C)	10⁶ TL	30,382	31,996	33,461	34,612	32,827	29,399	31,043	32,143	30,918	28,485	29,831	28,952
Unit Cost of Energy	TL/kWh	54.3	52.4	50.4	48.2	46.2	52.8	51.0	48.9	46.9	51.4	49.5	47.7

Fig. 9-8 Study on High Water Level and Effective Storage Capacity of Reservoir
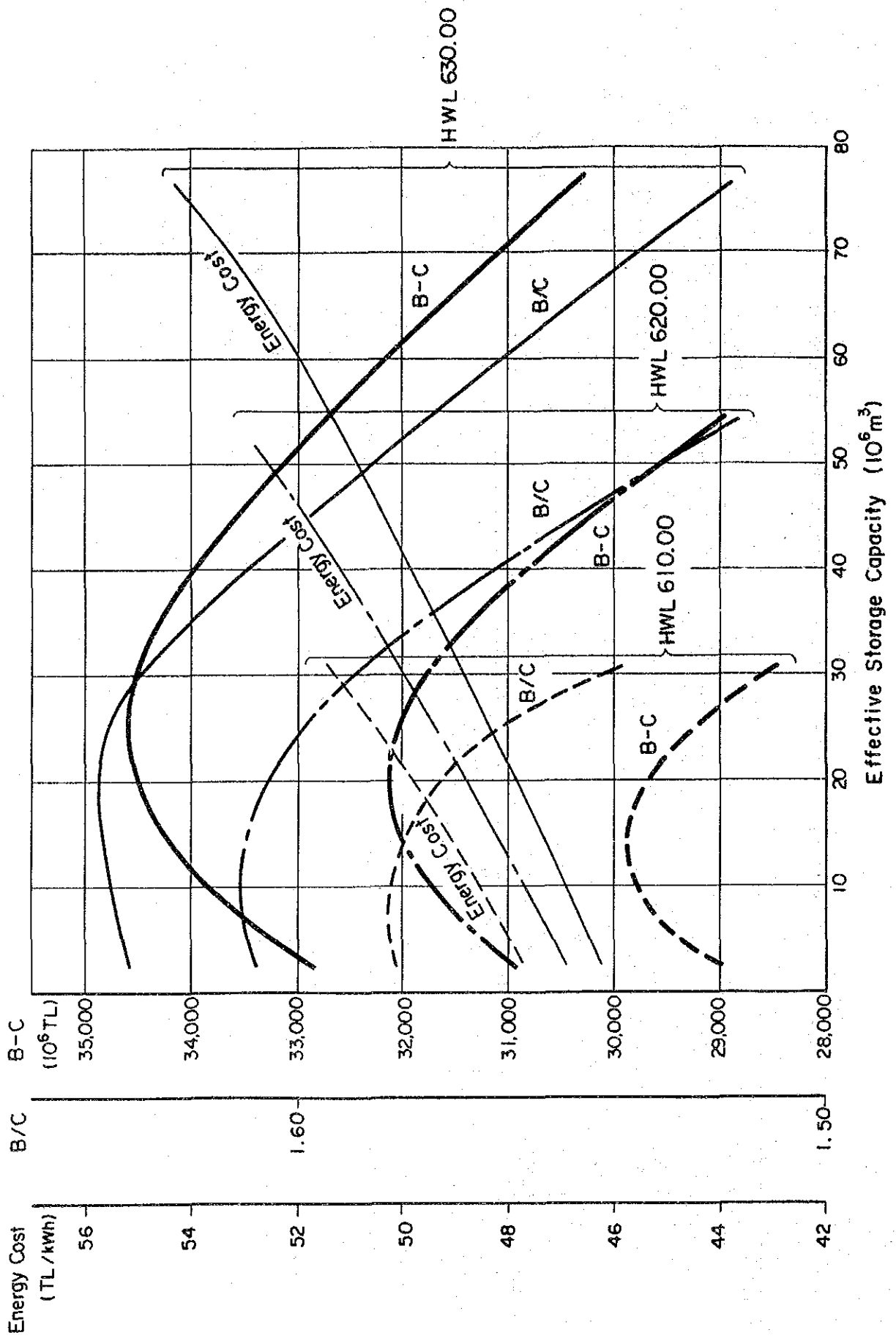
9.2.2 Study on Maximum Power Discharge

The maximum power discharge and installed capacity of the Goktas Project must be carefully studied considering the characteristics of the project and the peak duration. If the planned installed capacity is too large, the effective power output becomes insufficient in comparison with the installed capacity. This results in an uneconomical Project scale. If, however, the installed capacity is too small, the effective power output would be limited by the installed capacity and the peak duration becomes unnecessarily long.

A study was made for five cases, changing the maximum discharge from 81 m³/s to 162 m³/s for a minimum peak hour of six hours, considering the demand and supply balance. A study was also made for a peak hour of eight and ten hours.

The study result is shown in Table 9-11 and Figs. 9-9 and 9-10. The maximum discharge is set at 108 m³/s and the installed capacity 270 MW for the Goktas Power Plant in accordance with the above study.

9.2.3 Study on the Number of Turbine and Generator Units

The three alternatives of 1-unit, 2-unit and 3-unit as the number of units for main equipment are conceivable for the installed capacity of 270 MW for Goktas Power Plant Project.

(1) Unit Capacity for Main Equipment

The maximum capacity per unit of main equipment as seen from the standpoints of power system operation is to be decided by the whole capacity of the existing power system. That is, it is necessary that the power system will not be greatly affected at the time of faulting and stepping-out of the main equipment.

Since the installed capacity of 270 MW will be only about one percent of the peak load as seen from the demand forecast for 2001 A.D., the year of commissioning of this project, all three alternatives will not pose any problems in operation of the whole system accordingly.

(2) Construction Cost

The installed capacity of main equipment of 270 MW (1-unit plan) as seen from the standpoints of design, manufacture, transportation and installation, means a large size for a Francis type turbine and as close to the limit of manufacturing, it is to involve technical problems as well, but economical merit for the large size equipment can be expected in the cost of the project. However, in case of a large size machine, the main equipment pieces and parts would be split into blocks because of transportation limitations, and there will be demerits in performance and the installation schedule.

With a 90 MW x 3 units plan, not only the equipment cost will be comparatively higher but a longer installation schedule will be required. In case of this 3-unit plan, there will be also involved technical problems in connection with manufacture and installation of branch conduits for the penstock bifurcations.

(3) Operation and Maintenance

For dealing with inspection and maintenance e.g. an undergoing overhaul, etc. requiring outage of the main equipment for long periods of time, and with any troubles or failures in generating operation, it will be necessary to provide two or more units of the main equipment.

In case of 1-unit plan (270 MW), rapid response required by the existing power system will be a defect in the unit with such large capacity. And, as the minimum output available (25 - 30% of full output capacity) is rather large value, the degree of flexible operations will be reduced for partial loads genera-tion at and/or below the half loads at which turbine efficiency falls down extreamely and is probable vibrations and cavita-tions occurred on the turbine runner especially.

(4) Conclusion

Consequently, in view of the development scale of the project, the 2-unit plan of which an economical and reasonable plan concerning the degree of flexibility in operation is to be adopted.

Table 9-11 Study on Optimum Maximum Discharge and Peak Duration

Item	Unit	D-1	D-2	D-3	E-1	E-2	E-3	F-1	F-2	E-3	G-1	G-2	G-3	H-1	H-2	H-3
Maximum Discharge	m³/s		162			130			108			93			81	
Minimum Peak Hour	hr	6	8	10	6	8	10	6	8	10	6	8	10	6	8	10
Annual Inflow	10⁶ m³		1,743.2			1,733.3			1,744.4			1,668.3			1,618.5	
Annual Power Discharge	10⁶ m³								1,705.2							
Annual Spill	10⁶ m³		0.9			11.1			39.2			76.1			125.9	
High Water Level	m								630.0							
Low Water Level	m								620.0							
Available Drawdown	m								10.0							
Gross Storage Capacity	10⁶ m³								109.3							
Effective Storage Capacity	10⁶ m³								24.7							
Gross Head	m								304.9							
Effective Head	m								284.4							
Installed Capacity	MW		405.0			325.0			270.0			232.5			202.5	
Firm Peak Power	MW	319.8	253.6	202.2	298.7	243.0	202.9	265.2	233.3	195.8	228.4	218.5	190.0	198.9	198.9	182.3
Annual Energy Production	GWh	1,181.2	1,174.2	1,158.1	1,168.5	1,174.5	1,167.1	1,147.0	1,152.0	1,154.7	1,121.5	1,122.6	1,128.6	1,087.2	1,087.2	1,090.4
Plant Factor	%	33.3	33.1	32.6	41.0	41.3	41.0	48.5	48.7	48.8	55.1	55.1	55.4	61.3	61.3	61.5
Investment Cost	10⁶ TL	739,900	739,900	739,900	608,790	608,790	608,790	523,030	523,030	523,030	487,630	487,630	487,630	464,310	464,310	464,310
Annual Cost (C)	10⁶ TL	76,950	76,950	76,950	63,314	63,314	63,314	54,395	54,395	54,395	50,714	50,714	50,714	48,288	48,288	48,288
Annual Benefit (B)	10⁶ TL	102,431	86,992	74,745	97,256	84,554	75,471	89,007	81,771	73,187	79,900	77,643	71,215	72,263	72,263	68,512
Benefit Cost Ratio (B/C)		1.33	1.13	0.97	1.54	1.34	1.19	1.64	1.50	1.35	1.58	1.53	1.40	1.50	1.50	1.42
Surplus Benefit (B-C)	10⁶ TL	25,481	10,042	-2,205	33,942	21,240	12,157	34,612	27,376	18,792	29,186	26,929	20,501	23,975	23,975	20,224
Unit Cost of Energy	TL/kWh	66.3	66.7	67.6	55.1	54.8	55.2	48.2	48.0	47.9	46.0	46.0	45.7	45.2	45.2	45.1

FIG.9-9 STUDY ON OPTIMUM MAXIMUM DISCHARGE AND PEAK DURATION (B/C) (1)

B/C

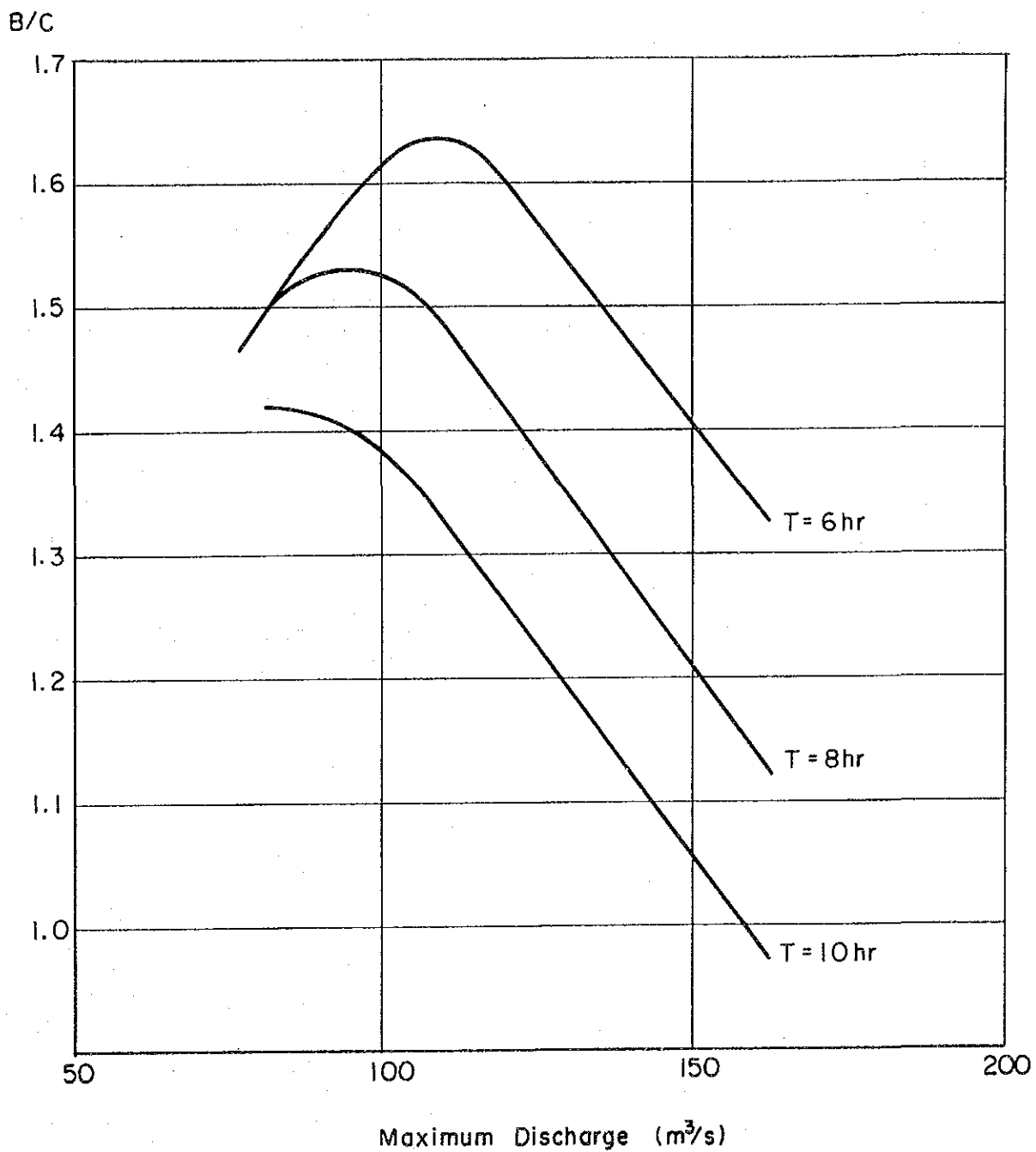Maximum Discharge (m³/s)

T = 6 hr

T = 8 hr

T = 10 hr

FIG. 9-10 STUDY ON OPTIMUM MAXIMUM DISCHARGE AND
PEAK DURATION (B-C) (2)

B-C
(10^6 TL)

40,000

30,000

20,000

10,000

0

T = 6 hr

T = 8 hr

T = 10 hr

50   100   150   200

Maximum Discharge (m^3/s)